THECHNICAL MAGAZINE

Department of Electronics & Communication Engineering

A.Y. 2023-24

















VELAGAPUDI RAMAKRISHNA SIDDHARTHA ENGINEERING COLLEGE

(AUTONOMOUS)

(Sponsored by Siddhartha Academy of General & Technical Education)

DEPARTMENT OF ELECTRONICS & COMMUNICATION ENGINEERING

Department Vision

To produce globally competitive and socially sensitized engineering graduates and to bring out quality research in the frontier areas of Electronics and Communication Engineering.

Department Mission

To provide quality and contemporary education in the domain of Electronics and Communication Engineering through periodically updated curriculum, best of breed laboratory facilities, collaborative ventures with the industries and effective teaching-learning process.

To pursue research and new technologies in Electronics and Communication Engineering and related disciplines in order to serve the needs of the society, industry, government and scientific community.

PROGRAM OUTCOMES

Program outcomes examine what a program or process is to do, achieve, or accomplish for its own improvement and/or in support of institutional or divisional goals: generally numbers, needs, or satisfaction driven. They can address quality, quantity, fiscal sustainability, facilities and infrastructure, or growth.

After completion of the Electronics & Communication Engineering programme, the students will be able to have:

PO1: Engineering knowledge: An ability to apply k nowledge of mathematics, science, fundamentals of engineering to solve electronics and communication engineering problems.

PO2: Problem analysis: An ability to identify, formulate and analyze electronics and communication systems reaching substantiated conclusions using the first principles of mathematics and engineering sciences

PO3: Design/development of solutions: An ability to design solutions to electronics and communication systems to meet the specified needs.

PO4: Conduct investigations of complex problems: An ability to design and perform experiments of complex electronic circuits and systems, analyze and interpret data to provide valid conclusions

PO5: Modern tool usage: An ability to learn, select and apply appropriate techniques, resources and modern engineering tools for modeling complex engineering systems.

PO6: The engineer and society: Knowledge of contemporary issues to assess the societal responsibilities relevant to the professional practice.

PO7: Environment and sustainability: An ability to understand the impact of professional engineering solutions in societal and environmental contexts and demonstrate knowledge of and need for sustainable development

PO8: Ethics: An understanding of professional and ethical responsibilities and norms of engineering practice.

PO9: Individual and team work: An ability to function effectively as an individual, and as a member in diverse teams and in multidisciplinary settings.

PO10: **Communication**: An ability to communicate effectively with engineering community and with society at large.

PO11: **Project management and finance:** An ability to demonstrate knowledge and understanding of engineering and management principles and apply these to manage projects.

PO12: Life-Long Learning: An ability to recognize the need for, and engage in independent and life-long learning in the broadest context of technological change.

ABOUT THE DEPARTMENT

Established in the year 1977, the department of ECE offers B. Tech Programme in Electronics & Communication Engineering with an intake of 240 and two M. Tech Programme in VLSI Design & Embedded Systems . The department has been accredited by NBA of AICTE four times. More than 40% faculties are with Ph.D. qualification. Led by a team of highly qualified experienced faculty with specializations such as RF & Microwave, Antennas, Digital Signal Processing, Wireless Communications, Digital Image Processing, VLSI and Embedded systems. The department provides excellent academic and research environment to the UG, PG and research students. A Centre of Excellence(TIFAC CORE- DST) in Telematics was established in the year 2009 with the state of the art facilities. Having successfully completed many research projects funded by UGC, AICTE, DST, NRSC-ISRO DLRL & ANURAG-DRDO etc., it is also recognized by JNTUK as "Research Center." Faculty members extend guidance to research scholars, produce Ph.D.'s and publish their findings in peer reviewed national and international journals and conferences.

Message by HoD

As a part of nurturing the students with qualities like teamwork, *technical* skills and a glimpse of the competitive world of *engineering* and *technology we are encouraging students to publish* articles in the frontier areas of electronics and communication engineering.

I am confident that all the faculty members and student community involved with this magazine have put their efforts in this in a way that the magazine both entertains and ignites the reader's mind. I would like to thank the editorial team members for bringing out this magazine regularly. I express my considerable appreciation to all the authors of the articles in this magazine. These contributions have required a generous amount of time and effort. It is this willingness to share knowledge, concerns and special insights with fellow beings that has made this magazine possible.

Dr. Venkata Rao Dhulipalla

J. Vouleala Ran

Technical Magazine 2022-23



Department of Electronics & Communication Engineering

Editorial Board ISSUE Academic Year
Dr D. Venkata Rao, Mr. K V Prasad JUNE- APRIL 2022-2023

TABLE OF CONTENTS

SNo	Title of the Article	Page No.
1	Mutual coupling Reductionin MIMO Antenna for UWB Application N. Venkateswari, M.D.S.S.D.Manisha, V.Sai Gopi chand	1-3
2	Optimized Dual Polarized MIMO Antenna With Slot And Parasitic Element Decoupling For Wireless Communication T.Mohith, D.Hemanth, Md.Sameer	4-6
3	Design & Simulation of Parallel Coupled Microstrip Bandpass filter for Wireless Communication Applications S. Geetha, B. Hemanth Kumar, B. Tejaswini	7-9
4	Prediction of Liver Diseases using Machine learning K.R.M.Aishwarya, P.Divya, V.Adarsh Venkata Sai	10-12
5	Smart Trolley for Quick Shoping K.Lohith, M.Thanmayee, M.Suraj Preetham	13-15
6	Matlab Implementation of monitoring system for High – Risk Cardiac Patients Ch.Mohitha, B.Naga Poojitha, Ch.Kishore	16-19
7	Development of LoRa Wan based Water Quality System K.Prasad, K.S.Sai Kiran, M.Venkatesh Babu	20-22
8	Enhancing Cognitive Radio Network Performance Through Channel Selection Algorithm S.Alekya, Sk.Nausheen, Ch.Swapna	23-26
9	Modified Karastuna Approximate Multiplier for Error- Resilient Applications P.Hareesha, T.Dheeraj	27-32
10	Determination of Crop Health & Treatment P.Jaxa Hruday ,A.BharathVenkata Siva Kiran	33-35

11	Vehicle Pollution Monitoring System using IoT K.S.Shanti Priya, N.VSai Teja, G.Roshan Chowdary	36-40
12	Detection of Marine Plastic Waste Using Machine learning P.Haarathi Padmavathi, P.B.Naveena, P.Hema nandini	41-43
13	MRI-CT fusion using Phase Conhruency of Intrinsic and Laplacian of Residue Maheshwar Reddy ,J.Prema Vani, B.Tejaswi	44-48
14	Design of a MIMO Antenna Isolated with an Inverted U-Shaped Ground Stub for Performance Enhancement P.Sree Pranavi, N.Poojitha, G.Susmitha	49-54
15	Pediatric Sleep Stage Classification P.Lurdhu merin, V.S.V.S.Prapoornetri, K.Ashok	55-56
16	Design and Analysis of Double U- Slot rectangular Patch Antenna for Wi-Fi and WiMAX Applications G.Bala Krishna, J.Waran Job, N.Om Venkata Vamsi	57-59
17	IoT Powered Intelligent Bike Safety System Afall Detection Algorithm M. Venkata Naga Vamsi, V. Sai Krishna, S. Karthikeya	60-62
18	mplementation of Dielectric Resonator Antenna M.Raghava, Sk.Nagur Basha ,N.Sanjay	63-64
19	Design of UWB MIMO for Bio-Medical Applications Ch.V.Sai Revanth, M.Hadi Abbas	65-68
20	Analysis of Smart Parking System Using Machine Learning Ch.Kowshik, N.Kaushik, Y.Yaswanth	69-71
21	Smart Bot for Face Recognition and Voice Controls E.Aditya Vardhan, B. Pooja, B. Kumar Sai	72-76
22	Design and Implementation of C Band Dielectric Resonator Antenna for 5G Communications A.R.V.Manoj, Sk.Ashraf, B.Yaswanth	77-81
23	Physical Layer Security Analysis of NOMA Network with Coorparative Relaying and RIS Under different Jamming Constraints D.B.S.Rohan, P.Naga Sridhar, D.Kumar Reddy	82-84

Student Members

- 1. T. Dheeraj- 208W1A04P0
- 2. B. Hemanth Kumar- 208W1A04J8
- 3. P. Hareesha- 208W1A04N6

DESIGN OF UWB MIMO ANTENNA WITH ENHANCED ISOLATION FOR WEARABLE APPLICATIONS

N. Venkateswari, V.Sai Gopichand, M.D.S.S.D. Manisha

Introduction:

Multiple antennas at the transmitter and receiver introduces signaling degrees of freedom that were absent in SISO systems. This is referred to as the spatial degree of freedom. The spatial degrees of freedom can either be exploited for "diversity" or "multiplexing" or a combination of the two. In simple terms, diversity means redundancy. A simple example of diversity is multiple antennas trying to receive the same signal. The received signal on the two antennas is corrupted by noise that is uncorrelated between antennas, therefore by combining the two signals a better-quality signal can be reconstructed. The analogy here is that by looking at the same object from two different vantage points, richer information on the object can be obtained. Diversity can also be achieved using multiple transmit antennas by using *Space Time Coding* (STC) techniques.

The second major MIMO technique is *Spatial Multiplexing*. Spatial multiplexing enables a MIMO transmitter/receiver pair to increase its throughput without increasing bandwidth usage or transmit power. Multiplexing increases throughput linearly with the number of transmit or receive antennas, whichever is lower. The transmitter sends signals carrying different bit streams from each of its antennas. Each receiver antenna receives a linear combination of the transmitted signals. The wireless channel is a matrix that is a function of transmit/receive antenna array geometry and the scatters/reflectors present in the environment.

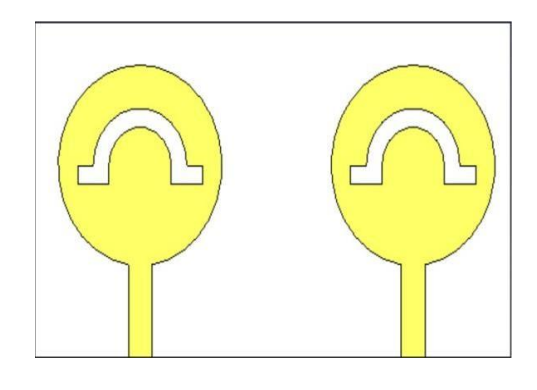


Fig.4.1 Front part

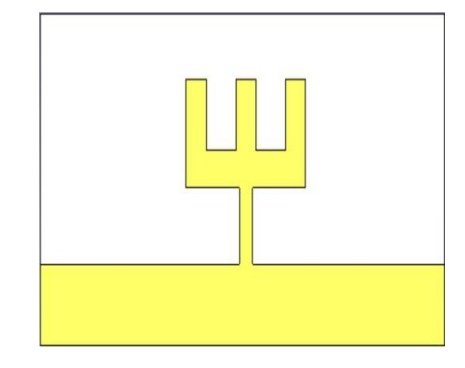
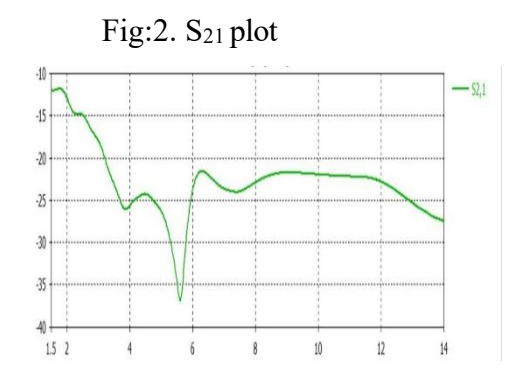


Fig.4.2 Back part

When a MIMO transmitter/receiver pair operates in an environment rich in scattering, the channel matrix becomes invertible, thus enabling the receiver to decode all the different signals transmitted from the various transmit antenna apertures, resulting in multiplexing gain. There is a trade-off between the amount of diversity and multiplexing gain a MIMO system can provide.

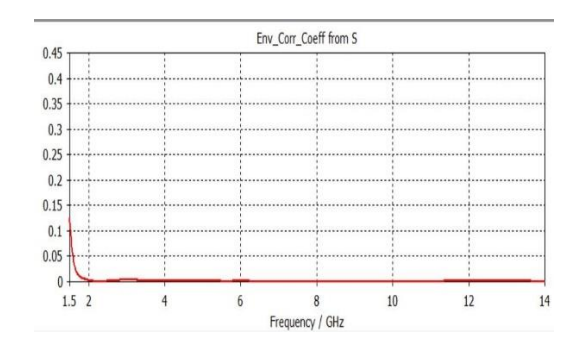
S₁₁/S₂₂: The most commonly quoted parameter in regards to antennas is S11. S11 represents how much power is reflected from the antenna, and hence is known as the reflection coefficient (sometimes written as gamma: or return loss. If S11=0 dB, then all the power is reflected from the antenna and nothing is radiated. If S11=-10 dB, this implies that if 3 dB of power is delivered to the antenna, -7 dB is the reflected power. The remainder of the power was "accepted by" or delivered. S₁₂/S₂₁: S21 represents the power transferred from Port 1 to Port 2. In general, SNM represents the power transferred from Port M to Port N in a multi-port network.

Fig:1. S₁₁ plot



DG (**Directivity Gain**): DG is a measure of the gain of an antenna compared to an ideal isotropic radiator. It indicates how well an antenna focuses its radiation in a particular direction. A higher DG value suggests that the antenna is more effective at concentrating its radiation in a specific direction, which can be useful in applications where directional coverage is desired.

ECC: The ECC is a key element for assessing the performance of the diversity in a MIMO antenna system. In regard to assess the competency of the pro-posed antenna model, it must approve that the ECC is relatively small, ideally under 0.5, suggesting the model to provide a strong diversity



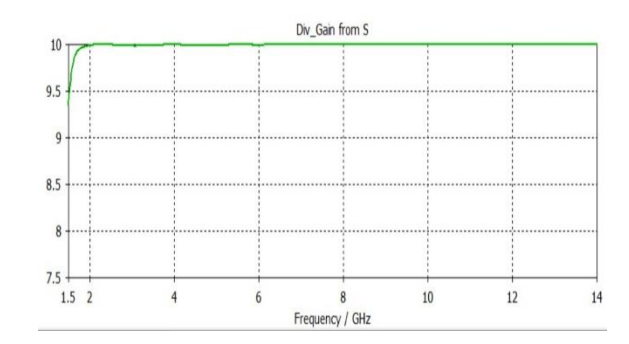
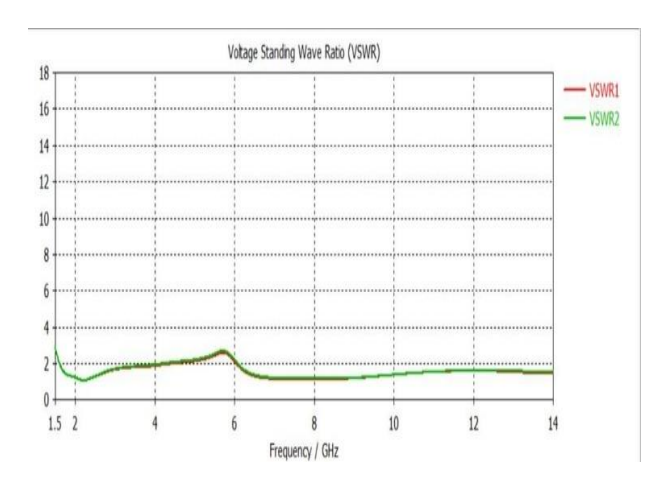


Fig:3. ECC plot

Fig:4. DG plot

VSWR: It stands for Voltage Standing Wave Ratio, and is also referred to as Standing Wave Ratio (SWR). VSWR is a function of the reflection coefficient, which describes the power reflected from the antenna. If the reflection coefficient is given by s11 or reflection coefficient or return loss.

FAR FIELD: The field, which is far from the antenna, is called as **far-field**. It is also called as **radiation field**, as the radiation effect is high in this area.



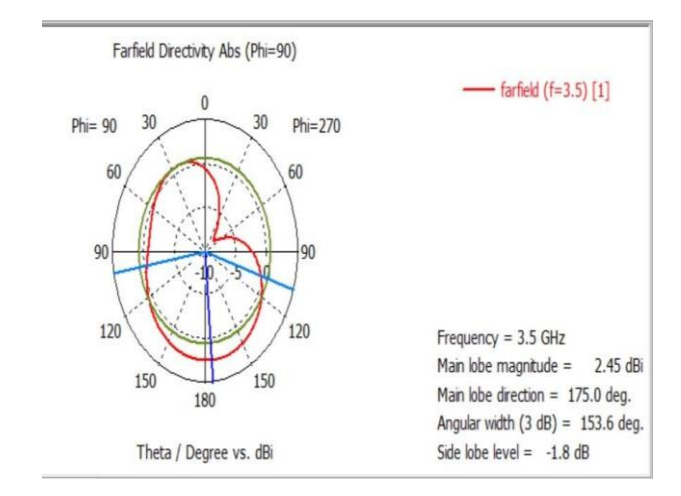


Fig:5VSWR plot

Fig:6 Far Fields

SURFACE CURRENTS: Surface current is a current flowing in the antenna, and has units of charge per unit time per unit length. A two-element wearable UWB-MIMO antenna with inverted E-shaped stub as a decoupling network is proposed. The decoupling structure provides an isolation enhancement of -34 dB in this communication. The proposed design is fabricated on a wearable jean's cloth, acting as a substrate, and a inverted E-shaped stub, mounted on the backside of antenna and attached to the partial ground for enhancing the port isolation. The proposed UWB- MIMO is simulated with dimensions $50 \times 35 \times 1.59 \text{ mm}^3$ and covers the entire UWB frequency. The diversity gain (DG) of the proposed design is greater than 9.9, with envelope correlation coefficient (ECC) less than 0.05 across the entire band. The results of the SAR provides that the antenna performs satisfactorily and is suitable for wearable applications. Simulation and fabricated model of the proposed antenna is a worthy candidate applicable for UWB MIMO applications.



Fig:7 Surface currents

OPTIMIZED DUAL POLARIZED MIMO ANTENNA WITH SLOT AND PARASITIC ELEMENT DECOUPLINGFOR WIRELESS COMMUNICATIONS

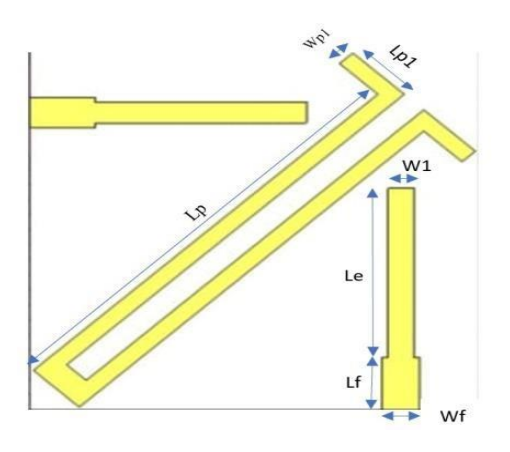
T. Mohith, D. Hemanth Sai Kumar, Md. Sameer

Introduction:

Multiple antennas at the transmitter and receiver introduces signaling degrees of freedom that were absent in SISO systems. This is referred to as the spatial degree of freedom. The spatial degrees of freedom can either be exploited for "diversity" or "multiplexing" or a combination of the two. In simple terms, diversity means redundancy. A simple example of diversity is multiple antennas trying to receive the same signal. The received signal on the two antennas is corrupted by noise that is uncorrelated between antennas; therefore bycombining the two signals a better quality signal can be reconstructed. The analogy here is that by looking at the same object from two different vantage points, richer information on the object can be obtained. Diversity can also be achieved using multiple transmit antennas by using *Space Time Coding* (STC) techniques.

The second major MIMO technique is *Spatial Multiplexing*. Spatial multiplexing enables a MIMO transmitter/receiver pair to increase its throughput without increasing bandwidth usage or transmit power. Multiplexing increases throughput linearly with the number of transmit or receive antennas, whichever is lower. The transmitter sends signals carrying different bit streams from each of its antennas. Each receiver antenna receives a linear combination of the transmitted signals. The wireless channel is a matrix that is a function of transmit/receive antenna array geometry and the scatters/reflectors present in the environment.

When a MIMO transmitter/receiver pair operates in an environment rich in scattering, the channel matrix becomes invertible, thus enabling the receiver to decode all the different signals transmitted from the various transmit antenna apertures, resulting in multiplexing gain. There is a trade-off between the amount of diversity and multiplexing gain a MIMO system can provide. A typical MIMO transmitter/receiver pair automatically finds an operating point on the diversity- multiplexing trade off curve based on instantaneous wireless channel conditions. The antenna has been designed on FR-4 substrate ($\varepsilon r = 4.4$, h = 1.57, $\tan \delta = 0.02$) and is composed of a pair of micro strip lines with step, a parasitic element placed between the pair of micro strip lines with step and three slots etched in the ground plane. The parameter values of the antenna are depicted as follows (in mm): Le = 11.25, L_f= 3.5, L_p = 26, L_{p1} = 3.8, W_f= 2,L_s=10.65,L_{s1}=29, Wl = 1.4, Wp = 3.5, Wp1=1.



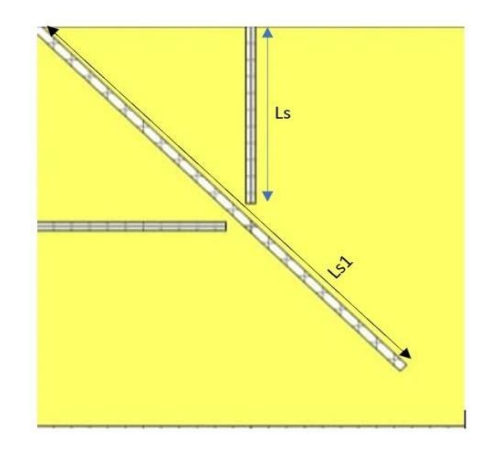
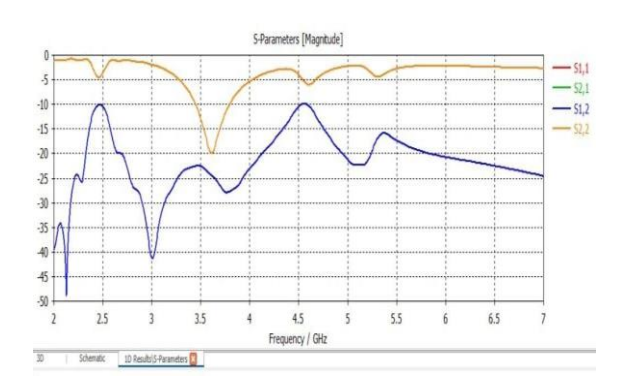


Fig.1 Front part

Fig 2: Back part

There was a notable concentration of current density on the ground plane situated between the radiating elements. To reduce this issue and enhance isolation, a diagonal slot was carved into this region on the ground plane. The lengths of these diagonal slots have been adjusted to achieve a substantial level of isolation between the ports, within the range of 25 to 30 mm.



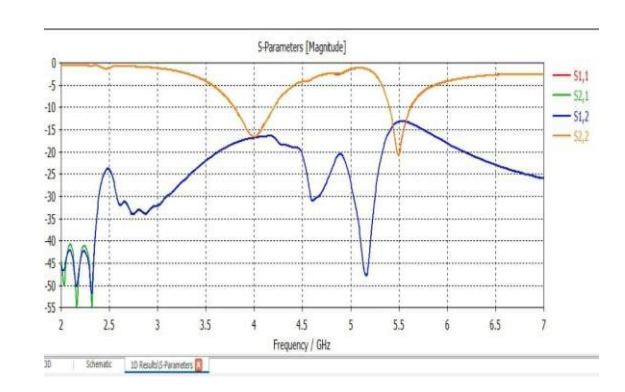


Fig: 3 - S₁₂ S₂₂ plot

Fig: 4 - S₁₂ S₂₁ plot

Fig 3 represents the 5G band communication which ranges from 3.35-3.5GHz.At the frequency 3.5GHz we get gain of -15Db .Fig 4 represents the WLAN application with frequency ranging from 5.18-5.95GHz.As show infig at those frequency the gain of -45dB.A compact two-element dual-polarized MIMO antenna for 5G applications and a compact two- element dual-polarized MIMO for 5G/WLAN applications are proposed. The design of bothMIMO antennas consists of a pair of micro strip lines with step and a parasitic element placed between the pair of micro strip lines with step and slots etched in the ground plane.

In the first MIMO antenna configuration, isolation better than 18 dB is achieved by the antenna. In the second MIMO antenna configuration, isolations better than 19.8 dB and 16.75 are achieved by the antenna for the first and second operating bands, respectively. Furthermore, for the second MIMO antenna configuration, key parameters of MIMO antennas such as ECC and DG are investigated, and appropriate values for ECC of lower than 0.06 and 0.11 are achieved by the first and second operating

band, respectively; besides, appropriate values for DG of higher than 9.994 and 9.971 areachieved by the first and second operating band, respectively. In addition, the ECC and DG results are compared with other works recently reported in the literature and the radiation efficiency is investigated and analyzed. Therefore, the MIMO antenna proposed in this work is suitable and a good candidate for use in 5G/WLAN applications.

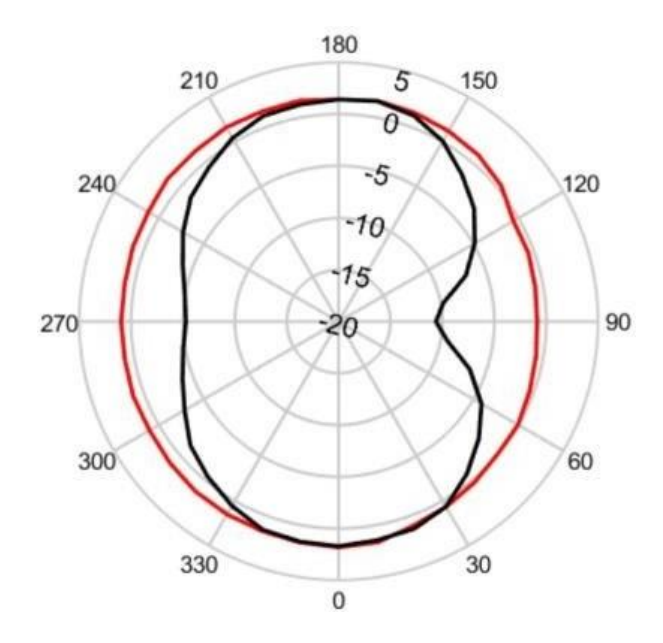


Fig 5 – Radiation Pattern at Frequency 3.5GHz

DESIGN & SIMULATION OF PARALLEL COUPLED MICROSTRIP BANDPASS FILTER FOR WIRELESS COMMUNICATION APPLICATIONS

S.Geetha, B.Hemath Kumar, B.Tejaswini

Introduction:

Microstrip bandpass filters are widely used in modern communication systems due to their compact size, low cost, and high performance. In recent years, the demand for high- speed wireless communication systems operating at higher frequencies has increased, which has led to the need for the design of bandpass filters operating at millimeter-wave frequencies. In this project, we designed and simulated the parallel-coupled microstrip bandpass filter operating in KU Band. The proposed filter is designed using the transmission line theory and the coupling matrix method. The filter is designed using a substrate with a dielectric RO3010 and a thickness of 1.28mm. The filter is designed to have a fractional bandwidth of 10% and passband ripple of 0.5db. The filter is simulated using a commercially available electromagnetic simulation tool (HFSS), and the simulation results are presented and The suggested filter demonstrates remarkable effectiveness by displaying a minimal insertion loss and exceptional selectivity The filter's performance is compared with the performance of other similar filters reported in the literature. The simulation results demonstrate that the proposed filter is superior to other reported filters in terms of its performance parameters. Overall, the proposed filter design and simulation methodology can be useful for the design of high-performance millimeter wave bandpass filters for modern communication system.

Methodology:

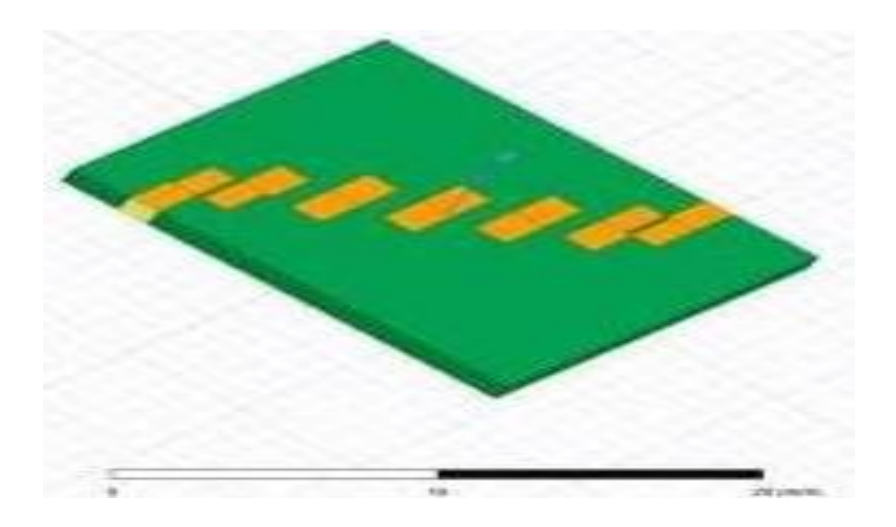


Fig 1: Block Diagram

The simulation process involves creating a 2D or 3D model of the filter in the simulation tool and setting up the simulation parameters, such as the frequency range and simulation type. The simulation

tool then solves the electromagnetic equations to calculate the filter's performance parameters, such as the S-parameters, insertion loss, and return loss. In the "Modeler" window, create a rectangular waveguide with the desired dimensions to operate at 15GHz. You can use the "Waveguide" option under "Primitive" in the toolbar to create a waveguide. Create a rectangular cavity by extruding a rectangle from the centre of the waveguide. The cavity should be designed to achieve the desired bandwidth and centre frequency. You can use the "Rectangle" option under "Primitive" in the toolbar to create the rectangle. Create two quarter-wave parallel-coupled resonators in the cavity. These resonators should be designed to resonate at the centre frequency and achieve the desired bandwidth. You can use the "Polyline" option under "Primitive" in the toolbar to create the resonator.

Connect the resonators to the input and output waveguide ports using short- circuited stubs. These stubs should be designed to provide impedance matching between the waveguide and resonators. You can use the "Stub" option under "Excitation" in the toolbar to create the stub. Add boundary conditions and set the simulation frequency range to 15GHz. You can use the "Boundary" and "Frequency" options under "Analysis Setup" in the toolbar to set these parameters. Run the simulation and observe the S-parameters to analyze the filter's performance.

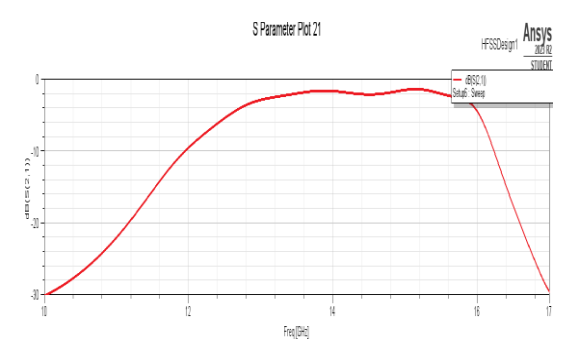


Fig 2: S₁₁ parameter of parallel coupled band pass filter

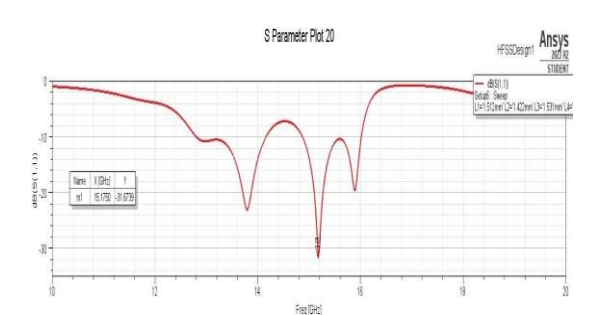


Fig 3: S₂₁ parameter of parallel coupled band pass filter

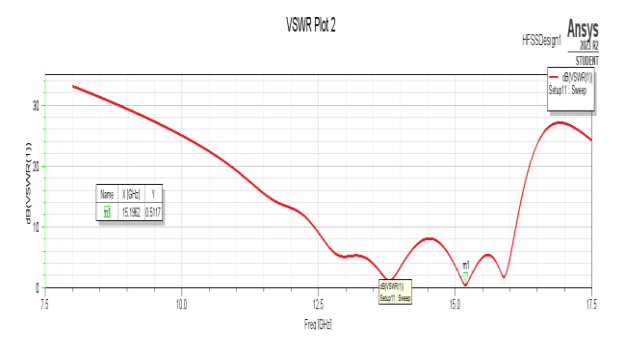


Fig 4: VSWR Plot of parallel coupled band pass filter

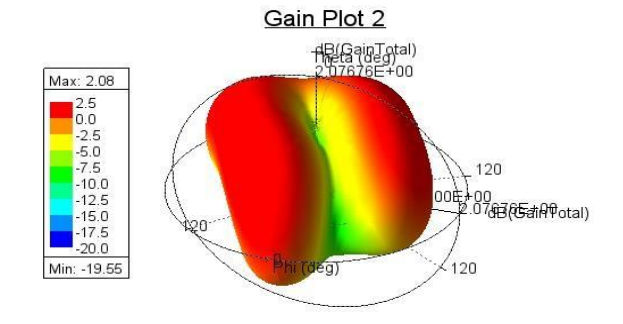


Fig 5: Gain Plot of parallel coupled band pass filter

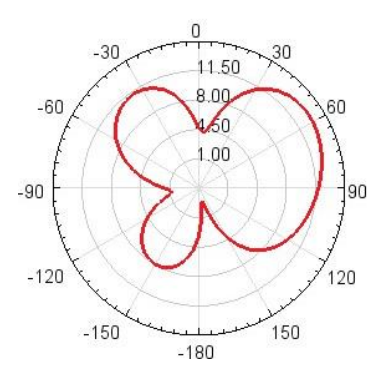


Fig 6: Radiation Plot of parallel coupled band pass filter

In this a parallel coupled Microstrip Bandpass filter with a centre frequency of 15 GHz for wireless communication applications, using a substrate of R03010 of Order 5 using HFSS software and it has 0.511 VSWR, insertion loss of 2 dB and return loss is less than 10 dB (-31 dB) with 21.73% of the bandwidth from 13.5 to 16.8 which is mainly used for radar communication and wireless communication systems.

PREDICTION OF LIVER DISEASE USING MACHINE LEARNING

K.R.M.Aishwarya, V.Divya, V.Adarsh Venkata Sai

Introduction:

Liver disease represents a substantial global health burden, affecting millions ofindividuals worldwide. Timely and accurate diagnosis of liver disease is pivotal for effective patient management and preventing adverse outcomes. Traditional diagnostic methods often rely on clinical observations, laboratory tests, and medical imaging, which can be time- consuming and may not always yield precise results. In recent years, the application of machinelearning (ML) techniques has emerged as a promising avenue for enhancing the predictive capabilities in the realm of liver disease. These ML methods leverage the power of computational algorithms to analyse vast and intricate datasets, enabling healthcare professionals to make informed decisions with improved accuracy. By harnessing the potential of ML, the critical need for more efficient and precise liver disease prediction methods need tobe addressed, ultimately improving patient care and outcomes.

Liver is the primary and most crucial body organ, and the maintenance of its health is essential for improved overall health. But the fact is that people generally overlook it in the case of health. Due to unhealthy lifestyle routines, most of the population across the globe aresuffering from acute to severe liver problems.

Liver diseases include: Viral infections, e.g., hepatitis A, hepatitis B, and hepatitis C, Immune system problems, e.g., autoimmune hepatitis, primary biliary cholangitis, primary sclerosing cholangitis Diseases caused due to drugs, poisons, or high alcohol consumption, e.g., fatty liver disease, non-alcoholic fatty liver disease (NAFLD), non-alcoholic steatohepatitis (NASH) and, cirrhosis, Inherited diseases, e.g., hemochromatosis, hyperoxaluria, alpha-1 antitrypsin deficiency, and Wilson disease Cancer and tumour, e.g., Liver Cancer, bile duct cancer, and liver cell adenoma.

Methodology:

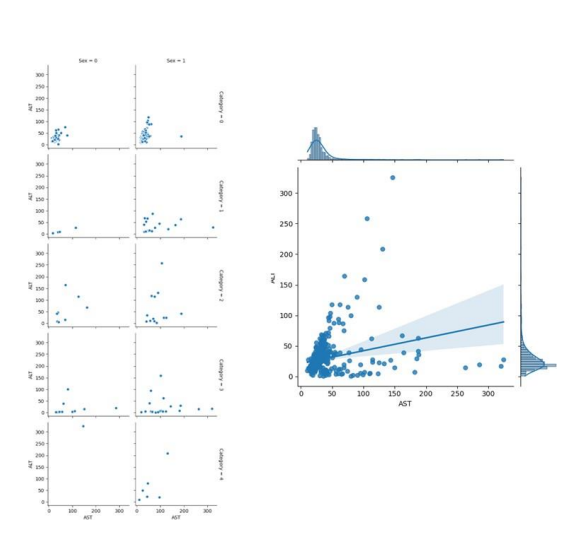


Fig.1: Relation between ALT & AST

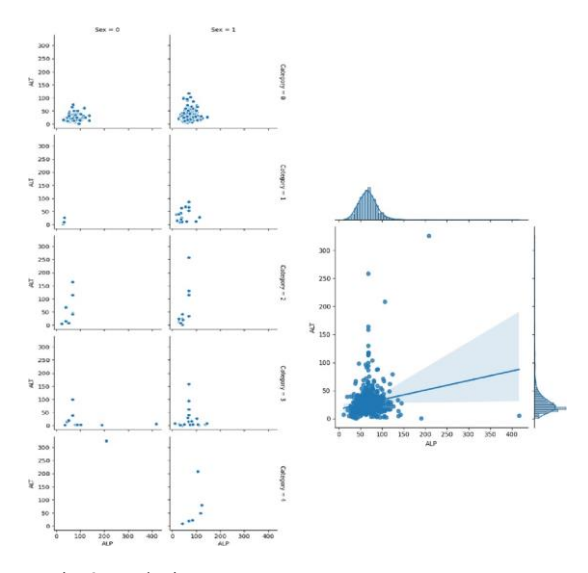


Fig.2: Relation Between ALP & ALT

Machine learning algorithms have demonstrated significant potential in the prediction and diagnosis of liver disease. These algorithms leverage the computational power of modern technology to analyze vast and intricate datasets, often including clinical, genetic, and imaging data. Unlike traditional approaches, ML models can identify subtle patterns, non-linear relationships, and hidden insights within these data, leading to enhanced diagnostic accuracy. Moreover, they have the capacity to adapt and improve their predictions over time as they learnfrom new data. By harnessing the capabilities of ML, we aim to develop robust models that can serve as invaluable tools for healthcare practitioners. Ultimately, our goal is to address the pressing need for more efficient and precise liver disease prediction methods, revolutionizing the landscape of liver disease management and patient care. In this, methodologies, datasets, challenges, and potential applications of ML will be addressed in the context of liver disease prediction, paving the way for improved healthcare outcomes and a deeper understanding of this complex medical condition.

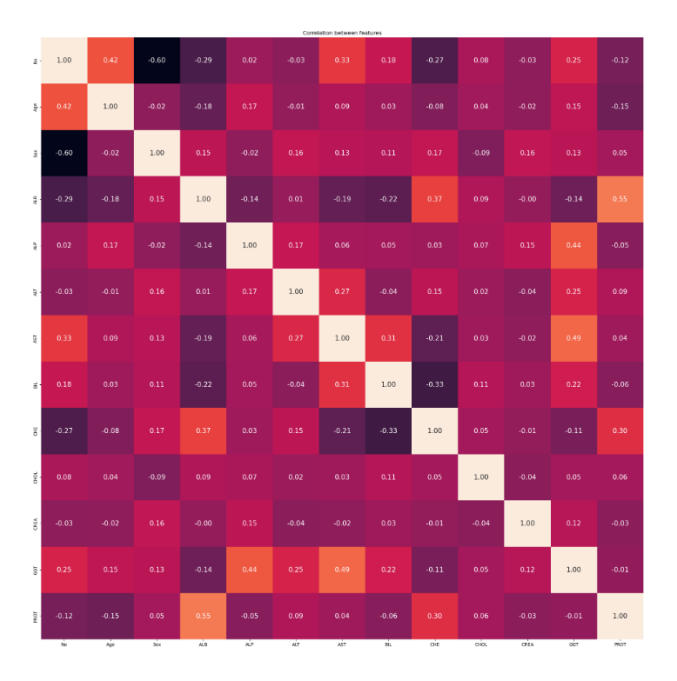


Fig 3: Correlation between the features

After, the preprocessing is done, the data is split into training data and testing data i.e., training data- 80% (492), testing data- 20% (123). The splitting is done by using train_test_split () function. The SVM model is fitted with the trained data after it is modelled. Then the classification and performance metrics like accuracy score, recall score, classification report are calculated whose results are shown in chapter 5 (results & conclusion). The same process is repeated for Random Forest classifier, Decision tree classifier, XGBoost, AdaBoost techniques. Then, the comparison is done among all the models.

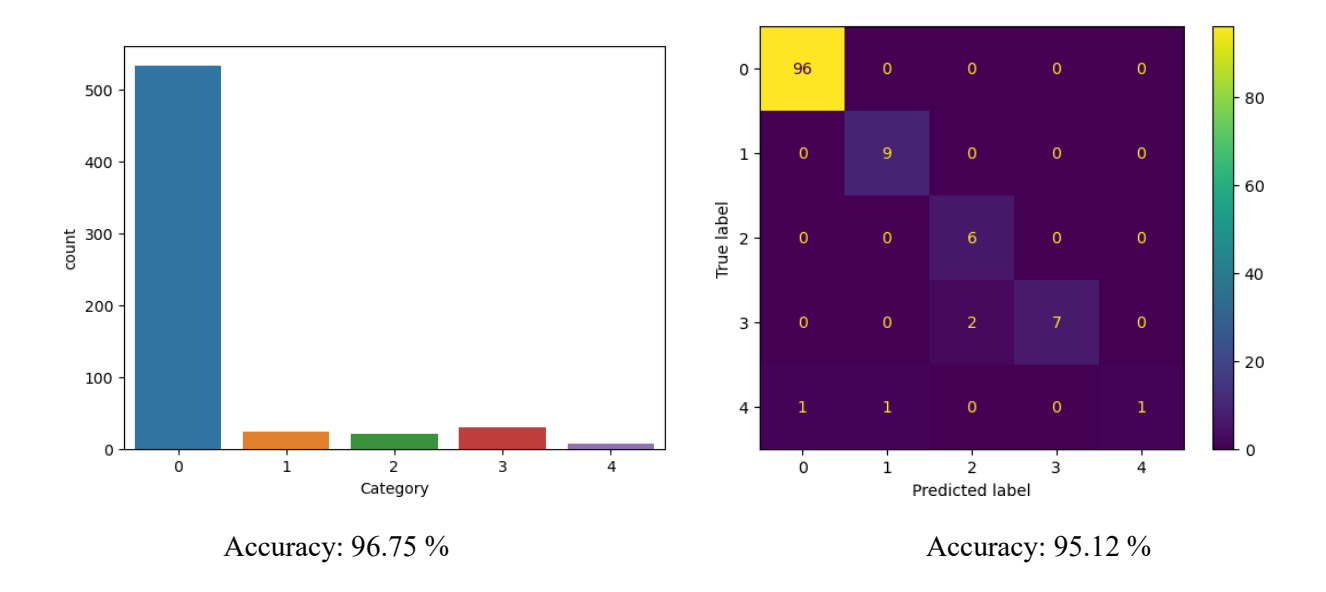
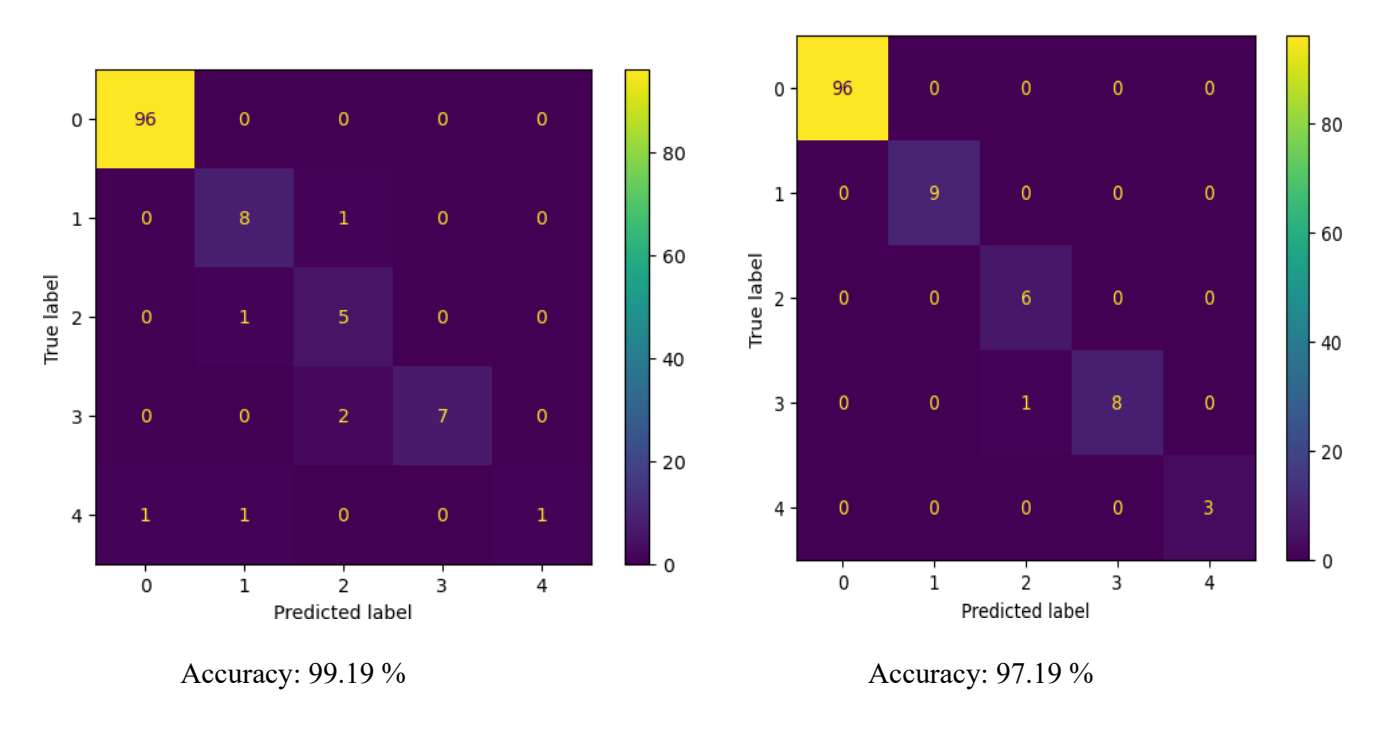


Fig. 4: Confusion matrix using SVM



Health condition of the patient with respect to liver disease can be predicted. If the patient has liver disease, then the stage of the disease can also be predicted bythis proposed model. Also from various algorithms, decision tree algorithm has the highest accuracy and is the best model to predict the liver disease.

SMART TROLLEY FOR QUICK SHOPPING

K. Lohith, M. Thanmayee, M. Suraj preetham.

Introduction:

Smart Trolley for Quick Shopping" project represents a groundbreaking advancement in the retail and shopping industry, leveraging cutting-edge technology to enhance the overall shopping experience for customers while optimizing store operations. Traditional shopping carts and trolleys are being transformed into intelligent, connected devices that offer a myriad of benefits for both shoppers and retailers.

This integrates a combination of sensors, RFID technology, and IoTconnectivity to create a shopping cart that is not only smarter but also more efficient. Theprimary objective of this project is to streamline the shopping process, reduce friction points, and provide a seamless, data-driven shopping experience. We can see manually operated trolleys in some shopping centers like Big Bazaar, Reliance Mart, D-Mart etc. Moving a manually operated trolley today is a daunting job in malls and retail areas because of the heavy weight of items and packed billing counters. In order to overcome this issue, "Smart Trolley For Quick Shopping" was proposed. An automated moving trolley with sensors is designed for the convenience of customers. The sensor on the trolley, scans the purchased item and keeps moving. Upon atotal purchase, the person has to go to the payment billing counter. The billing system will be placed in the trolley consists of an RFID reader. If a product is placed in the trolley, the product code will be identified by using an RFID reader connected to the trolley. When the new product is added, the cost will be calculated to the overall bill. Therefore, the billing would be performed in the trolley itself, which will be observed on the LCD.



Fig1. Jammed billing counters with manually operated trolleys

In depth, "Smart Trolley For Quick Shopping" is an automated customer favorable trolley, designed with the goal of making the system reliable, simpler, faster and more effective. Customer satisfaction is one of the most important aspects of any company. It can also increase sales for supermarkets by making it easier for customers to find the products they want.

The proposed system can reduce costs for supermarkets by reducing the amount of time that employees spend helping customers find products. It can improve the customer experience by making it easier for customers to find the products they want and by providing them with information about products. There are improvisations that can be made in the future in the new framework that we have put in place.

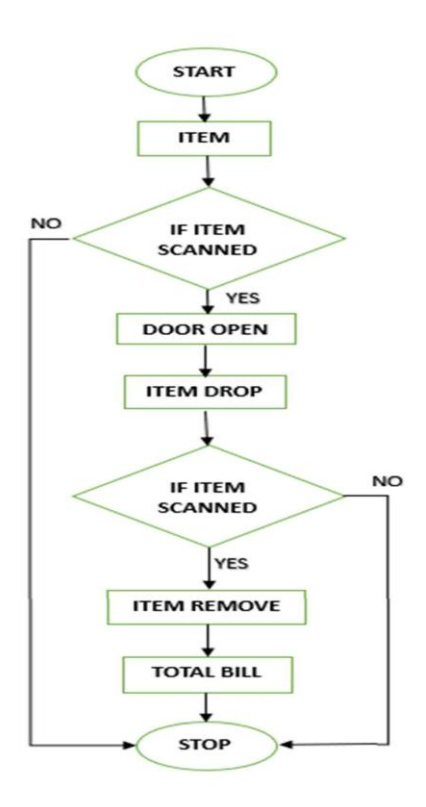


Fig2. Flowchart



Fig 3. Designed Prototype



Fig 4.Application

This system can offer several benefits for supermarkets and customers alike. Supermarkets can benefit from reduced labor costs, increased sales, improved customer satisfaction, and enhanced data collection and analytics. Customers can benefit from a faster and more efficient shopping experience, real-time spending tracking and budgeting, convenient mobile payment, and personalized recommendations and offers. Overall, smart trolleys integrated with mobile applications have the potential to revolutionize the way people shop for groceries.

The designed system will offer several benefits for both supermarkets and customers, including: Reduced labor costs and increased sales for supermarkets. A faster and more efficient shopping experience for customers. Real-time spending tracking and budgeting for customers. Convenient mobile payment for customers. Personalized recommendations and offers for customers. A sustainable shopping experience. Smart trolleys are still under development, but they have the potential to make a significant impact on the retail industry. It can also help customers to save time and money, and make the shopping experience more enjoyable. Overall, smart trolleys are a promising new technology with the potential to revolutionize the grocery shopping experience.

MATLAB IMPLEMENTATION OF MONITORING SYSTEM FOR HIGH-RISK CARDIAC PATIENTS

Ch. Mohitha, B. Naga Poojitha, Ch. Kishore

Introduction:

In Healthcare, we know that when it comes to your heart, experience matters. And our board-certified cardiac electrophysiologists diagnose and treat more patients with abnormal heart rhythms than any other health care provider in San Diego. Recognized as leaders for their groundbreaking research, our renowned electrophysiologists are continually looking for new and better ways to manage and treat heart rhythm disorders; ensuring patients have access to the most advanced technology. Throughout the cardiovascular network, electrophysiologists work hand-in-hand with your primary care physician, cardiologist and medical colleagues to provide the best possible treatment options for all types of arrhythmias. The electrical system of your heart initiates each heartbeat and creates signals that trigger the heart to pump.

These electrical signals control the heart rate and rhythm. A normal heartbeat has a specific pattern of electrical flow throughout the heart. Since among all the components in an ECG signal QRS complex is of paramount importance, accurate QRS detection is essential for ECG monitoring. For example, the QRS complex is most closely associated with heart rate variability (HRV) that is derived from the RR interval between consecutive QRS complexes and is thus crucial to the diagnosis of arrhythmia and cardiac diseases. In the proposed system, ECG MIT-BIH (ecgdb) 108 dataset is considered and the RAR file is downloaded and extracted, the .mat file is downloaded and saved in the appropriate folder. The dataset consists of the Amplitude of the ECG signal end to end, here we consider the Sampling frequency of 360Hz and sampling is done for it and stored in the MATLAB variable ECG. The data is of double datatype <650000*2>.

This system mainly consists of the high pass filter (HPF), low pass filter (LPF), and QRS Wavelet Decomposer. From Fig.2, we can know the constructed circuit for the low pass filter by using the coefficients given in the module description used as the right shifters. From Fig.3, the high pass filter is designed in the MATLAB 2021a Simulink file. Now the Wavelet Decomposer is designed by using the LPF, HPF, adders and the delay unit. The below Fig.4 gives the Architecture of the Wavelet Decomposer which consists of the blocks.

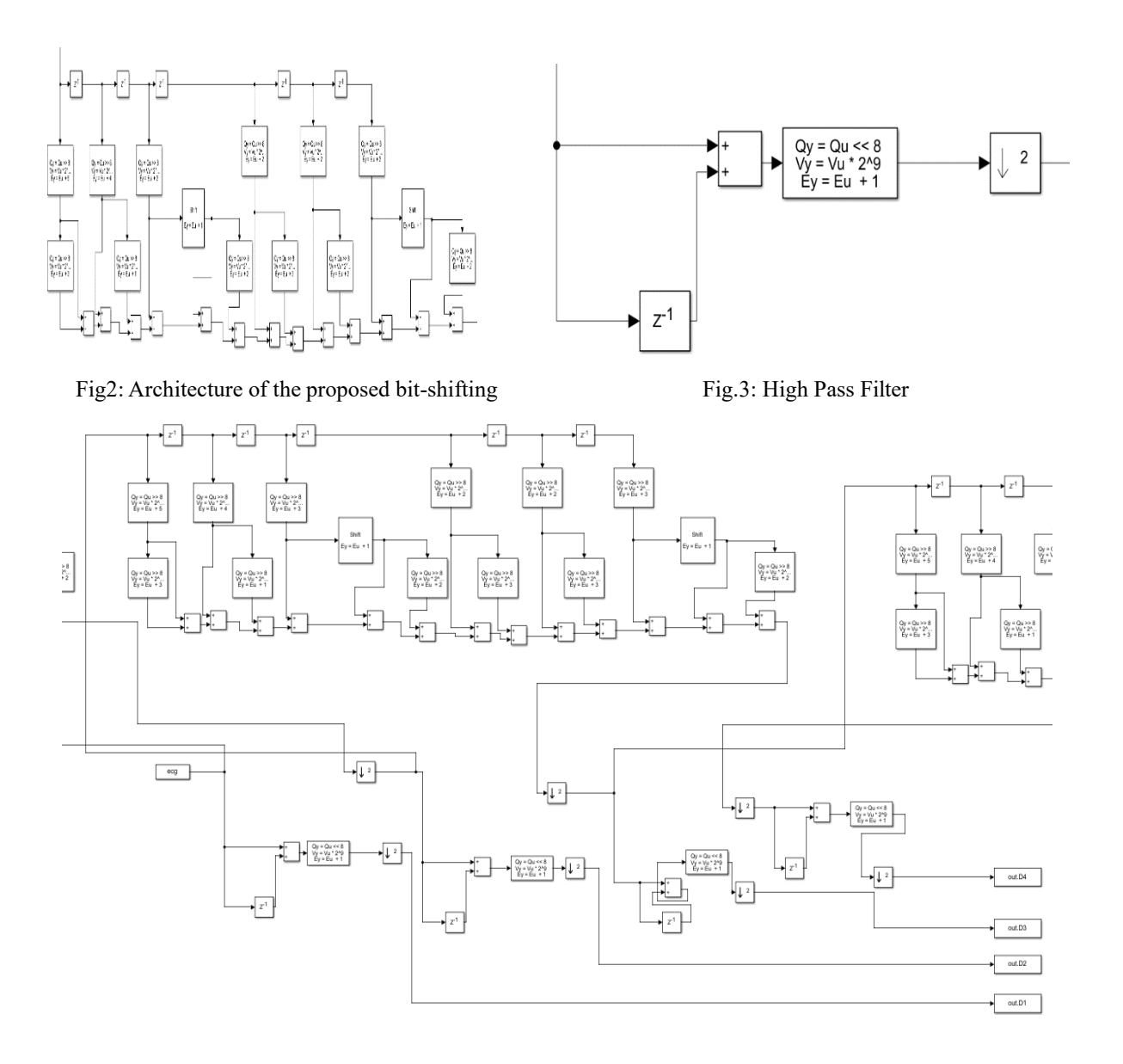
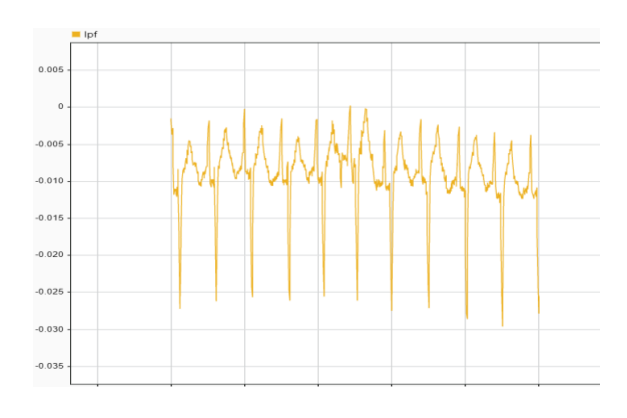


Fig.4 Wavelet Decomposer Block diagram in the MATLAB Simulink

Three LPF's and four HPF's are used in the proposed architecture. With each state of the LPF filter bank process, the spectrum range is reduced by a half; hence the width in the frequency domain is progressively narrowed and the frequency resolution is thus improved at the expense of time resolution. This is due to a down-sampling operation right after each stage of LPF processing. In DWT, a "down-sampling by 2" operation is required and this also preserves the total energy of the signal to be constant. For the down-sampling circuit, here a counter is implemented to generate the control signal that makes the sampling time of each stage reach to a power of 2.

RESULTS



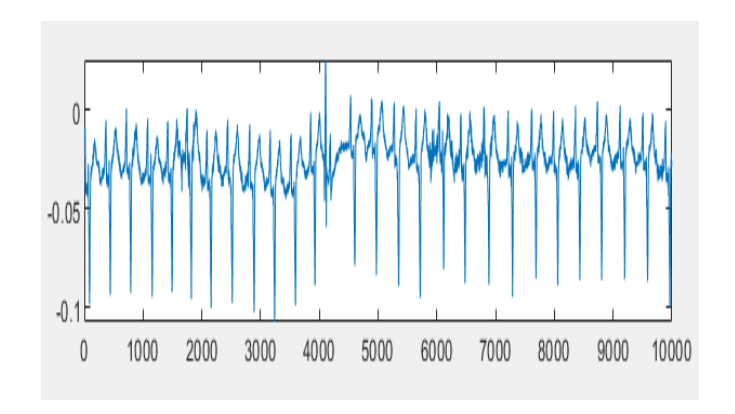
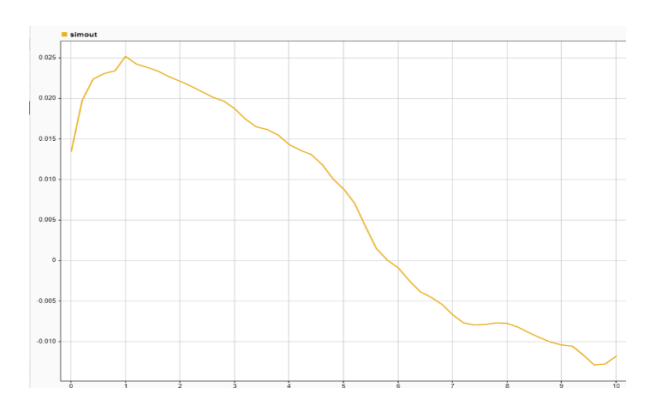
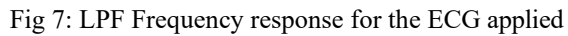


Fig 5: Output of LPF for Input ECG from MIT-BIH Database 108

Fig 6: Input ECG





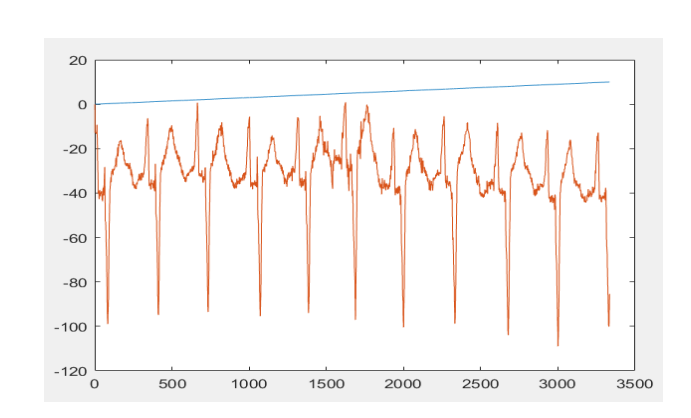


Fig 8 D1

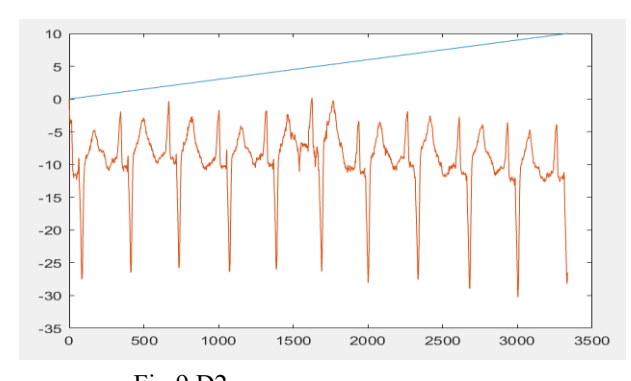


Fig 9 D2

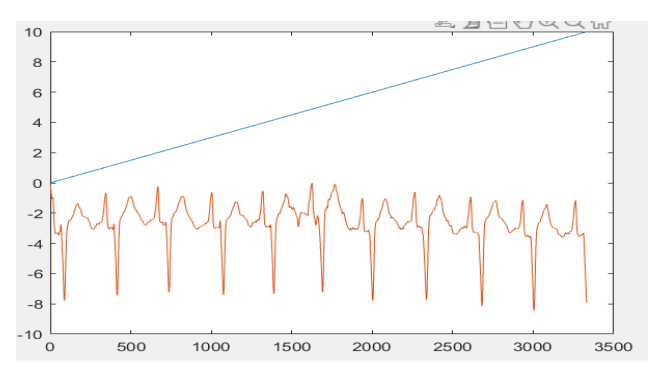


Fig 10 D3

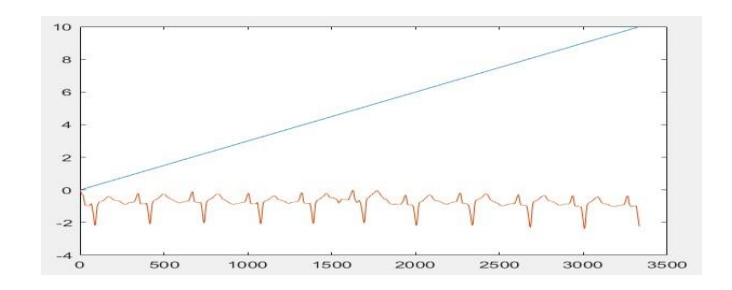


Fig 11 D3

CONCLUSION

The low pass filter, high pass filter, and wavelet decomposer by applying the ECG from MIT-BIH 108 dataset and verified the results for the LPF and the Wavelet Decomposer by using MATLAB software and verified the frequency response and plotted the results for D1,D2,D3,D4 . However, we still have two modules remaining, which are signal multiplication and noise detection.

DEVELOPMENT OF LORAWAN BASED WATERQUALITY SYSTEM

K. Prasad, K.S. Sai Kiran, M. Venkatesh Babu

Introduction:

As human activities intensify and environmental challenges escalate, the need for effective water quality monitoring systems becomes increasingly-evident. The quality of water directly impacts public health, agricultural productivity, industrial processes, and the overall well-being of ecosystems. Therefore, ensuring reliable and efficient monitoring of water quality has emerged as a crucial priority for water management authorities and regulatory bodies.

Traditional water quality monitoring methods often suffer from limitations such as high costs, time-consuming data collection, and restricted coverage. As a response to these challenges, advancements in communication technologies have paved the way for more sophisticated and cost-effective monitoring systems. In recent years, the emergence of Low Power Wide Area Network (LPWAN) technologies, such as Long Range Wide Area Network (LoRaWAN), has revolutionized the field of remote data transmission.

A traditional water quality monitoring system utilizes numerous analog sensors to determine water parameters, resulting in higher power consumption. To achieveefficient results, the system must possess the following key features: Broad coverage area for transmitting data from end devices deployed in remote locations. Minimal infrastructure and cost-effective implementation for the proposed system. High data security to safeguard sensitive information. Low power consumption by the system to extend battery life.

Methodology:

Here LoRa shield to transmit the sensor node data to cloud server via LPS8gateway. By using TTN The Things Network we need to create an application for the device and then the end device needs to be registered with the corresponding keydetails. Gateway has to be configured first with the device node.

Step 1: Hardware Setup

Connect the Arduino UNO to the Shield-LoRa-RFM. Now connect the sensors according to their respective pins.

Step 2: Arduino IDE Setup

Install the latest open-source Arduino IDE. Get the MCCI LoRaWAN LMIC library installed. And other required libraries if necessary.

Step 3: The Things Network

Create an account in The Things Network website. And add a new application. Then register the end device manually. AppEUI, DevEUI, and AppKey found in end device registration are used in Arduino sketch.

Step 4: Upload The Code to Arduino. Open Arduino IDE. Write the LoRa code for the transmission of node data to The ThingsNetwork(TTN). Use the USB cable for linking the Arduino board with your PC.Step 5: Testing

Upload the code into the LoRa shield. Login to TTN server and open the application created before. Verify the output the by the node device.

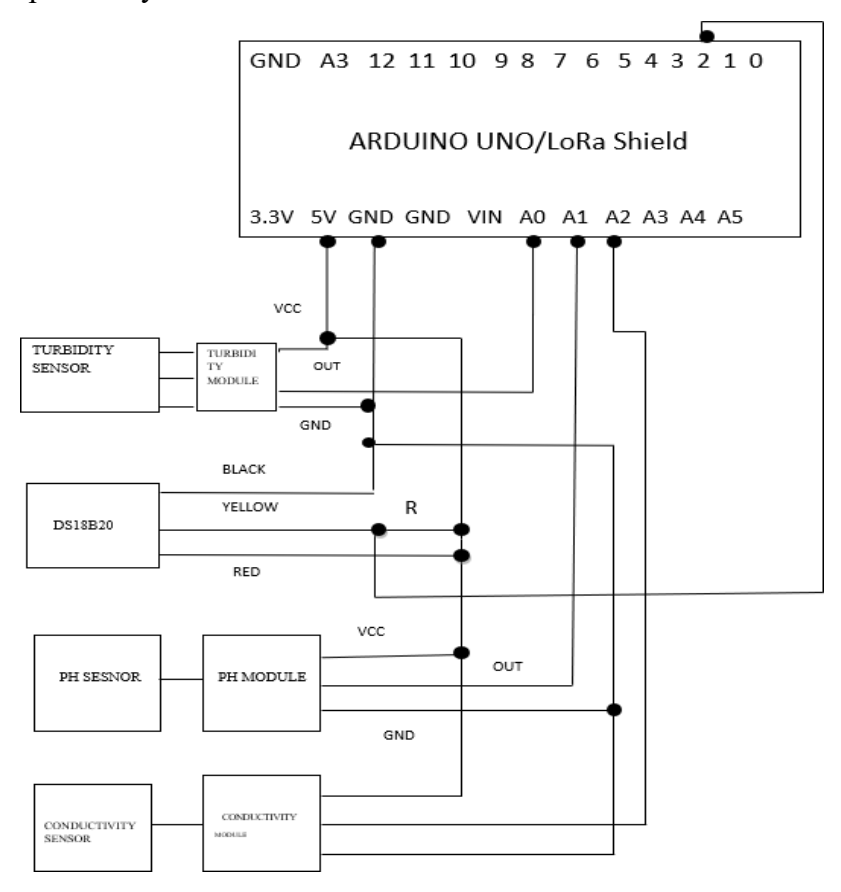


Fig 1: Block Diagram

Flow Chart:

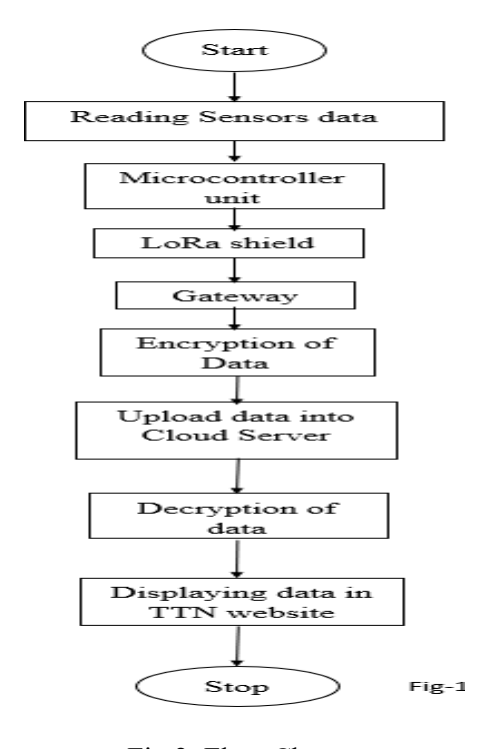


Fig 2: Flow Chart

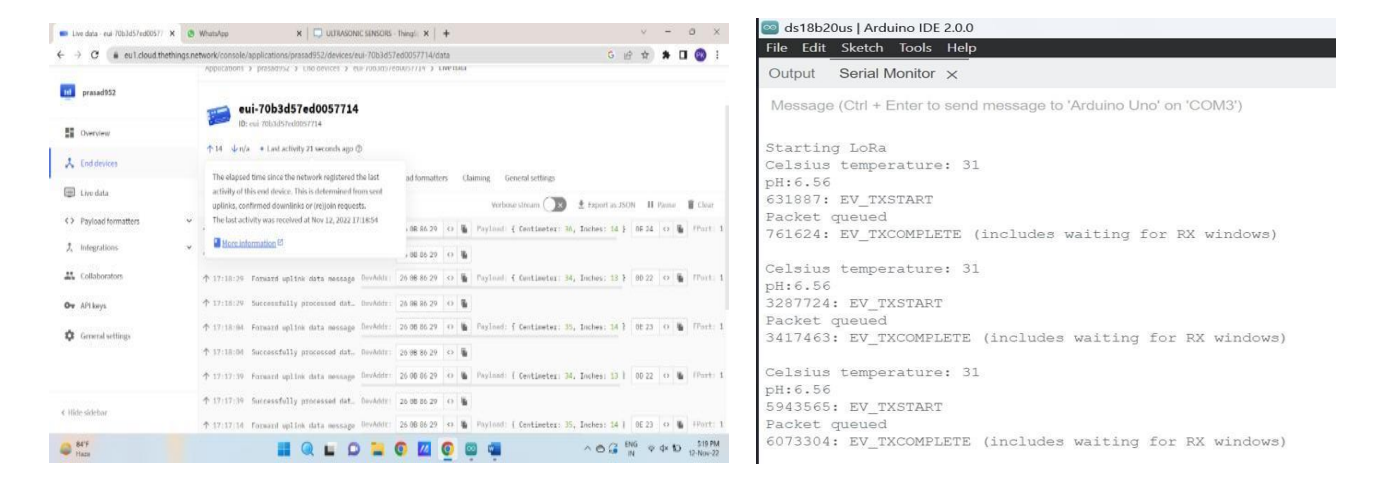


Fig 3: Results

CONCLUSION:

The system utilizes LoRa WAN technology for efficient data transmission a dedicated TTN server. This enables real-time monitoring and analysis of essential water quality parameters like pH, turbidity, TDS, and temperature. By leveraging the capabilities of these cutting-edge solutions, the proposed system offers a robust and scalable approach to continuously monitor water quality parameters in a cost-effective manner. By harnessing the power LoRaWAN and leveraging the TTN server infrastructure, water management authorities and regulatory bodies can access real-time data, enabling prompt detection of anomalies and proactive decision-making to ensure the provision of clean and safe drinking water to communities.

ENHANCING COGNITIVE RADIO NETWORK PERFORMANCE THROUGH CHANNEL SELECTIONALGORITHM

S. Alekhya, Sk. Nausheen, Ch. Swapna

Introduction:

Cognitive Radio (CR) is an adaptive, intelligent radio and network technology that can automatically detect available channels in a wireless spectrum and change transmission parameters enabling more communications to run concurrently and also improve radio operating behavior. In which a transceiver can intelligently detect which communication channels are in use and which are not, and instantly move into vacant channels while avoiding occupied ones. This optimizes the use of available radio-frequency (RF) spectrum while minimizing interference to other users. In its most basic form, CR is a hybrid technology involving software defined radio (SDR) as applied to spread spectrum communications.

Possible functions of cognitive radio include the ability of a transceiver to determine its geographic location, identify and authorize its user, encrypt or decrypt signals, sense neighboring wireless devices inoperation, and adjust output power and modulation characteristics. There are two main types of cognitiveradio, full cognitive radio and spectrum sensing cognitive radio. Full cognitive radio takes into account all parameters that a wireless node or network can be aware of. Spectrum-sensing cognitive radio is used to detect channels in the radio frequency spectrum.

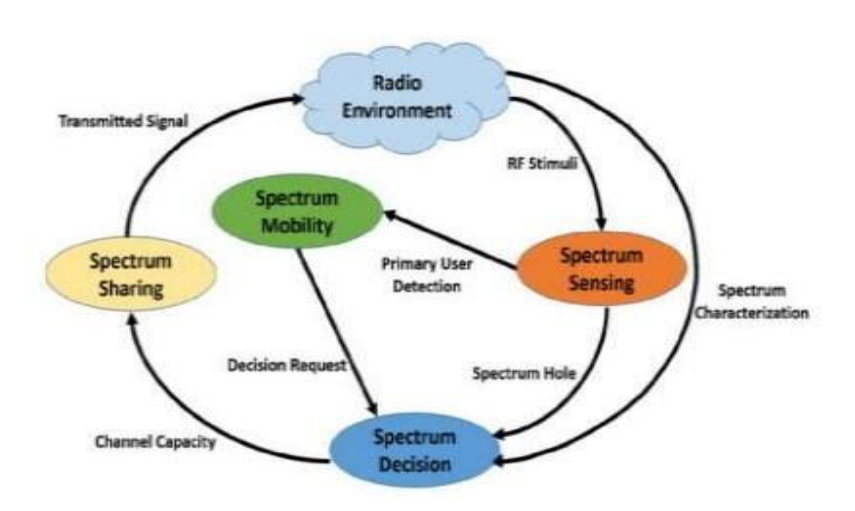


Fig.1 Cognitive cycle

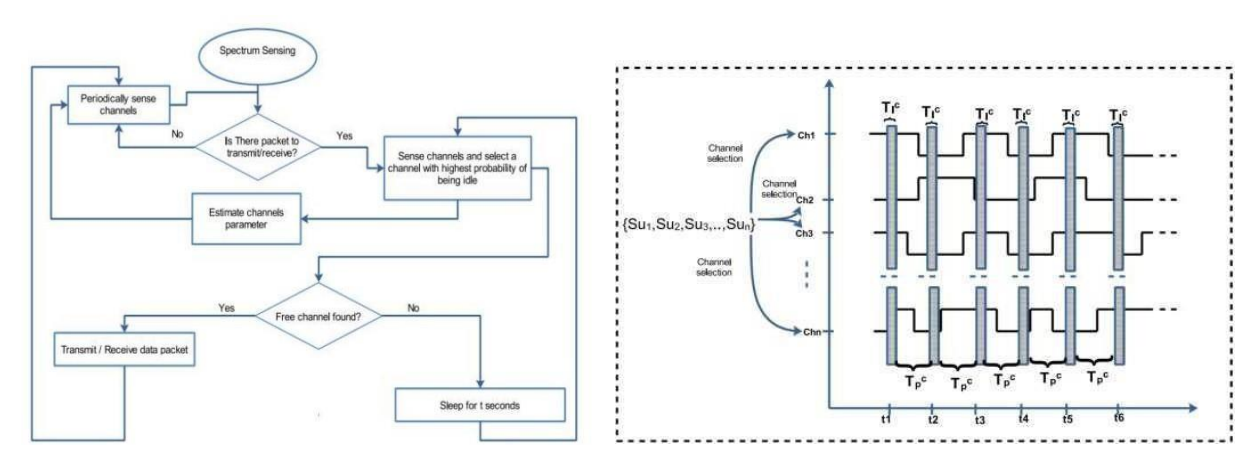


Fig. 2 Sensing strategy flow diagram selection

Fig. 3 Graphical representation of SU channel

The Fig shows a level of complexity at which data is aggregated can influence the OR rule requires a simple aggregation technique which allows faster data aggregation and higher detection with lower accuracy. A major drawback of this rule is that, an increase in probability of detection leads to an increase in the probability of detection. In contrary, AND rule decreases the probability of detection with the decrease in probability of false alarm. Although results obtained using this rule are accurate and reliable, the chances of detecting PU signal are very low. In N-out-M aggregation rule, N can be chosen in such a way that the probability of detection remains in an acceptable level. In such cases, the detection would bevery accurate. The manner in which data is aggregated using AND, and OR rule, introduces delays due torobustness in data aggregation.

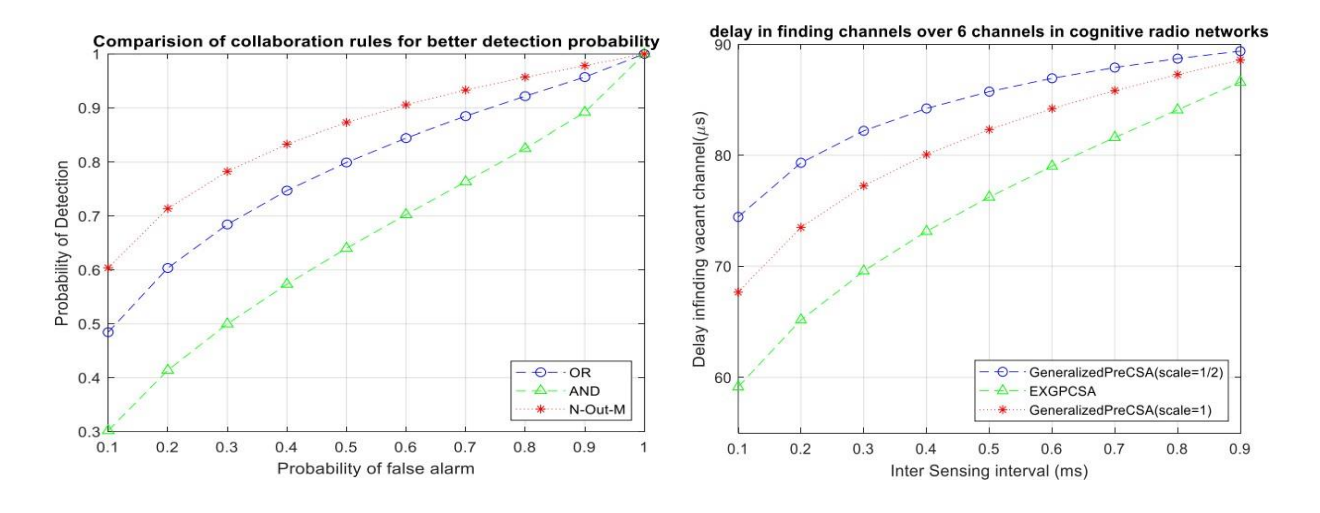
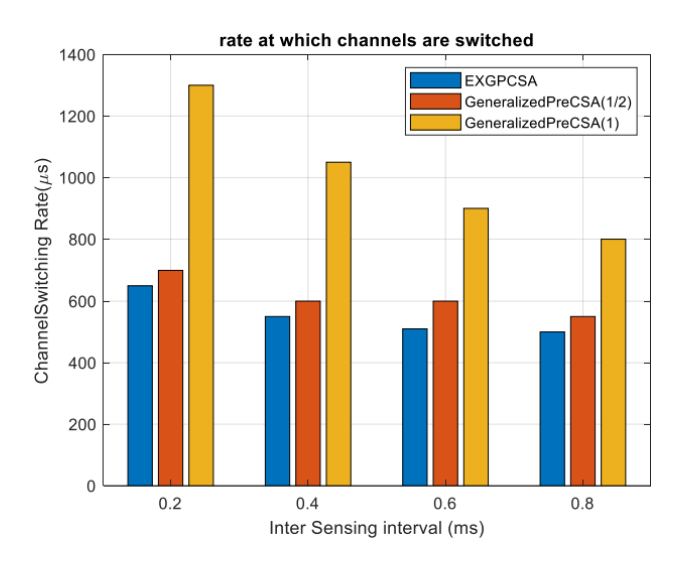


Fig. 4 Probability of Detection

Fig. 5 Delay in finding idle channels

The Fig shows the ordering and selection of channels influences the transmission rate of data. EXGPCSA allows multiple channels to be sensed simultaneously while ordering them in the descending order of their idling probabilities. This greatly reduces delays in available channels for data transmission. As it can be noticed, delays in finding the available channels increases with the increase in inter-sensing interval. If achannel is being sensed for longer periods, delays increase

which compromises the throughput. The Fig shows the rate at which nodes switch between channels when inter-sensing intervals are increased. SUs switch from one channel to the other searching for free channels for transmission. It is desirable to have few channel searches before finding the next available channel to reduce searching delays. Channelswitching rate remains higher when intersensing interval is small. This is due to the fact that sensing is performed within a very short period of time and this causes high overheads and more channel switches.



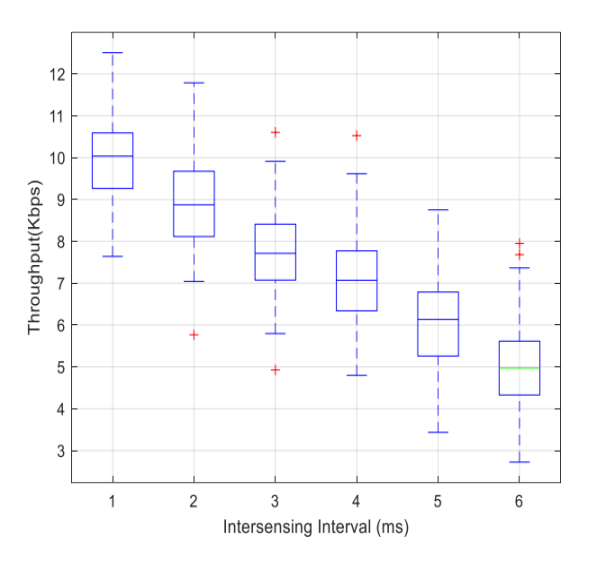


Fig. 6 Channel switching rate

Fig. 7 Throughput of SU in GPCSA

The Fig shows the throughput generated by SUs when EXGPCSA was simulated in the range while the throughput of the Generalizes Pre CSA was in the range. Considering, average throughput from these ranges, we observed that EXGPCSA has higher throughput when intersensing interval. The same trend was observed. It can also be observed that EXGPCSA outperformed generalized predictive CSA scenario. The results show that 25% of SUs in EXGPCSA recorded achievable throughput. It was in this sensing interval scenario that all the schemes had the highest achievable throughput. The throughputs generally dropped as the intersensing intervals were increased. There may be many causes of this but one of them is delay in sensing. Increasing sensing interval causes delays in data transmission and in many cases may lead to spectrum under-utilization due missed opportunities. These factors have degraded achievable throughput as depicted.

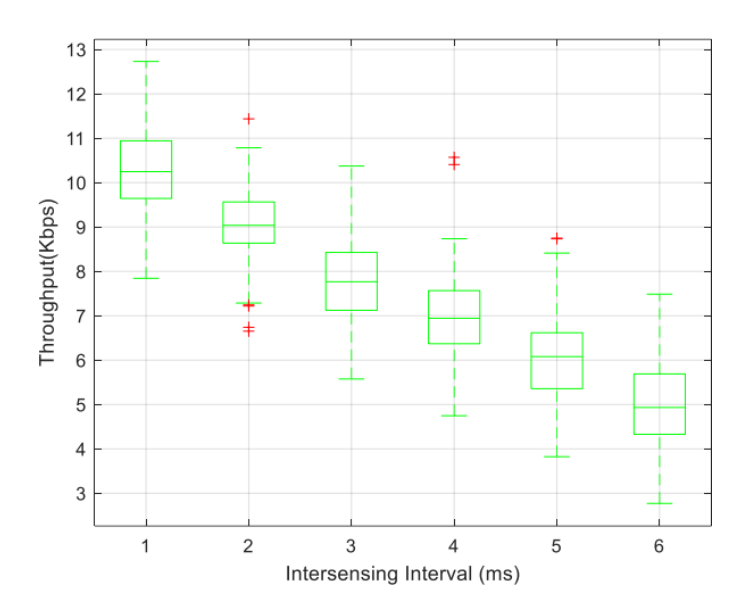


Fig. 8 Throughput of SU in EXGPCSA

A robust approach was taken in designing and implementing EXGPCSA in which the collaborative sensing, parallel sensing, and data aggregation rules were considered. This approach is very complex in nature and required necessary techniques to achieve better performance. Hence, a channel selection technique and sensing strategies were employed to intelligently enable SUs to adapt to their environment. EXGPCSA consistently achieved better results compared to the generalized predictive CSA. We can therefore, conclude that EXGPCSA significantly outperformed the generalized predictive CSA.

MODIFIED KARATSUBA APPROXIMATE MULTIPLIERFOR ERROR-RESILIENT APPLICATIONS

P.Hareesha, T.Dheeraj

Introduction:

In many computational tasks, multiplication plays a fundamental role, and its accuracy is of utmost importance. However, in certain applications where high precision is not to critical, trading off accuracy for improved performance and reducedenergy consumption becomes an attractive proposition. This has led to the emergence of approximate computing techniques that aim to strike a balance between accuracy and efficiency. Numerous applications of arithmetic operations include recognition, machine learning, data mining, and multimedia processing. In signal processing applications, in particular, they might induce computational mistakes.

In order to minimize these errors, it is vital for electronic systems to reduce energy usage. A number of methods exist at various levels to reduce power or energy usage, but approximation computing is the most desired strategy. The introduction of approximations and the analysis of their outcomes must be done with caution. In contrast to conventional multipliers, an approximate multiplier is a digital circuit that performs multiplication with a specific amount of error tolerance. This allows for greater speed or lower power consumption. An approximation multiplier can be useful in the context of error-resilient applications since it can accept faults in the multiplication process without adversely compromising system performance as a whole. The most popular technique among these various ones is approximation computing.

Considering error-resilient apps, in which the applications have less power consumption, to make the point clearer. The profusion of the input data, iterative calculations, and the absence of a single perfect output are the causes of the mistake resilience. So, to effectively develop error-tolerantapplications in approximate designs, contemporary methodologies are used. Theperformance of AMs for image processing applications is great, however by prolonging the AMs, accuracy was compromised for reducing the area, power consumption, or latency. The Karatsuba algorithm is a well-known technique for multiplying large numbers efficiently. It utilizes a divide-and-conquer approach to break down the multiplication process into smaller, more manageable operations.

By exploiting this algorithm's characteristics, we can modify it to create an approximate multiplier that provides faster computation and lower energy consumption while allowing controlled levels of accuracy loss. The modified Karatsuba algorithm for approximate multiplication leverages the inherent redundancy in multiplication operations and introduces approximations at strategic points within the algorithm. By relaxing certain computations or employing simplified approximations, we can considerably reduce the number of

arithmetic operations required and thus achieve energy savings.

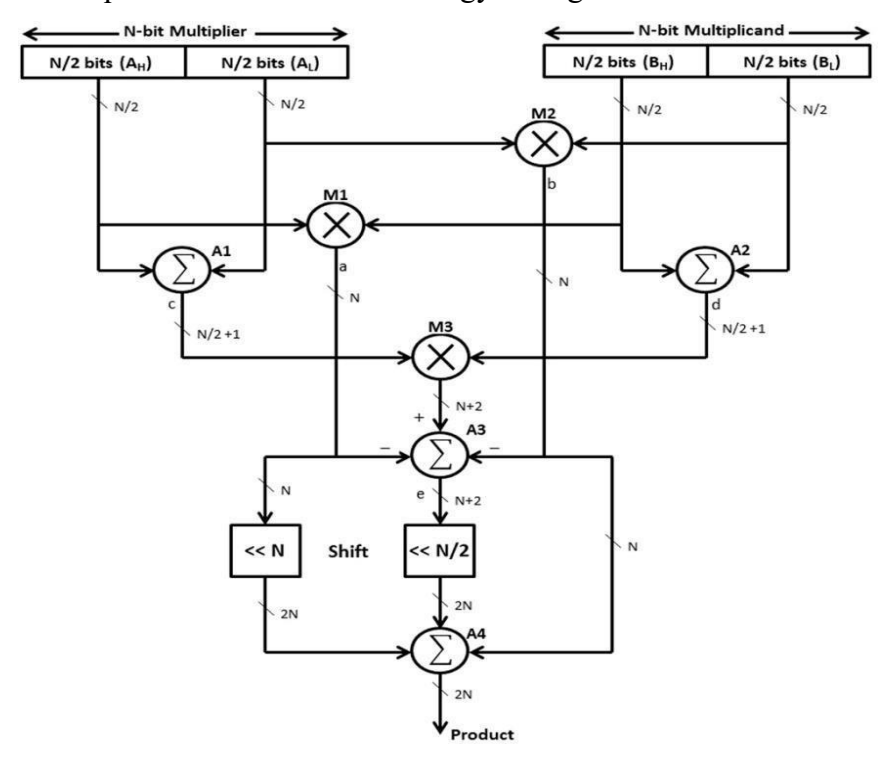


Fig 1: Karatsuba Multiplication Algorithm

However, it's important to carefully designand analyze the trade-off between accuracy and computational efficiency to ensure that the introduced errors remain within acceptable limits for the given application. Approximate multiplier using the modified Karatsuba algorithm. Through experimental evaluations and comparisons with conventional multiplication methods, we expect to highlight thebenefits and limitations of our proposed approach and provide insights into the potential applications where approximate multipliers can be employed effectively. A careful balance must be struck between the degree of approximation, the need for error resilience, and the required system performance when designing an approximate multiplier for error resilient applications.

Approximate computing is a technique where computations are performed with a certain level of imprecision or approximation, sacrificing accuracy for gains in efficiency, performance, or energy consumption. The four broad classes of applications suitable for approximate computing are: Applications that use chaotic real-world data for analog inputs. Applications designed for human perception and using analog output. Applications include online search and machine learning that lack a singular solution. Applications that iteratively process vast volumes of data and the equality of results depends on the number of iterations are known as convergent and iterative applications.

Image sharpening is a common technique used in image processing to enhance the details and edges in an image. One way to achieve image sharpening is byusing different multipliers or filters to emphasize high-frequency components and enhance edges. There are several types of filters that can be used as multipliers for image sharpening. Unsharp Masking is a popular image sharpening technique that involves subtracting a blurred version of the image from the original image. The blur operation acts as a low-pass

filter, and subtracting it from the original image emphasizes the high-frequency components, such as edges and details. The resulting image is then added back to the original image to enhance sharpness.

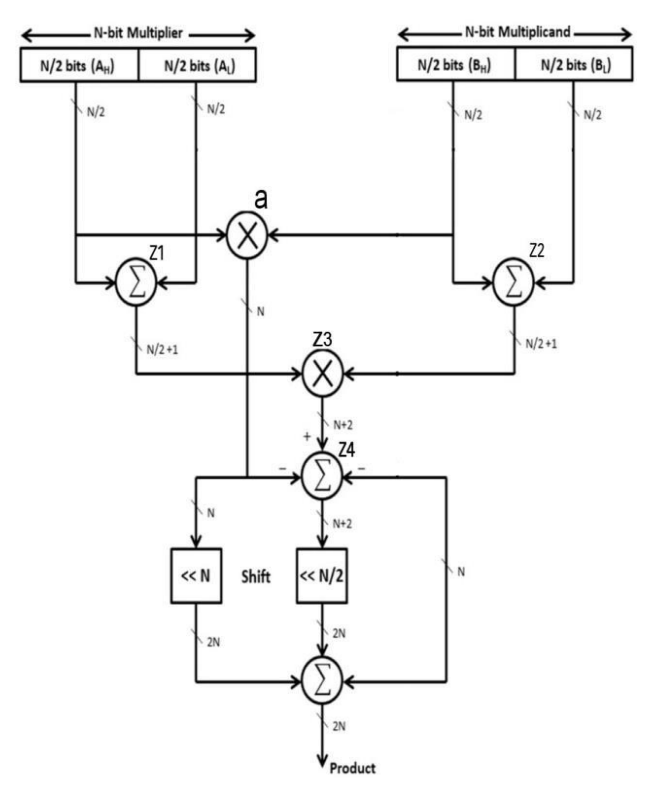


Fig 2 Hybrid OR based Approximate Multiplier Algorithm

A high-pass filter allows high-frequency component pass while attenuating low-frequency components. By using a high-pass filter as a multiplier, you can accentuate the edges and details in an image. Different multipliers and filters can produce varying degrees of sharpness and may have specific strengths and weaknesses depending on the image content and the desired outcome. Each pixel value is commonly represented using 8 bits when doing image multiplication on 8x8-bit pictures, allowing for a range of values from 0 to 255. The relevant pixels in the input pictures are multiplied together generate a new output image during the per-pixel multiplication procedure.

Column 7	Column 6	Column 5	Column 4	Column 3	Column 2	Column 1	Column 0
Stage 1	X ₃ Y ₃ Column 6	X ₃ Y ₂ X ₂ Y ₃ Column 5	X ₃ Y ₁ X ₂ Y ₂ X ₁ Y ₃ Column 4	$\begin{bmatrix} X_3Y_0 \\ X_2Y_1 \\ X_1Y_2 \end{bmatrix}$ X_0Y_3 Column 3	X ₂ Y ₀ X ₁ Y ₁ X ₀ Y ₂ Column 2	$\begin{bmatrix} X_1Y_0 \\ X_0Y_1 \end{bmatrix}$ Column 1	X ₀ Y ₀ Column 0
	X ₃ Y ₃	X ₃ Y ₂ X ₂ Y ₃	X ₃ Y ₁ — X ₂ Y ₂ — X ₁ Y ₃	X ₃ Y ₀ X ₂ Y ₁ X ₁ Y ₂ X ₀ Y ₃	X ₂ Y ₀ X ₁ Y ₁ X ₀ Y ₂	X ₁ Y ₀	X ₀ Y ₀
Y[7]	Y[6]	Y[5]	Y[4]	Y[3]	Y[2]	Y[1]	Y[0]

Fig.3. Proposed AM Architecture

Our investigation focused on image multiplication, which involves multiplication of two pictures pixel by pixel. The purpose was to analyze the characteristics of approximation multipliers in real-world image processing. By employing a designed multiplier, we obtained the product and scaled it down to an 8-bit grayscale result. In Figure, image (x) represents the input image1, which is the cameraman image, while image (y) represents the input image2, which is the ruler image. We perform the multiplication of images (x) and (y)to obtain image (z), which is the resultant image. The multiplication process utilizes the multiplier with the proposed OR based approximate multiplier. It's worth noting that both input images are 8-bit images.

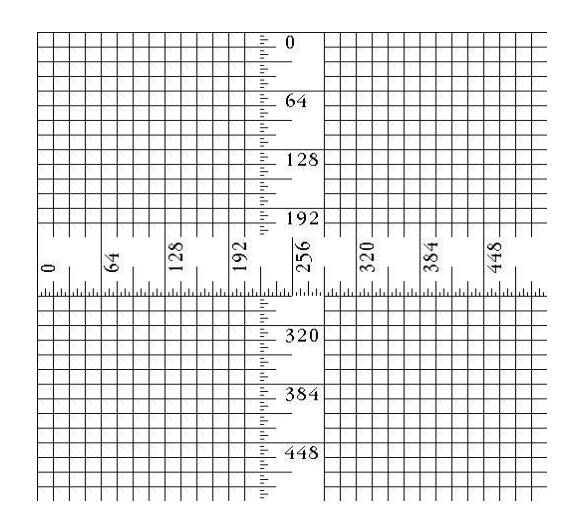


Fig.4 (y) "ruler" input image-2



Fig.5. (x) "cameraman" input image-1



Fig. 5.3. (z) Image Multiplication output using multiplier

suggested AM exhibits remarkable accuracy when compared to current AMs. Additionally, it demonstrates efficiency in terms of power, area, and latency compared to previous AMs. The estimated reductions in area, delay, and power are 78.83%, 33.75%, and 46.15%, respectively, in comparison to preceding AMs. One notable advantage of the suggested architectural AM is its ability to incorporate real-time components. This feature enhances its versatility and applicability in 12 various domains. The field of AM, as a whole, is a multidisciplinary discipline that is currently experiencing significant growth and holds tremendous potential. However, it is crucial to approach the introduction of approximations and the analysis of their outcomes with caution. Extensive study and research are necessary before AM can be considered a mainstream design paradigm. Specifically, areas that require further investigation include quality (error) analysis and computation, automated approximation approaches, and scalable solutions for complex systems. Toestablish AM as a widely accepted design paradigm, it is important to address these research areas and develop comprehensive solutions. By doing so, we can unlock the full potential of AM and leverage its benefits across diverse fields and applications.

DETERMINATION OF CROP HEALTH & TREATMENT

Jaxa Hruday Pemula , Anakapalli bharath venkata siva kiran

Introduction:

Utilizing technology in modern agriculture to improve crop health and reduce environmental impact is an ongoing goal. In-order to revolutionize plant health management, this project offers a system that combines hardware and sophisticated image processing methods. This sophisticated system, which makes use of a Raspberry Pi, a camera, and two motors, intends to change farming practices. It offers a unique method of pesticide spraying by concentrating on the examination of leaf health through color classification, guaranteeing accuracy and efficiency.

In the past, farmers have depended on eye inspection to spot damaged leaves, which has resulted in widespread pesticide use, frequent overapplication, and negative environmental effects. The Raspberry Pi, which has image processing algorithms, is used in this project to analyze video in real-time. The technology accurately distinguishes between healthy and unhealthy leaves by obtaining crucial information about leaf health based on color features.

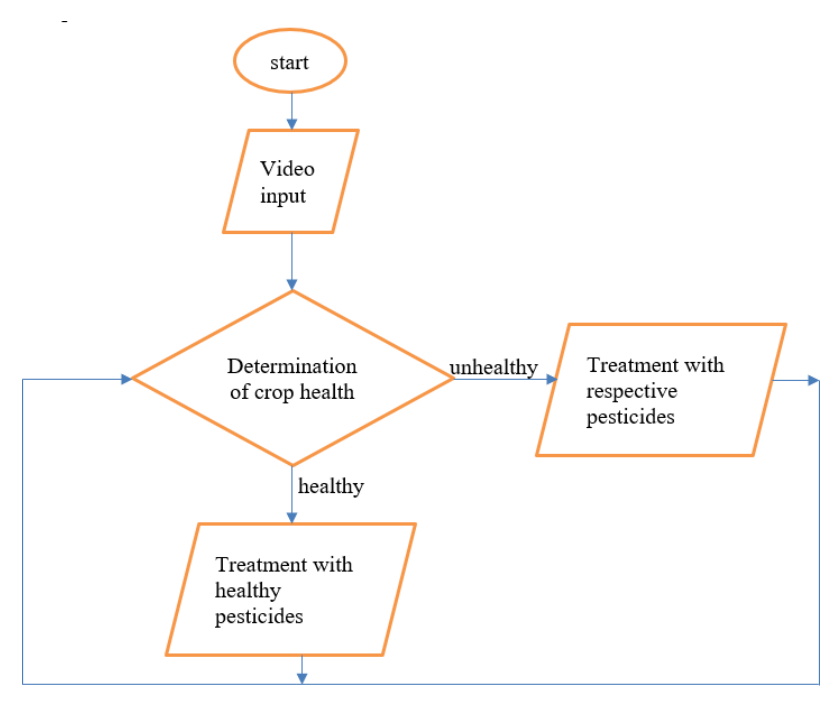


Fig-1: Flow chart

The integration of motorized pesticide spraying devices is what makes this concept innovative. These motors are connected to certain pesticide dispensers and are placed appropriately. The device recognizes a healthy leaf and turns on the associated motor, which releases pesticide. On the other hand, when an unhealthy leaf is found, the system activates the other motor, turning on pesticide for unhealthy leaves. This focused strategy guarantees careful usage of pesticides, optimizing their use and reducing their environmental impact.

It's important to note that this project is highly complex and may require advanced hardware, image processing algorithms, motor control, and automation skills. The accuracy of color analysis, precise

motor control, and the choice of pesticides are critical factors to consider when developing such a system. Additionally, safety measures should be in place to ensure the responsible use of pesticides and to minimize environmental impact.

```
import cv2
    import numpy as np
    class VideoStream:
        def __init__(self,resolution=(640,480),framerate=30):
            self.stream = cv2.VideoCapture(0)
            ret = self.stream.set(cv2.CAP PROP FOURCC, cv2.VideoWriter fourcc(*'MJPG'))
            (self.grabbed, self.frame) = self.stream.read()
8
            for i in range(len(scores)):
9
            if ((scores[i] > min conf threshold) and (scores[i] <= 1.0)):</pre>
10
                image using max() and min()
                ymin = int(max(1,(boxes[i][0] * imH)))
                xmin = int(max(1,(boxes[i][1] * imW)))
                ymax = int(min(imH,(boxes[i][2] * imH)))
14
15
16
                xmax = int(min(imW,(boxes[i][3] * imW)))
                cv2.rectangle(frame, (xmin,ymin), (xmax,ymax), (10, 255, 0), 2)
                object_name = labels[int(classes[i])]
                label = '%s: %d%%' % (object name, int(scores[i]*100)) # Example: 'person: 72%'
                labelSize, baseLine = cv2.getTextSize(label, cv2.FONT_HERSHEY_SIMPLEX, 0.7, 2) # Get font size
20
                label ymin = max(ymin, labelSize[1] + 10) # Make sure not to draw label too close to top of window
```

Fig-2: Code for cam and leaf health identification



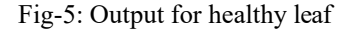




Fig-6: Output for unhealthy leaf

The project is an example of innovation practice in agriculture, where effectiveness, accuracy, and environmental awareness are essential. This comprehensive system makes plant health management by utilizing the capabilities of the Raspberry Pi, image processing algorithms, and motors.

A key component of the system that demonstrates the power of technology in agriculture is real-time leaf health analysis. It gives farmers rapid and accurate information about plant health by properly identifying between healthy and diseased leaves based on their color and its characteristics.

This project's role in cost reduction cannot be understated, as it optimizes resource allocation, enhancing farmers' profitability while fostering economic sustainability. Its adaptability and scalability make it accessible to a diverse range of farming operations, from small family farms to large commercial enterprises, and across various crops and geographies. Beyond technological advancements, it represents a combination of IOT and deep learning, setting the stage for broader

innovations in both fields. In summary, the Crop Health Treatment System can be used to change agriculture into a future where technology and sustainability go hand in hand to increase the yield and decrease the health hazards of farmers.

VEHICLE POLLUTION MONITORING SYSTEM USING IOT

K. S. Shanti Priya, N. V Sai Teja, G. Roshan Chowdary

Introduction:

Air pollution poses a significant threat not only to the environment but also to all living organisms on our planet. An alarming 75% of total carbon monoxide emissions can be attributed to automobiles. In urban areas, these emissions contribute substantially, accounting for 50-90% of the overall air pollution burden. While it is virtually impossible to eliminate emissions entirely, their monitoring and control can be effectively managed through the implementation of a pollution detection system.

Governments have established standard emission levels in accordance with Bharat Stage norms. Unfortunately, due to inadequate vehicle maintenance, emission levels often surpass these norms. This necessitates a mechanism for informing vehicle owners about the harmful pollution levels emanating from their vehicles. If no corrective action is taken by the vehicle owner, the system can escalate this information, coupled with the vehicle's location, to the relevant pollution regulatory authority. Such data can prove invaluable in identifying and curbing pollution sources within a given area, empowering authorities to take necessary actions against vehicle owners to mitigate pollution. This process operates in real-time, with the ability to provide immediate, granular data on polluting vehicles to the pollution regulatory body. The entire orchestration of this system is efficiently managed and controlled through the utilization of a microcontroller, ensuring a seamless and effective response to environmental concerns. The innovative approach outlined in this proposal harnesses an embedded system to overcome the limitations inherent in conventional air quality monitoring methods. This forward-thinking solution involves the integration of several key components to facilitate comprehensive air quality assessment.

By interfacing an Arduino microcontroller with a PMS7003 sensor for PM2.5 dust particle measurement and an MQ-7 sensor for carbon monoxide detection, this system delivers robust air quality insights. Notably, the incorporation of a NodeMCU enables seamless data transmission to a web server, affording users remote access to real-time air quality information. This not only enhances data accessibility but also enables users to monitor air quality through web-based platforms.

The advantages of this proposed method are manifold. The system employs a buzzer and an LCD display, ensuring immediate feedback and visual cues to alert users when air quality thresholds are breached. This feature is instrumental in cultivating heightened awareness and encouraging swift

actions to safeguard public health.

In stark contrast to traditional methods, the embedded system's adaptability shines through, as it can be deployed in diverse environments, offering a broader coverage area for comprehensive air quality monitoring. Furthermore, its low maintenance requirements and ease of calibration render it suitable for extended, long-term deployment.

In summation, the proposed embedded system represents a user-centric, efficient, and cost-effective solution for air quality monitoring. The figures 3.2.1 and 3.2.2 represents the Block diagram and circuit diagram of the Vehicle Pollution Monitoring System.

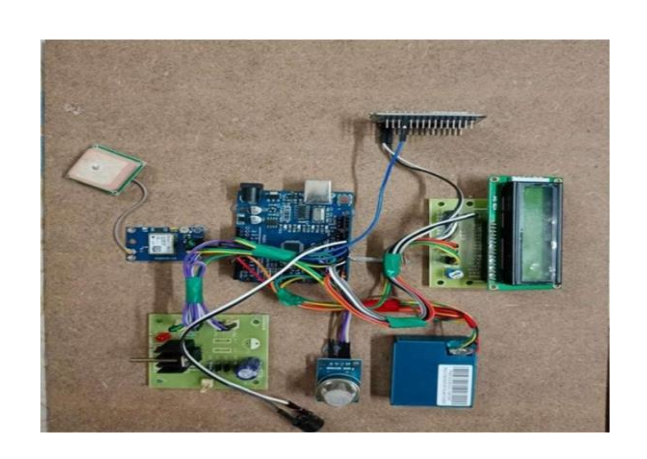


Fig :2 Circuit Diagram

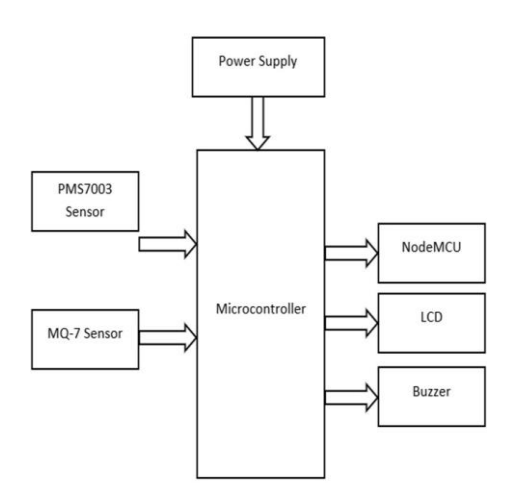


Fig :2 Block Diagram

The model underwent initial testing under controlled room temperatures before being subjected to real-world conditions, specifically exposure to vehicular emissions. Leveraging the Thingspeak, Internet of Things (IoT) platform and implementing code modifications, the threshold values were adjusted during room temperature assessments. During real-time testing, the threshold values are calibrated in adherence to Bharat stage norms, ensuring a comprehensive evaluation reflective of environmental standards. Situated proximate to the exhaust terminus(as shown in Fig), the circuit diligently monitors Carbon Monoxide and particulate matter levels, employing a five-second delay between each data acquisition iteration. This meticulous approach underscores the precision and reliability of the monitoring system in capturing dynamic pollutant concentrations.



Fig 3. Testing the model by placing it near the exhaust terminal

As delineated in the methodology section, the monitoring protocol incorporates a proactive alert mechanism. Upon surpassing the predefined threshold values for pollutants, an automated notification will be promptly dispatched to the vehicle owner. This notification serves to apprise the owner of the detected issue, thereby facilitating timely and informed interventions to address and rectify the observed environmental concerns.

This responsive alert system enhances the overall efficacy and impact of the pollution monitoring framework. The dispatched message is shown in Fig 4.

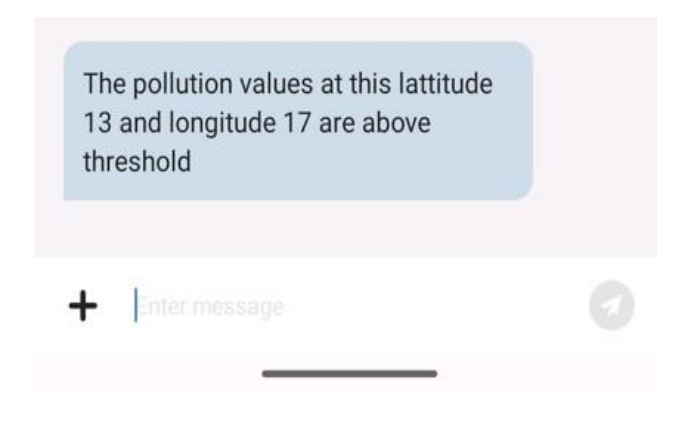
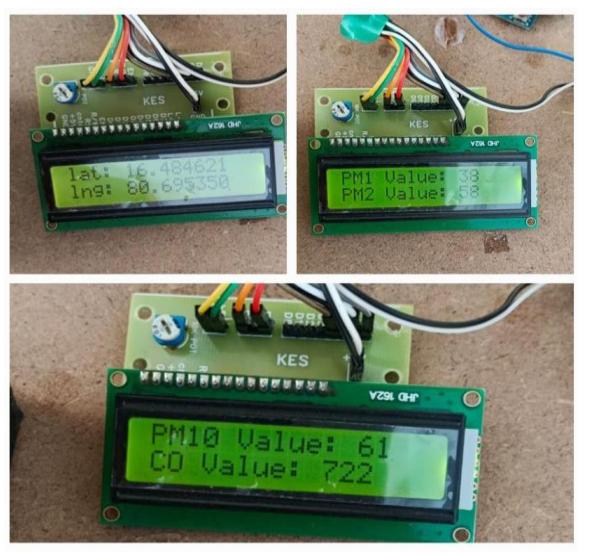


Fig 4. The dispatched message



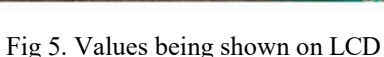






Fig6. LCD when the values cross threshold value

Furthermore, in alignment with our earlier discussions, the circuit is equipped with an instantaneous alert mechanism in the form of an audible buzzer. Upon detection of pollutant levels exceeding the predetermined thresholds, the buzzer is activated, emitting a distinct alert signal lasting for a duration of five seconds. This immediate auditory notification serves as an additional layer of responsiveness, ensuring that the vehicle owner is promptly informed of the environmental anomaly. The integration of this alert feature reinforces the system's capacity for real-time, on-site notification, enhancing its utility in facilitating swift and effective responses to emerging pollution concerns. The circuit also display the values of Carbon Monoxide, Particulate matter and the location with the help of LCD as shown in Fig 5.

After presenting the pollutant values, if any measurement exceeds the designated threshold, the system will activate an audible alert via the buzzer. Simultaneously, the LCD screen will prominently indicate that the recorded values have surpassed the acceptable limits, signaling a potential environmental concern. The indication is as in Fig 6. Moreover, the model provides the capability to monitor and analyze the temporal trends of the detected pollutants. Leveraging the robust features of the Thingspeak platform, users can access comprehensive graphical representations and data trends, offering a nuanced understanding of the pollutant dynamics over time. This functionality contributes to a holistic assessment of environmental conditions, enabling stakeholders to discern patterns, identify potential sources of concern, and formulate informed strategies for pollution mitigation.

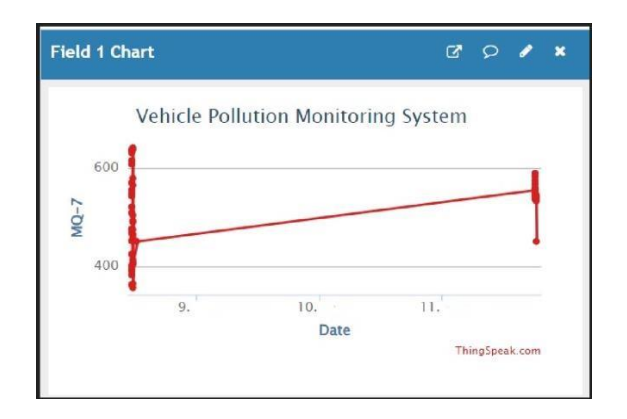


Fig 7. The graph of MQ 7 sensor particle

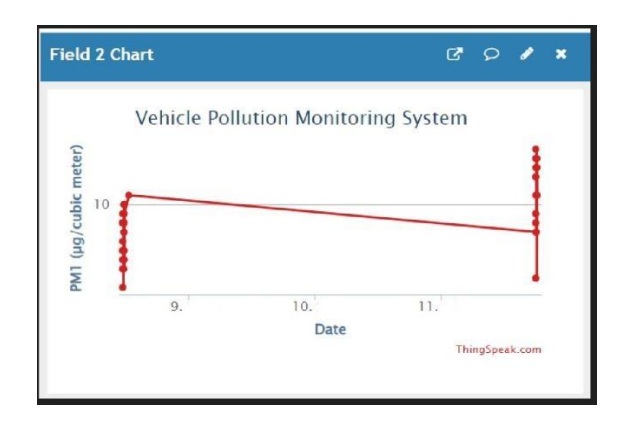
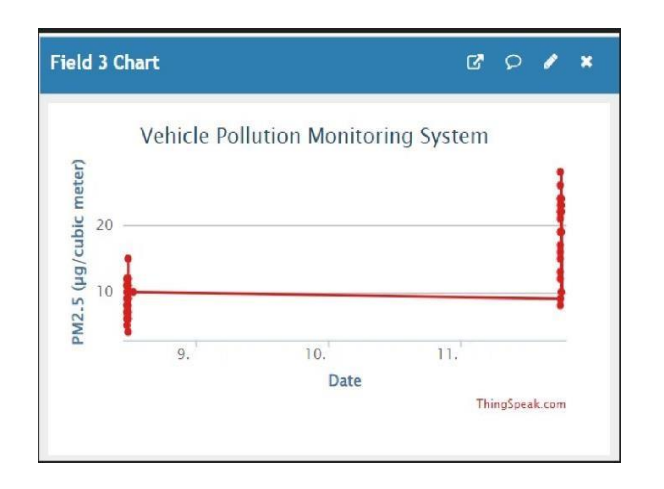


Fig 8. The graph of PM 1



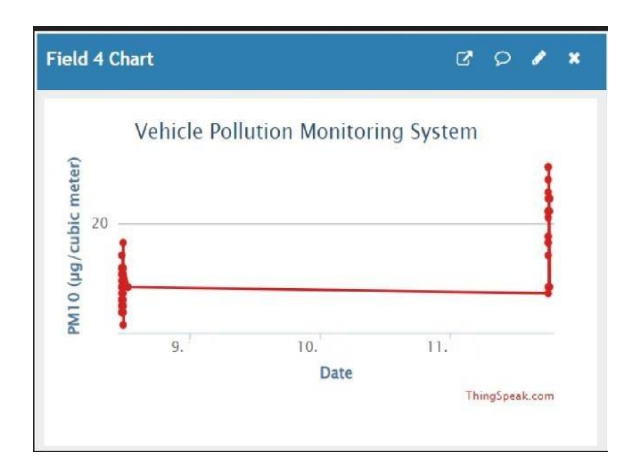


Fig 9. The graph of PM 2.5 particle

Fig 10. The graph of PM 10 particle

DETECTION OF MARINE PLASTIC WASTE USING MACHINE LEARNING

Haarathi Padamati, P. B. Naveena , P. Hema Nandini

Introduction:

Plastic pollution is a pressing environmental concern that poses a significant threat to aquatic ecosystems. Plastics, due to their durability and low biodegradability, can persist in water bodies for many years, causing harm to marine life and disrupting the balance of aquatic ecosystems. To address this issue, there is a growing need for efficient methods to detect and monitor plastic debrison the water surface. Detecting plastics on water surfaces is a crucial step in understanding the extent of the problem, implementing effective mitigation measures, and protecting our oceans and water bodies. Detecting plastic on water surfaces using machine learning is a promising approach that combines technology and artificial intelligence to address the issue of plastic pollution in aquatic environments. Machine learning models can be trained to automatically identify and classify plastic debris from various sources, including satellite or drone imagery. Plastic pollution is a global environmental challenge that affects both freshwater and marine ecosystems. Plastics, ranging from microplastics to larger debris, can harm aquatic life, leach harmful chemicals, and create unsightly and hazardous conditions in our water bodies.

Importance of Detection: Detecting plastics on the water surface is essential for several reasons: Assessment: It allows scientists and researchers to assess the extent and distribution of plastic pollution in different water bodies. Mitigation: Effective detection informs the development of mitigation strategies to remove and prevent plastic pollution.

Environmental Impact: Understanding plastic presence helps evaluate the environmental impact and potential threats to aquatic ecosystems. Introduction to Plastic Detection on Water Surface:

Plastic pollution is a pressing environmental concern that poses a significant threat to aquatic ecosystems. Plastics, due to their durability and low biodegradability, can persist in water bodies for many years, causing harm to marine life and disrupting the balance of aquatic ecosystems. To address this issue, there is a growing need for efficient methods to detect and monitor plastic debrison the

water surface. Detecting plastics on water surfaces is a crucial step in understanding the extent of the problem, implementing effective mitigation measures, and protecting our oceans and water bodies. Challenges in Detection: Detecting plastics on water surfaces presents challenges due to the vastness of water bodies, the diversity of plastic types, and their buoyant and often fragmented nature.

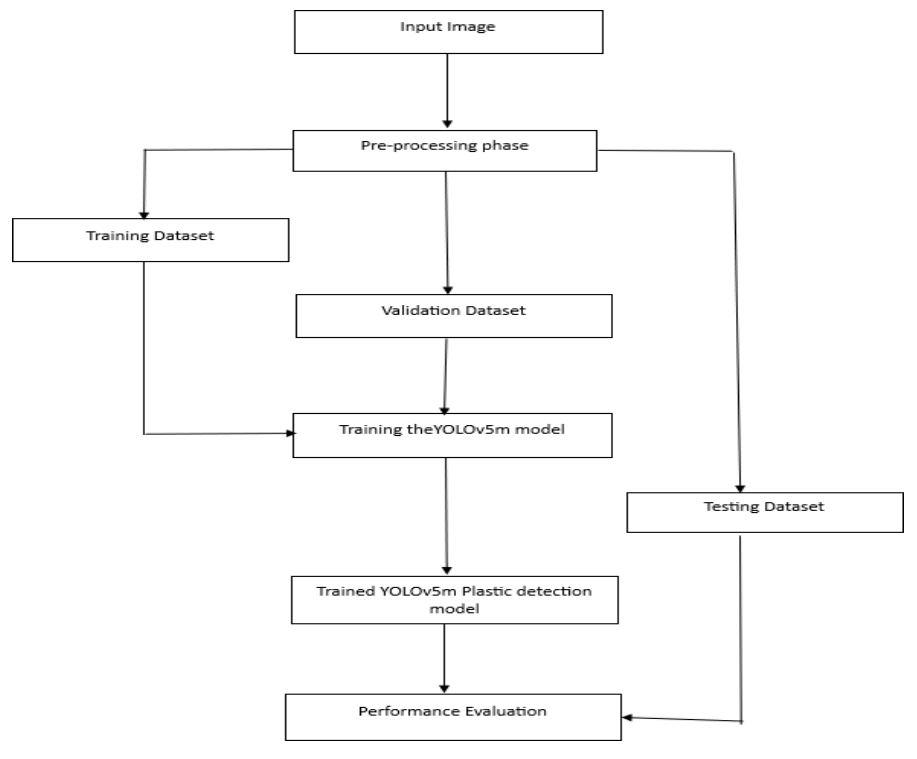


Fig: 1 Block Diagram

Neural Network Performance on the Validation Data Set There is only a small amount of variation in the accuracy between each of the trained models. By increasing the image size from the default 640 pixels to 1280 pixels in Model 2, accuracy was slightly improved, shown by the slight rise in map and F1 score in comparison to Model 1. When using YOLOv5m in Model 3, accuracy remained similar to Model 2 despite the use of a larger and more complex model. Using the full image resolution in Model 4 with the YOLOv5s architecture, accuracy slightly improved compared to Model 2. Despite this slight increase in accuracy, Model 2 was chosen as the final model due to its lower computational requirements, making it more suitable for deployment.

Neural Networks Performance on the Test Data Set The model was 95.23% accurate at detecting the presence or absence of plastics in the test data set and validation data set. However, when differentiating between object types, the model accuracy significantly decreased to 65.3%. The model often either detected the plastic as the incorrect object type or was unable to detect the item, as shown. When differentiating between object types, the model accuracy was significantly lower than the model accuracy from the validation data set. This is likely due to the validation data set containing frames from the same videos that were used in the training data set; however, the test data are a separate entity. The test data set represents real-world footage, which contains a large amount

of variation in the environment and in the items, making the objects more difficult to detect.



Fig 2. Input image of plastic in the water



Fig 3. Detected image



Fig 4. Underwater Input Image



Fig 5. Percentage of plastic detected image

MRI-CT FUSION USING PHASE CONGIRACY OF INTRINSICAND LAPLACIAN OF RESIDUE

Maheshwar reddy ,Prema vani, Tejaswi

Introduction:

The aim of multimodal image fusion is to combine favorable data from source images taken by various sensors into a single image. The result of the fused image will have accurate data in the input images without any noise. Image fusion technique has been widely used in many fields including agriculture, medical imaging, biometric, remote sensing. In agriculture fusion technique is used for crop recognition and detection. In medical field, magnetic resonance (MR) imaging and computed tomography (CT) contains high resolution are examples for anatomical imaging methods. Single-photon emission computed tomography) (SPECT) and positron emission tomography (PET) are examples for Functional imaging methods which determines the activity of organs at specific region. Since every modality possesses distinct advantages and disadvantages, it is typically inadequate for a comprehensive medical diagnosis on its own. Image fusion technique used to integrate the features of input images into single image.

In recent years, the advancements of image fusion in the medical field have been made development of various fusion techniques. These techniques can generally classifies into two main categories: spatial domain methods and transform domain methods. Spatial domain methods are chosen based on the features of spatial data. The advantage of spatial domain techniques is their ability to perfectly preserve the detailed information present in the source images. Consequently, the fused image retains all the information that was originally present in the source images. Spatial domain techniques perform better in like multi-focus [3], [4], [5] image fusion due to their ability to preserve spatial information. However, they do have a notable drawback: they struggle to effectively integrate data from the certain location in each input image, except for methods that involve weighted averaging of image pixels. Unfortunately, these weighted averaging methods often lead to decreased in the sharpness of the detailed data in the resulting output image.

In contrast, transform domain-based methods are employed in the field of medical image fusion. Transform domain techniques first converts the input images into specific coefficients. These coefficients are fused by fusion rules, and then resulting fused coefficients are inversely transformed to produce the fused output image. Among these methods, multiscale transform (MST) and sparse representation(SR) based techniques have gained popularity in recent years. MST-based algorithms operate in the frequency

domain and involve decomposing input images into high and low frequency components using transformations like NSST, DWT, and NSCT. Subsequently, different fusion rules are applied to the high frequency and low frequency components to generate the fused image. On the other hand, Sparse representation based algorithms, are rooted in timedomain processing and rely on dictionary learning to obtain sparse coefficients from the source images. In summary, both sparse representation and MST transform methods are prominent approaches within the transform domain and are widely used in image fusion. In sparse representation, the source images are encoded sparsely as sparse coefficients through a straight forward Max - 11 fusion rule. This approach ensures that the resulting fused image retains outstanding detailed information. This method typically increases computation costs that are approximately 2 to 3 times greater compared to alternative transform domain methods. The MST algorithm stands out as the prevailing choice for image fusion within the transform domain. In the context of multi-modality medical image fusion, MST-based techniques like shearlet transform (ST), curvelet transform (CVT), Wavelet transform (DWT), non-subsampled shearlet transform domain (NSST) and non-subsampled contourlet transform (NSCT), empirical mode decomposition (EMD) are widely employed.

Many researchers have used EMD in image fusion to remove the artefacts of preset basis functions in traditional fusion methods such as the Fourier transform as well as the wavelet transform. Unfortunately, current EMD-based image fusion techniques have a limited impact because of certain limitations has been addressed in image fusion. In order to enhance the effectiveness of EMD-based image fusion techniques, we initially a multichannel bidimensional EMD approach employing morphological filtering, denoted as MF-MBEMD. This method was employed to decompose the source images into multiple Intrinsic Mode Functions (IMFs) of varying scales, along with a single residual component. Here the high frequency components (IMFs) are fused by the Phase congruency fusion rule where as low frequency components (residuals) are fused by the local Laplacian energy based fusion rule.



Fig1: Block Diagram of method implementation

A summary of the proposed methodology and contributions is provided in the following. We employ a general learning-based decomposition models suitable for fusing images from various imaging modalities. Hence This combination of these techniques would require a well-defined problem and careful integration to achieve a better result.

We performed fusion on various data sets and calculated metrics like peak signal to noise ratio (PSNR), structural similarity index (SSIM) and mean square error (MSE) for estimating the performance of algorithm, and then we discussed about how framework are selected to our technique. After getting results we compared the efficiency of employed algorithm with the other techniques like Arithmetic average fusion, Edge structure aware fusion, NSCT. All this process and output images which was shown are performed by using MATLAB2021 on laptop with Intel Core i4 CPU and 4.0 GB RAM. Figure 5.1 shows the testing data sets of MRI-CT. Fused results of our method is shown in figure 5.3, and figure 5.4, figure 5.5.

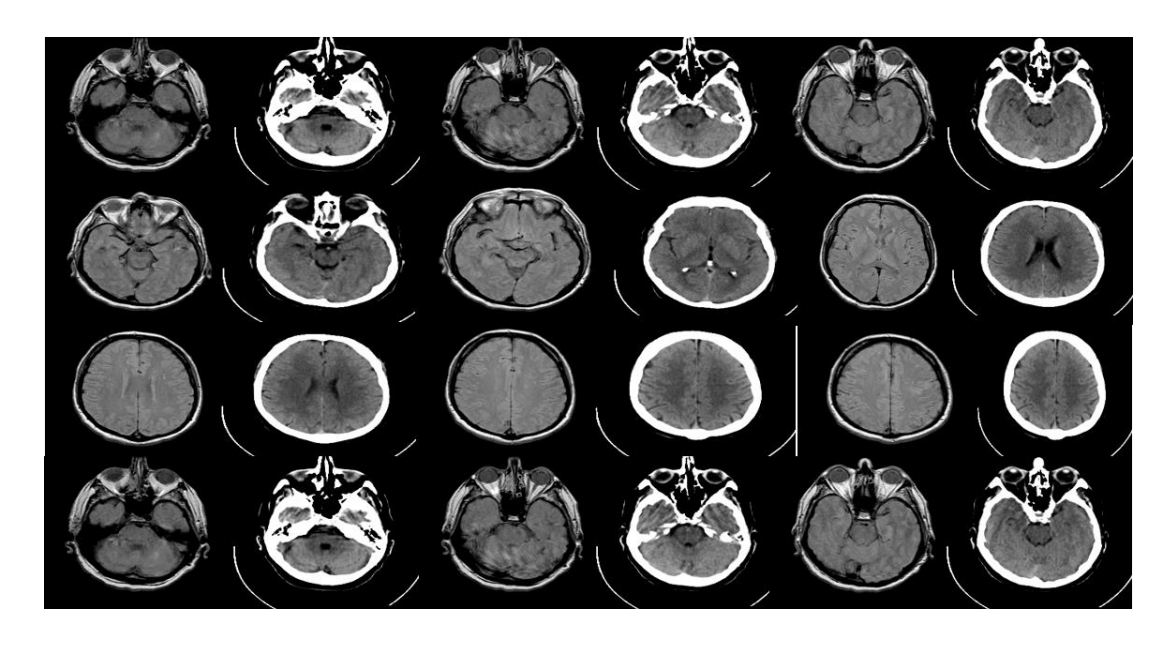


Fig 2: Training datasets of MRI-CT images

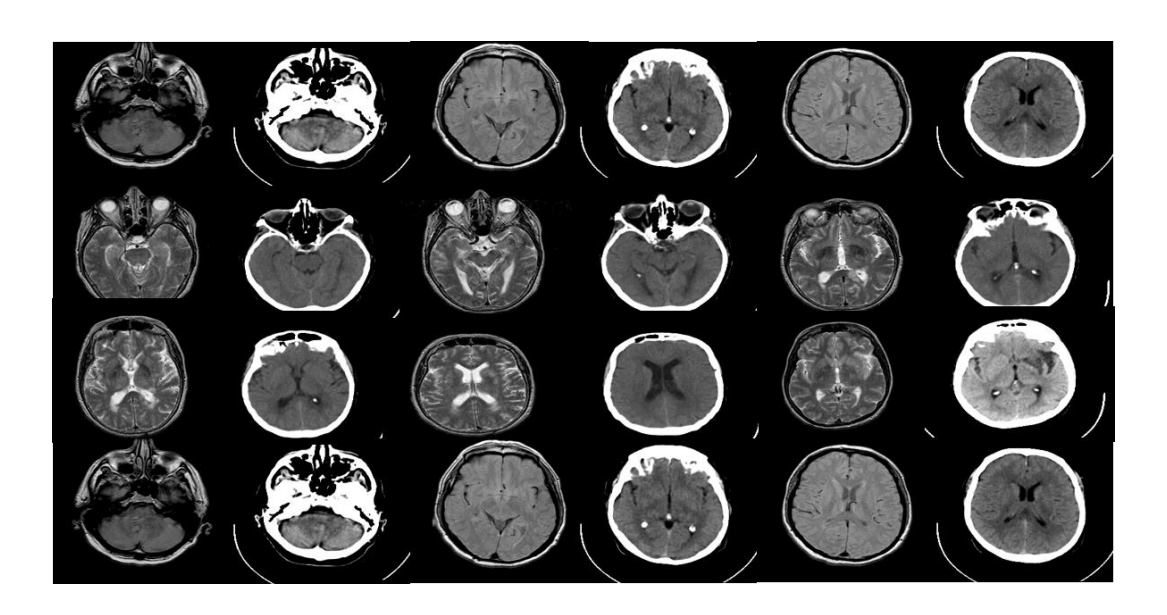


Fig 3: TESTING DATASETS

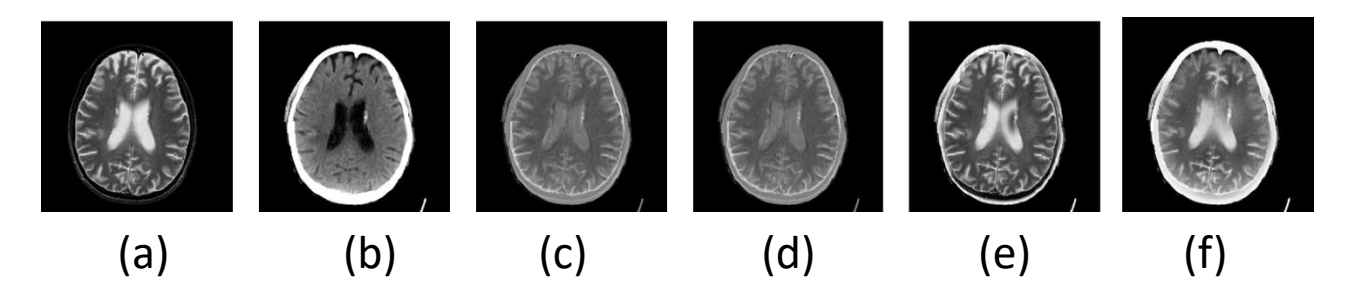


Fig 4: Fused Results of Various Techniques: (c), (d), (e) and (f) images are fused images of (a)MRI and (b) CT. (c) Average Fusion method, (d) is Structure Aware method, (e) is NSCT method and (f) is our method.

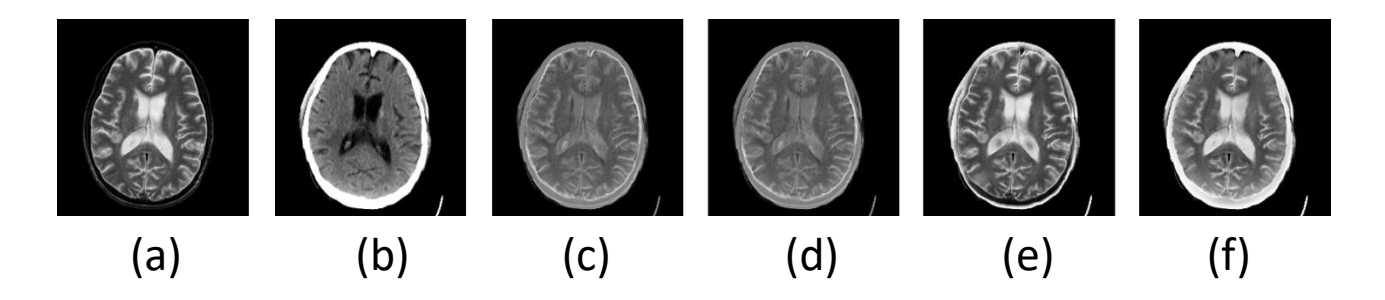


Fig 5: Fused Results of Various Techniques: (c), (d), (e images are fused images of (a)MRI and (b) CT. (c) Average Fusion method, (d) is Structure Aware method, (e) is NSCT method and (f) is our method.

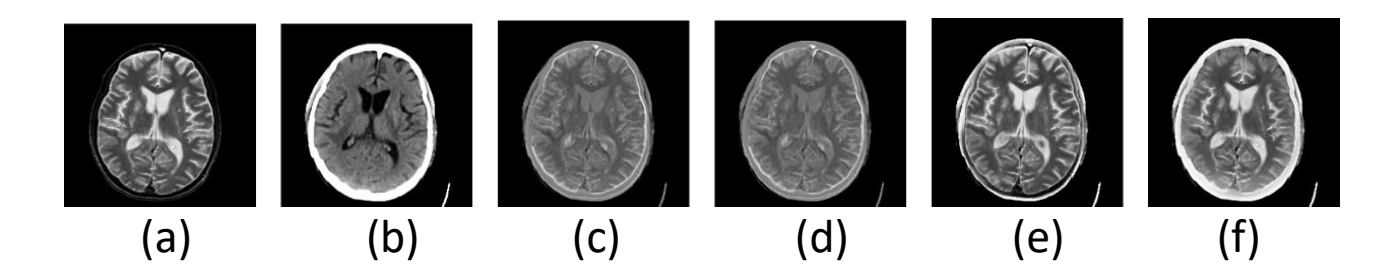


Fig 6: Fused Results of Various Techniques: (c), (d), (e) and (f) images are fused images of (a)MRI and (b) CT. (c) Average Fusion method, (d) is Structure Aware method, (e) is NSCT method and (f) is our method.

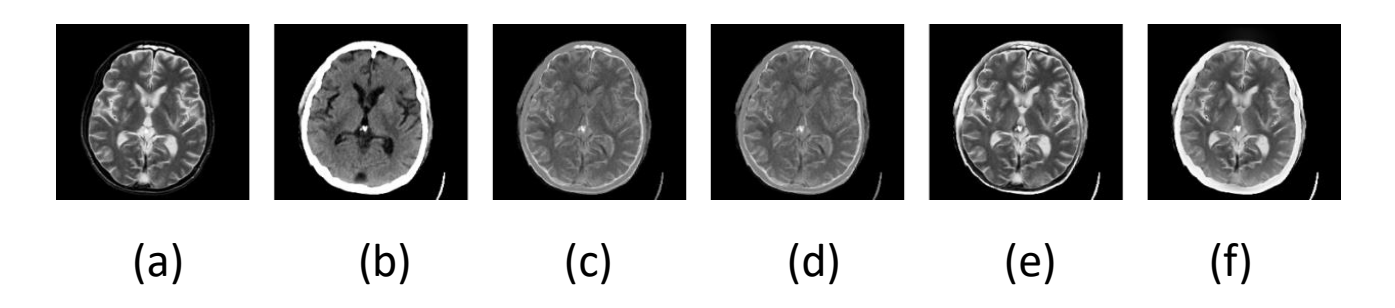


Fig 7: Fused Results of Various Techniques: (c), (d), (e) and (f) images are fused images of (a)MRI and (b) CT. (c) Average Fusion method, (d) is Structure Aware method, (e) is NSCT method and (f) is our method.

This approach for fusion of multi-modality medical images in the EMD domain, using phase congruency (PC) and Local Laplacian Energy (LLE). The technique comprises three main steps: initially, the input medical image pairs decompose into IMFs and Residue using EMD. The IMFs are fused by phase congruency and residual component are fused using local Laplacian energy-based fusion rule. Finally, to get resultant output image inverse EMD is performed. Experimental results validate that this method performs good in both visual and objective quality metrics along with maintaining competitive computational efficiency for fused images

DESIGN OF A MIMO ANTENNA ISOLATED WITH AN INVERTED U-SHAPED GROUND STUB FOR PERFORMANCEENHANCEMENT

P.Sree Pranavi, N.Poojitha, G.Susmitha

Introduction:

In the field of wireless communication and electromagnetic wave propagation, the design and optimization of antennas play a pivotal role. Antennas serve as the interface between electronic devices and the electromagnetic spectrum, facilitating the efficient transmission and reception of signals. One of the critical aspects of antenna design is ensuring resonance at specific frequencies, as this directly impacts the performance and effectiveness of the communication system.

Wireless systems have been deployed through the world to help people and machines to communicate with each other independent of their location. Wireless communication is highly challenging due to the complex, time varying propagation medium. If we have only one transmitter and one receiver in wireless system, the transmitted signal that is send into wireless environment arrives at the receiver along a number of diverse paths, referred to as multi paths. These multi paths of signal are mainly because of reflection, refraction scattering and diffraction due to these factors the received signal varies as a function of frequency, time and space.

These variations are referred to as fading and which cause deterioration of the system quality. Furthermore, wireless channels suffer of cochannel interference (CCI) from other cellsthat share the same frequency channel, leading to distortion of the desired signal and also low system performance. Therefore, wireless systems must be designed tomitigate fading and interference to guarantee a reliable communication. The frequency range of 8.1-8.5 GHz falls within the microwave spectrum, which is widely utilized for various applications such as satellite communication, radarsystems, and wireless networks. Designing an antenna that resonates within this frequency range requires careful consideration of electromagnetic principles and engineering techniques to achieve optimal performance. Multiple-input and multiple-output (MIMO)is the use of multiple antennas at boththe transmitter and receiver to improve communication performance. It is one of several forms of smart antenna technology. MIMO technology has attracted attentionin wireless communications, because it offers significant increases in data throughput link range without additional bandwidth or increased transmit power.

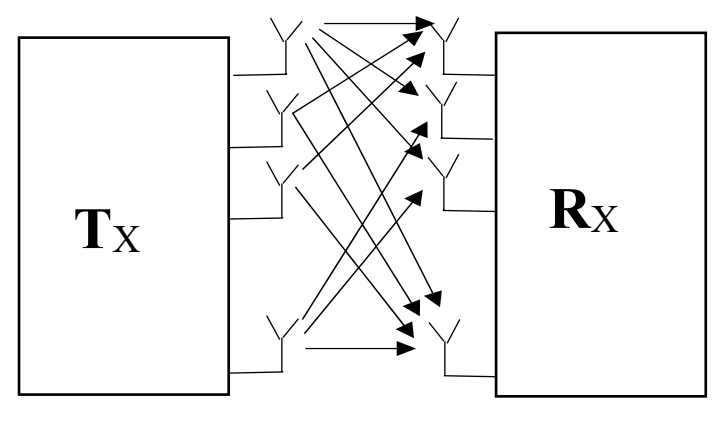
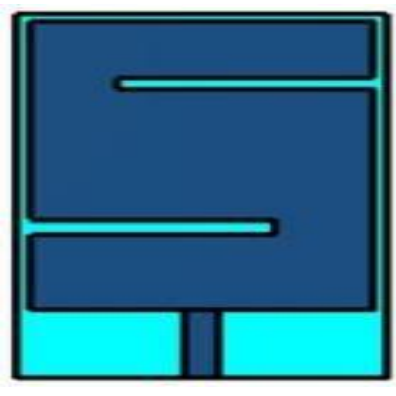


Fig 1 MIMO model

It achieves this goal by spreading the same total transmit power over the antennas to achieve an array gain that improves the spectral efficiency (more bits per second per hertz of bandwidth) or to achieve a diversity gain that improves the link reliability (reduced fading) .The antenna is designed on a thin semi-flexible substrate of Rogers 5880 ($\epsilon r = 2.2$, loss tan = 0.0009) with a thickness of 0.51 mm. The dimensions of single-elementantenna structure are only 14 mm × 25 mm that is equal to 0.114 λ o× 0.204 λ o, where λ o is the free space wavelength at the resonating frequency of 2.45 GHz. Miniaturization is attained through etching four open-end slots on the rectangular patch along the x-axis on both the sides. L-shaped partial ground plane is used for better impedance matching and wider bandwidth.



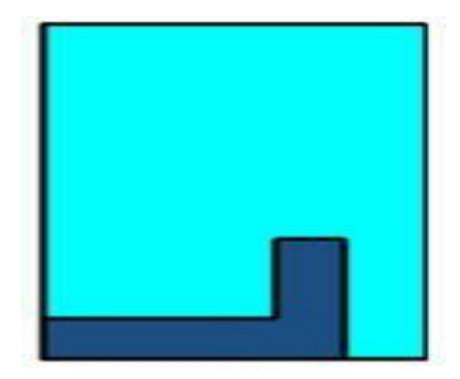


Fig 2 front view

Length of the slots and otherparameters are optimized to tune the desired resonance using Computer Simulation Technology (CST) microwave studio. In step 1, the antenna is designed by cutting two open-end slots at the two opposite corners of the radiator. First slot is etched at the lower left corner which provides wideband resonance at 3.5 GHz. Length CW1 of the slot is varied from8 to 11 mm to obtain optimal performance. It can be observed that increasing the length of the slot helps to reduce the resonating band but degrades impedance matching. Therefore, CW1 = 11 mm is considered for further

design which provides resonance at 3.9 GHz. Second slot is etched at the upper right corner which adds inductive effectin the structure.

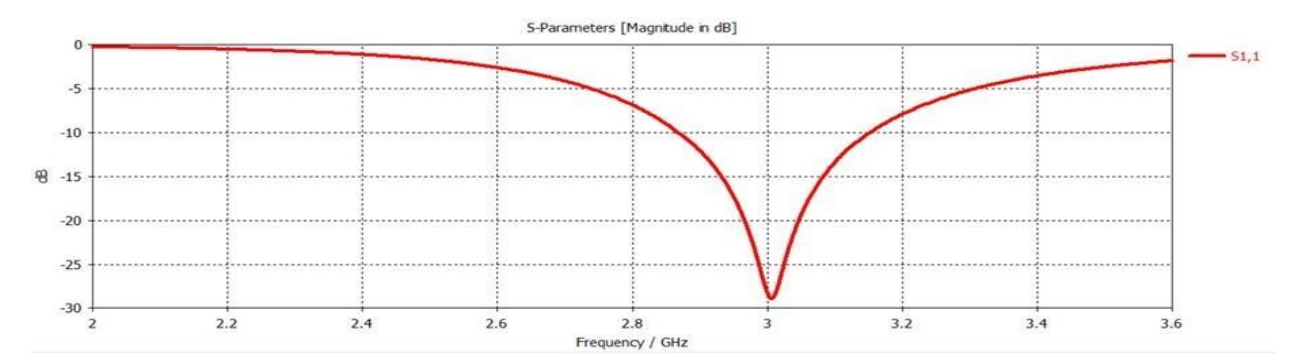


Fig 4. Reflection coefficient of the designed single element antenna

It helps to reduce the resonating band from 3.9 to 3.0 GHz with goodimpedance matching as shown in fig 4. Effect of varying length CW4. The increasing value of CW4 has an almost negligible effect on return loss. In the second step the two slot are joined making a S-shape to increase the frequency of the antenna. The shapes are adjusted according to the required resonating frequency. The design of step2 is shown in the fig 5. The reflection coefficient of the designed antenna is shown as in fig 6.

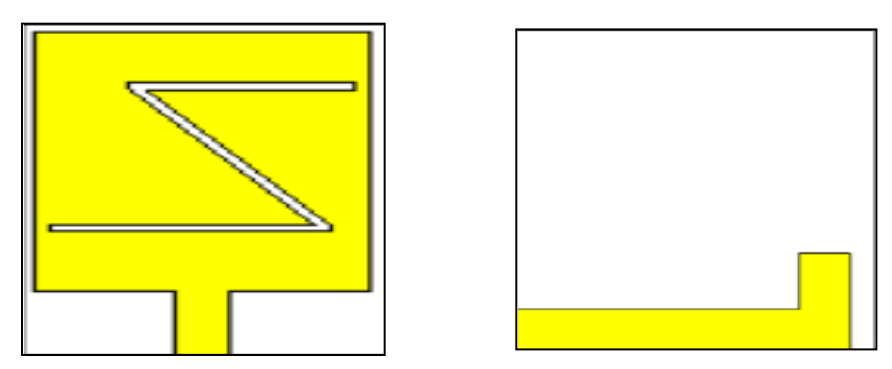


Fig 5. Front view and back view of the single element antenna

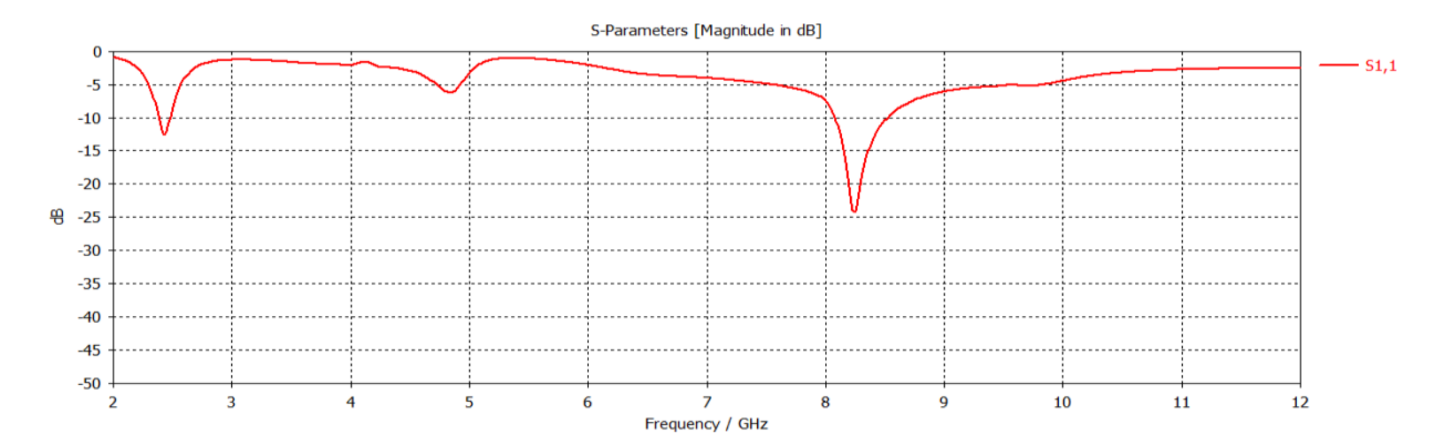


Fig 6. Reflection coefficient of single element antenna

To design a MIMO antenna, two mirror image antenna elements are placed parallel to each other. It was difficult to maintain high isolation between two elements without a decoupling structure. Therefore, to improve the isolation, inverted U-shaped stub is added at the ground plane acting as a parasitic resonator. Length of this stub is 47 mm ($2 \times \text{Lc} + \text{Wc}$), which is approximately equal to the value calculated in equation. Length of inverted U-shaped stub satisfies the resonating length at 8.25 GHz.

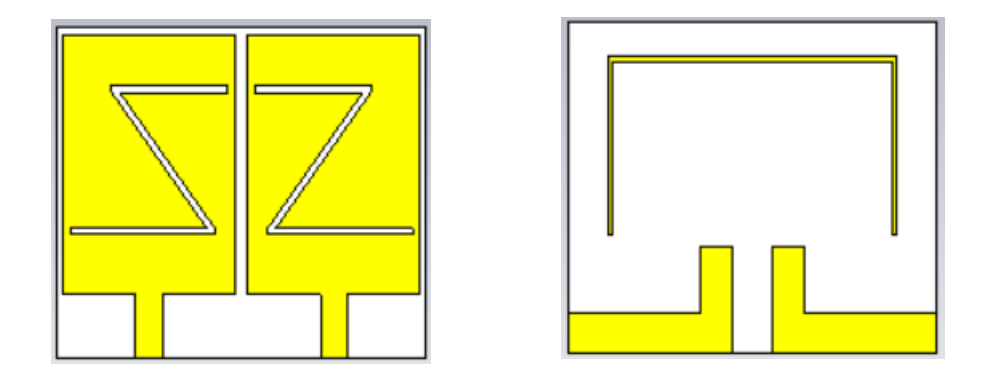
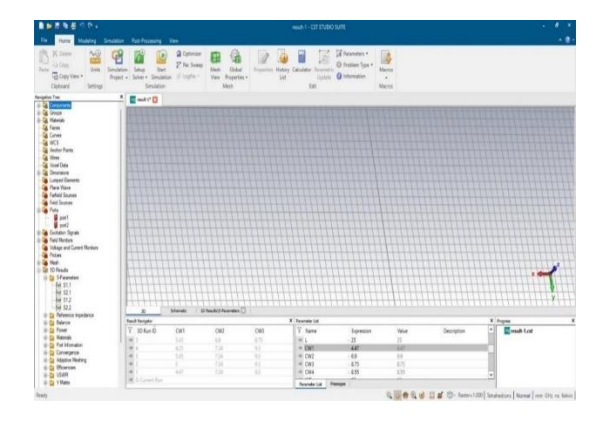


Fig 7. Front view and back view of MIMO antenna along its dimensions

The designed antenna is resonated ate the frequency of 8.1-8.5 GHz. The S11 and S21 parameters are simulated. The S11 at the frequency of 8.25 GHz is -24.3 dB and S21 at that frequency is -34.3 dB.



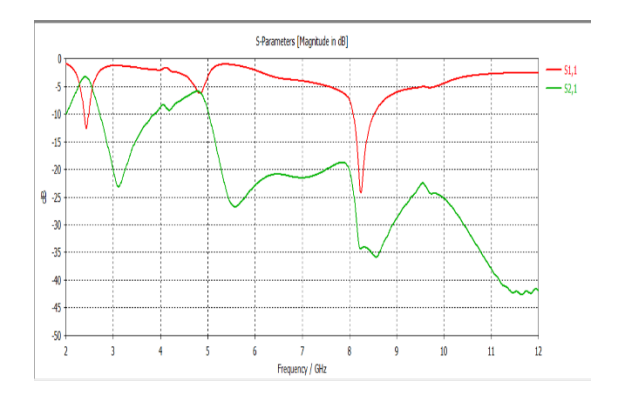
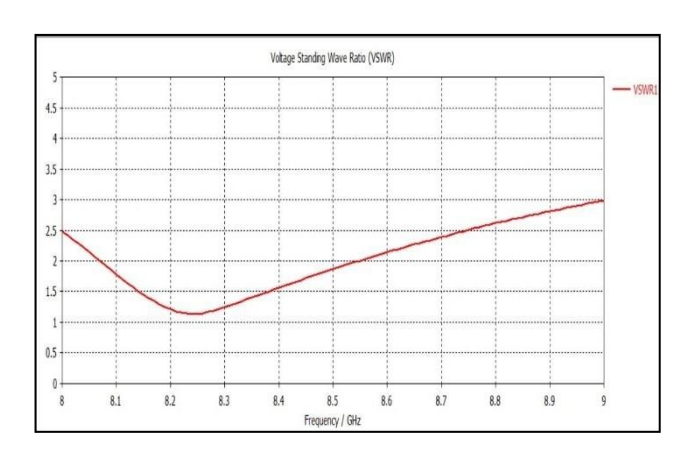


Fig 8 CST SOFTWARE

Fig. 9 . S11 and S21 Parameters



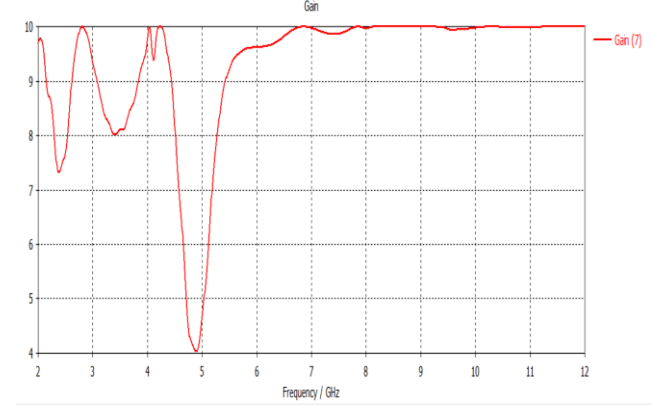


Fig 10. VSWR of the MIMO antenna

Fig 11 Gain

VSWR shows how efficiently the radio frequency power is transmitted between a source and a load. The VSWR of the designed antenna is obtained to have the range between 1 to 2 in the frequency range of 8.1 – 8.5 GHz. The gain achieved for MIMO antennas contribute to increased data rates, improved reliability, and better overall performance in wireless communication systems. The Gain for the designed MIMO antenna is 10 dB. The radiation pattern of an antenna is a graphical representation of how the antenna radiates or receives electromagnetic energy in three-dimensional space. It provides valuable information about the directional characteristics of the antenna andis crucial in various aspects of antenna design, deployment, and communication system performance.

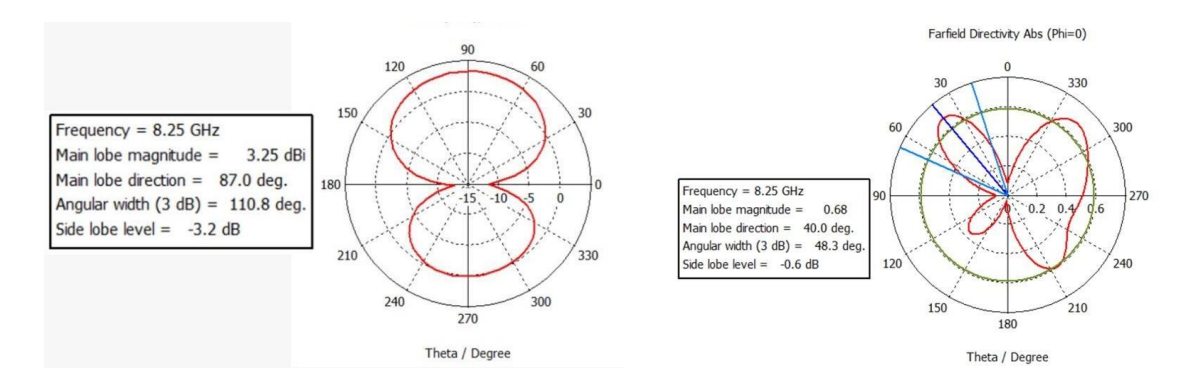


Fig 12 Radiation Pattern

Fig 13 Directivity

Directivity is a measure of how focused or concentrated the radiation or reception pattern of an antenna is in a particular direction. It is expressed as a ratio of the radiation intensity (or reception sensitivity) in the maximum direction to the average radiation intensity (or sensitivity) over all directions. Surface current density is a concept in electromagnetics that describes the distribution of electric current across a surface.

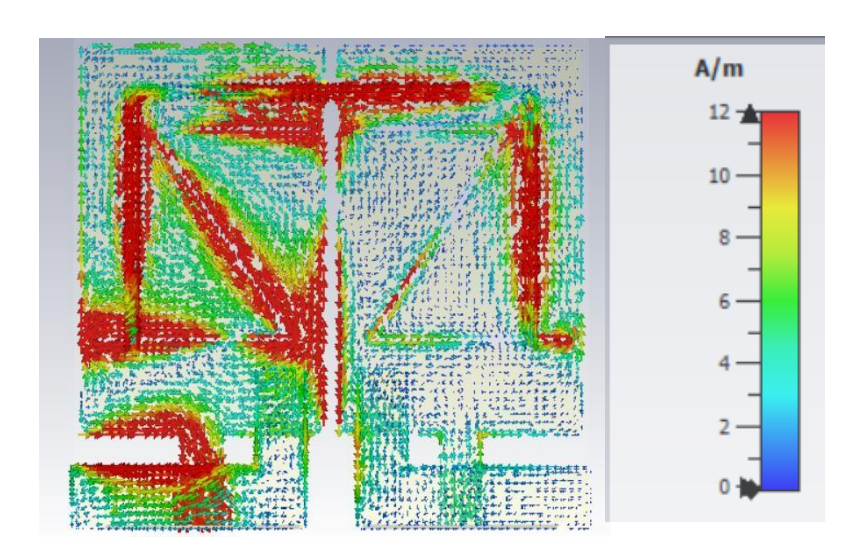


Fig 14 Surface Current Density of the MIMO antenna

PEDIATRIC SLEEP STAGE CLASSIFICATION

P Lurdhu Merin, V S V S Prapoornetri, K Ashok

Introduction:

At present, most of the computing tasks of the remote sleep monitoring (such as sleep staging) are deployed on platforms with large-scale computing resources such as computing centers, which largely limit the convenience to people. Sleep-induced diseases such as insomnia, drowsiness, obstructive sleep apnea (OSA) and other sleep disorders are becoming more and more common and have become a major medical challenge. For children, high-quality sleep helps children's intellectual development and is closely related to children's cognitive function, learning and attention. If school- age children are not able to get enough and good sleep, it will affect their mental development and cause emotional, behavioral, and attention problems.

Polysomnography (PSG) recordings is used to diagnose sleep-related diseases, which include electroencephalogram (EEG), electrooculogram (EOG), electrocardiogram (ECG), electromyogram (EMG), breathing exercises (chest and abdominal), oral and nasal airflow, body movement, blood oxygen saturation (SaO2) and other physiological parameters. Sleep stage scoring is to divide the physiological parameters in the polysomnography chart into 30 s continuous epochs according to the time axis, and divide these epochs into different sleep stages according to the American Academy of Sleep Medicine (AASM) rules. Sleep stage scoring can be performed using single-channel EEG or multiple physiological parameters. The hypnogram obtained from the results of sleep staging can intuitively reflect the sleep of subjects throughout the night, and is used to evaluate sleep quality and sleep-related problems.

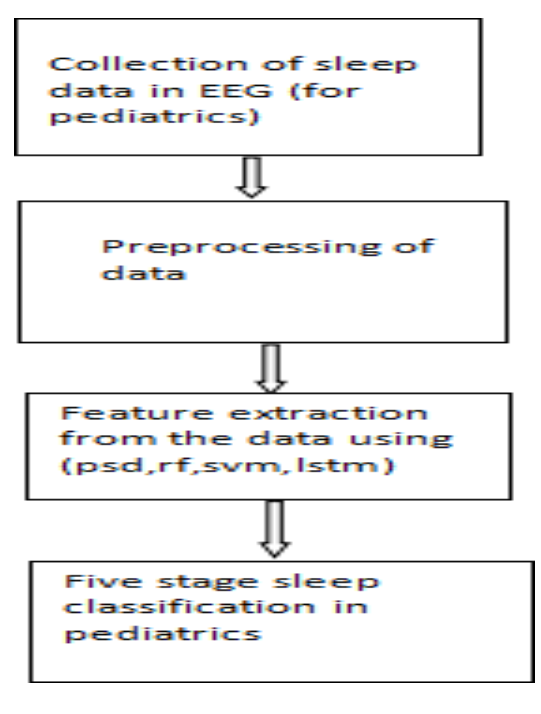


Fig 1: Flow Chart

The HNN-based classifier yields the best performance metrics using 30 s time series in combination with an instantaneous frequency using a 19-channel, three-stage classification, with an overall accuracy, F1 score, and Cohen's Kappa, equal to 92.21%, 0.90, and 0.88, respectively. An effective combination of temporal and spatial time domain clues with time-varying frequency domain information plays a pivotal role in pediatric, automatic sleep staging. Sufficiently reasonable performance of the HNN-based approach coping with highly complicated pediatric EEG signatures hopefully sheds light on the clinical feasibility of DNN-based automatic sleep staging for pediatric neurology.

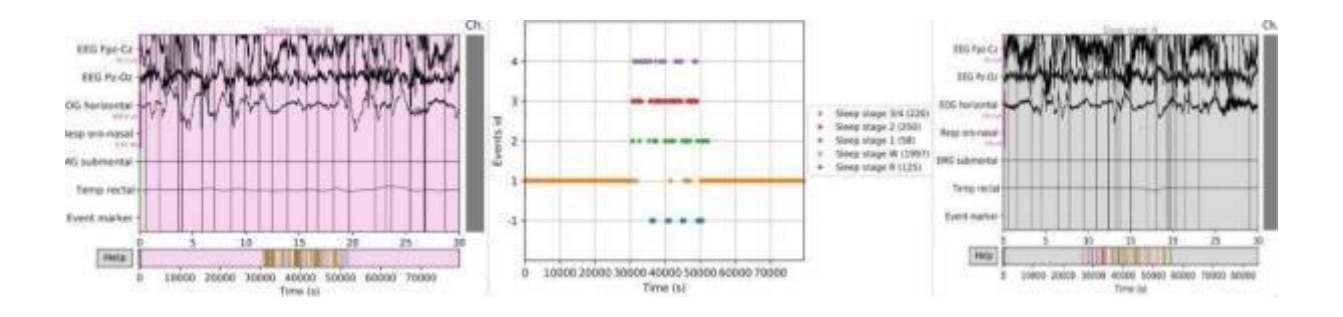


Fig 2: Simulation Result

EOG, EMG and EKG are considered as input signals and all the sleep stage classification is done accordingly and we demonstrated the influences of the length of input signals, number of channels, and types of input signals on the HNN-based automatic sleep-stage classification for pediatric scalp EEG datasets in the time and frequency domains. Therefore, Pediatric Sleep stage classification is a great benefit in clinical neurology and helps us detect any kind sleep related disorders which we can diagnose before hand and take the necessary solutions.

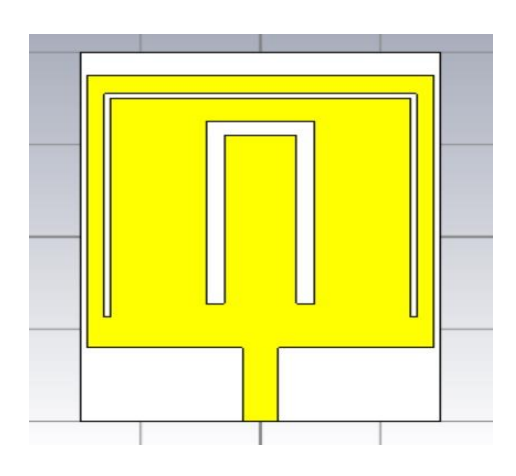
DESIGN AND ANALYSIS OF DOUBLE U-SLOT RECTANGULAR PATCH ANTENNA FOR Wi-Fi AND WIMAX APPLICATIONS

G. Balakrishna, J. Waran job , N.Om venkata Vamsi

Introduction:

The continuous development in mobile communication system has tend to increased in demand for multiband high gain and high isolation antenna which cover the GSM, Wi-Fi, and WiMAX (1.8,2.4,3.5HGz) bands. In addition, the demand for wideband antennas has risen to accommodate the growing number of service bands. Multiband microstrip patch antennas are a type of antenna that can operate at multiple frequencies. Multiband microstrip patch antennas have a number of advantages over other types of multiband antennas. They are relatively easy to design and fabricate, and they can be very compact. Additionally, they can be integrated with other electronic components on a single circuit board. In this paper we focus on the applications of GSM, Wi-Fi, and WiMAX.

Wideband microstrip antenna with a single-layer, single-patch configuration measuring 8.65" x 4.90". This antenna achieves an impedance bandwidth of 10–40% without additional parasitic patches. The radiation patterns remain stable with half-power beamwidths of 59 degrees at 812MHz and 57 degrees at 1.1GHz in the x-z plane, and 65 degrees at 812MHz and 70 degrees at 1.1GHz in the y-z plane, resulting in a bandwidth (VSWR = 2) of -47%, a double U-slot patch antenna with dimensions 144mm x 76mm is designed using a foam layer of thickness equivalent to -9% of the wavelength. This configuration achieves an impressive impedance bandwidth of 44%. The antenna's half-power beamwidths are 57 degrees in the H-plane and 73 degrees in the E-plane, with cross-polarization levels well below 20dB in the broadside direction.





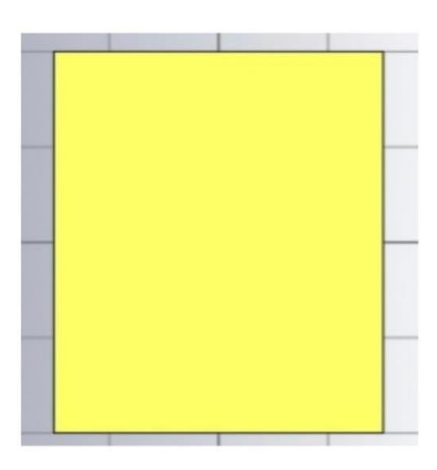


Fig 2:BACK VIEW

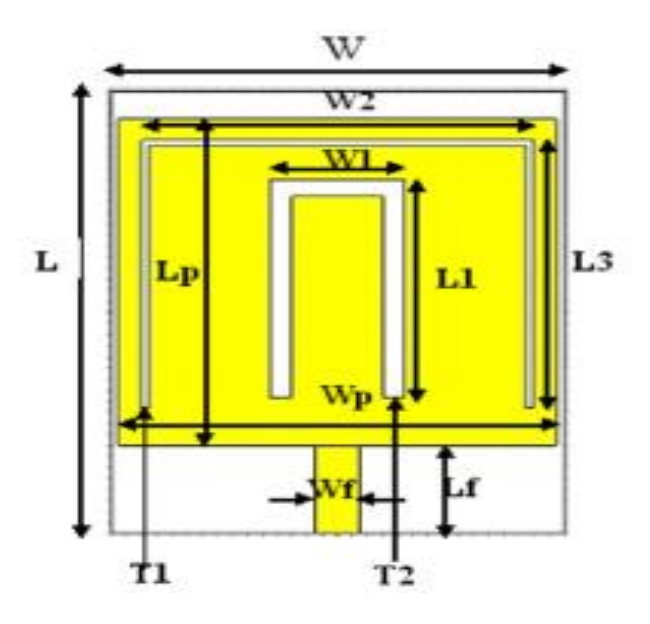


Fig.3: optimized model

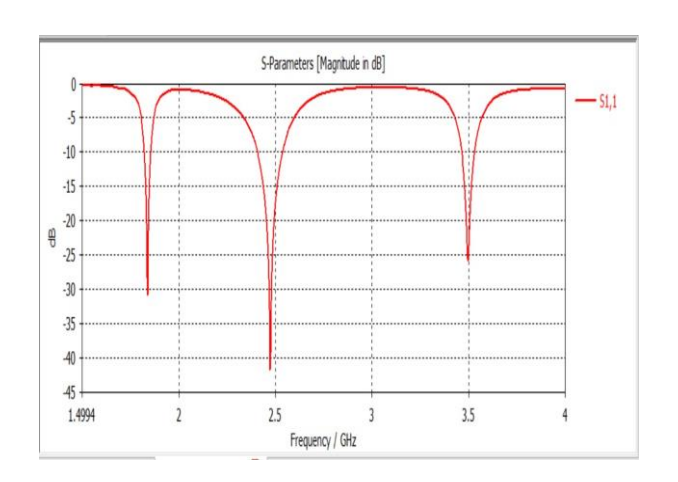


Fig4.: S11 plot

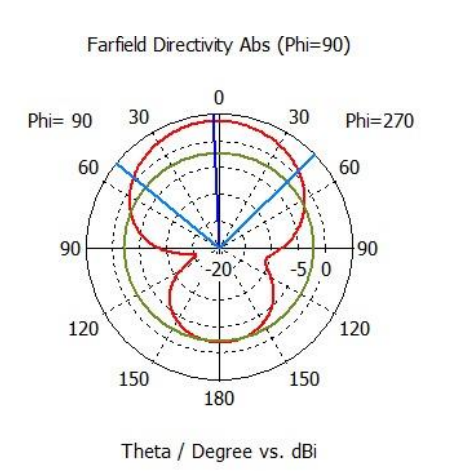


Fig 6: Radiation pattern for 2.4 GHz frequency

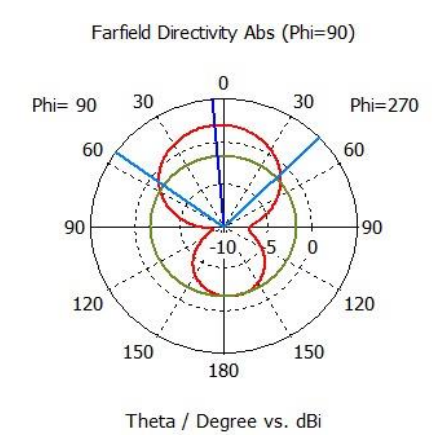


Fig 5: Radiation pattern for 1.8 GHz frequency

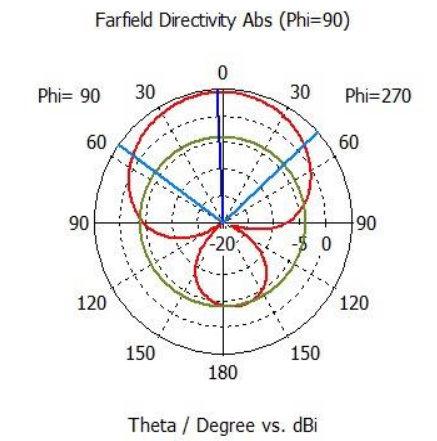


Fig 7: Radiation pattern for 3.5 GHz frequency

A simple, low-cost, low-profile double U-slot microstrip patch antenna was designed and measured to operate at the three desired resonant bands; 1.8 GHz, 2.4 GHz and 3.5 GHz. Measured return loss and radiation patterns compared fairly well with the simulated results. The measured error was less than 2% for the resonant frequencies and less than 10% for the resonant bandwidth. Our antenna, merits over those studied in the literature, that it has a relatively more compact size, simpler to design, has a higher gain and serves wider applications. The size of the antenna could be further decreased by using a substrate with a higher dielectric constant. such On the other hand, wider resonant bandwidths and even higher gain could be achieved if a dielectric material; such as Rogers /Duroid, with a relatively lower dielectric constant and a lower dielectric loss is used, instead of FR4. Further U-slots could be added to the patch, if more resonant bands are desired but efforts for further optimization become more challenging.

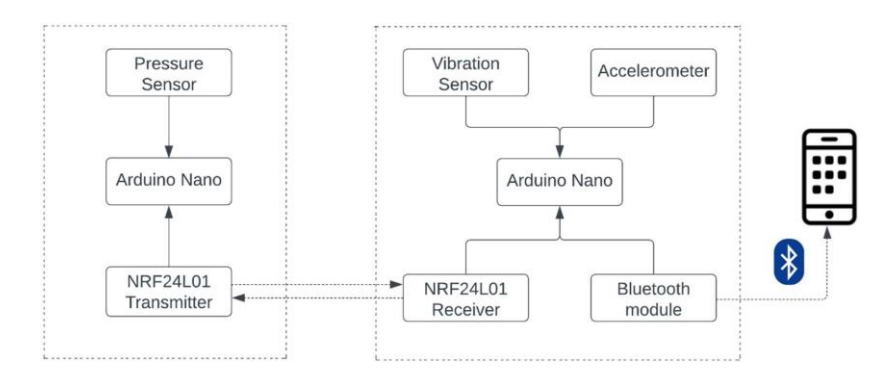
IoT POWERED INTELLIGENT BIKE SAFETY SYSTEM: A FALL DETECTION ALGORITHM

Venkata Naga Vamsi Marriwada, Sai Krishna Vallepu ,Karthikeya Sesham

Introduction:

Road accidents have developed as a serious global concern in today's fast- paced society, ranking as the tenth greatest cause of mortality worldwide. Bike riders are among the most vulnerable on our roadways, as they face particular hazards and obstacles as they navigate through traffic and varied road conditions. It is critical to develop creative solutions that prioritize rider safety in order to address the growing incidence of bike-related accidents and fatalities. This project proposes a ground-breaking prototype that intends to improve bike rider safety by incorporating cutting-edge technology and smart sensors, promoting responsible riding practices and lowering the occurrence of accidents and injuries.

The use of GPS technology to monitor and mitigate over speeding is the core of this unique system. Excessive speed is a significant cause of bike accidents, and theapp responds by giving visual and aural alerts when predefined speed restrictions are exceeded. This real-time feedback allows riders to make informed judgements, reducing the desire to accelerate and improving overall road safety. In addition, the system includes an accelerometer sensor and vibration sensors, which detect rapid changes in bike acceleration and vibrations. These sensors act as watchful guardians, ready to send out fast alerts in the case of a fall. In the event of anaccident, such early detection can dramatically cut reaction times, potentially saving lives and minimizing injuries.



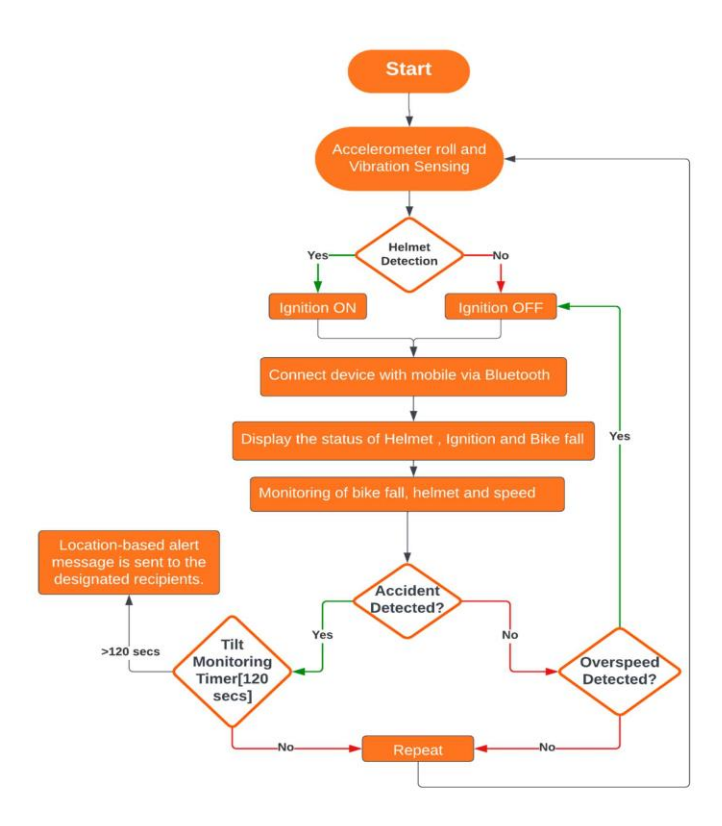


Fig-1: Module



Fig- 5 : Alert Message

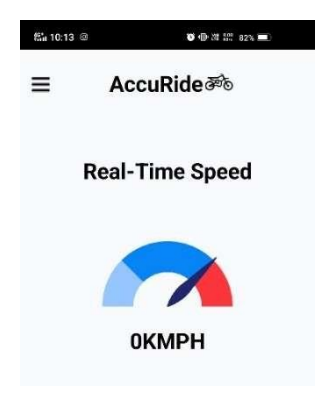


Fig-6: Real-Time Speed

The overspeed detection module, which utilizes GPS technology in conjunction with a companion mobile app, has proven to be a robust tool for curbing over speeding. Real-world testing revealed that the system reliably detects over speeding violations and immediately takes control of the bike's ignition, ensuring the rider's speed is reduced to safe levels. This proactive approach effectively promotes responsible riding practices and enhances rider safety.





Fig-7: NRF24L01 Module

Fig-8: Helmet with NRF24L01

The mobile application, a crucial component of our system, has shown excellent resultsin facilitating rider interaction with the safety system. Real-time alerts, auditory warnings, and the ability to notify concerned emergency contacts were all successfullytested and demonstrated. The app's user-friendly interface enhances user engagementand serves as a vital link in ensuring timely responses to safety events.





Fig-9 App Interface

Fig-10: Emergency Numbers Interface

Overall, four modules, when integrated and tested collectively, showcasea significant potential to encourage responsible riding practices and reduce accidents and injuries for bike riders. These results underscore the importance of a multi-faceted approach to rider safety, combining advanced technology with user-friendly applications to enhance safety on the road.

IMPLEMENTATION OFDIELECTRIC RESONATOR ANTENNA

M.Raghava ,sk.NagurBasha ,N.Sanjay

Introduction:

A singly fed wideband circularly polarized DRA, including a rectangular DRA, conformal metal strip of Roman three shape for excitation purpose, parasitic strip, and the ground plane made up of PEC. The size of the DRA is kept similar as in [20], where having a height (H), width (B) and depth of (C) 26.1 mm, 25.4 mm, and = 14.3 mm, respectively. Additionally, the relative permittivity of DRA has $\mathcal{E}_r = 10$. Conformal metal feed comprises up to 5 separate strips used to excite the antenna. After the numerous parametric sweeps, the optimized dimensions of the feeds are h_3 & $h_4 = 12$ mm, $w_1 = 7.0$ mm, h_5 & $h_6 = 4$ mm. The widths of all the strips are optimized at 1mm. For the PEC ground plane, a square plate of 35x35 cm2 has been used. DRA has been placed in the middle of the ground plane. The proposed antenna can be used vehicle to infrastructure and vehicle to vehicle applications. We designed Circularly polarized Dielectric resonator antenna (DRA) is proposed for future 5G new radio applications. A Roman feed circularly polarized DRA was introduced of operating frequency 3.7- 4.2GHz and excited by different higher order modes to cover the whole 5G new radio bands. Parasitic metal strips are introduced for novel feed mechanism to get good characteristics parameters for 5G newradio band sub- 6GHZ frequency application.

S Parameters: S-parameters (or scattering parameters) are used to describe how energy can propagate through an electric network. S-Parameters are used to describe the relationship between different ports, when it becomes especially important to describe a network in terms of amplitude and phase versus frequencies, rather than voltages and currents. From the S- parameter matrix, you can calculate characteristics of linear networks such as gain, loss, impedance, phase group delay, and voltage standing wave ratio (VSWR). The operating frequency of the above antenna is 4.5GHz.

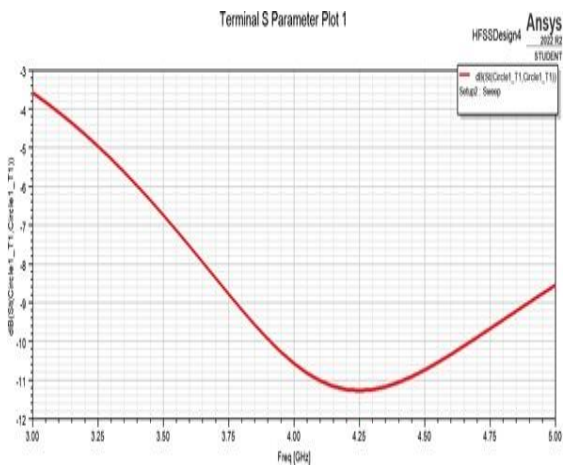


Fig 1: S parameter plot

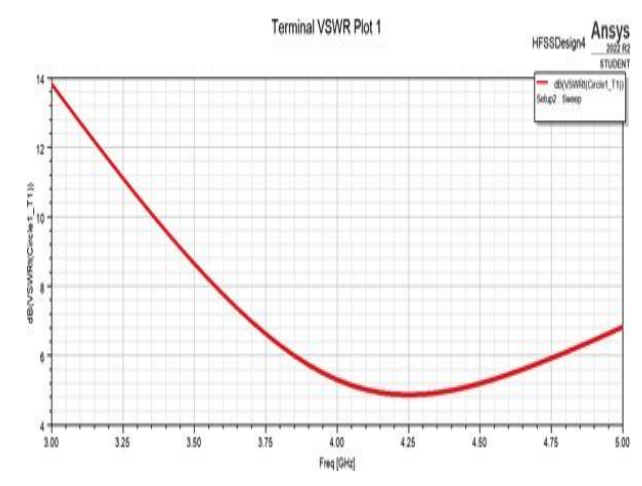


Fig 2: VSWR plot

VSWR Plot: VSWR (Voltage Standing Wave Ratio) is a measure of how efficiently radio- frequency power is transmitted from a power source, through a transmission line, into a load (for example, from a power amplifier through a transmission line, to an antenna). In an ideal system, 100% of the energy is transmitted. VSWR value under 2 is considered suitable for most antenna applications. The antenna can be described as having a "Good Match". So when someone says that the antenna is poorly matched, very often it means that the VSWR value exceeds 2 for a frequency of interest.

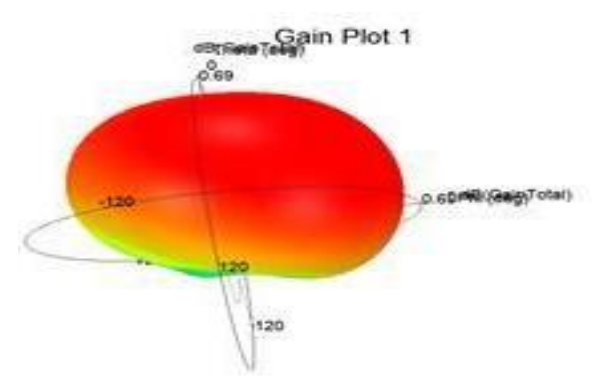


Fig 3: Gain Plot

In dielectric resonator antenna a novel roman three-feed CP DRA for sub-6 GHz 5G NR band was examined and has been successfully investigated in this article initially, the proposed antenna has produced a very narrow S11 and CP bandwidth. It has been revealed that by just deploying a parasitic metallic strip on the wall of the DRA nearby the novel feed, the antenna has exhibited a very broad10- dB impedance operation of 27.73% (3.26 – 4.35 GHz) and CP waves of 23.71% (3.37–4.23 GHz) that can easily cover 5G NR Band (n77/n78). Because the proposed wideband CP DRA has a simple structure and feeding mechanism and stable gain and radiation patterns, it is a good candidate for 5G NR band (sub-6 GHz) applications.

DESIGN OF UWB MIMO FOR BIO-MEDICAL APPLICATIONS

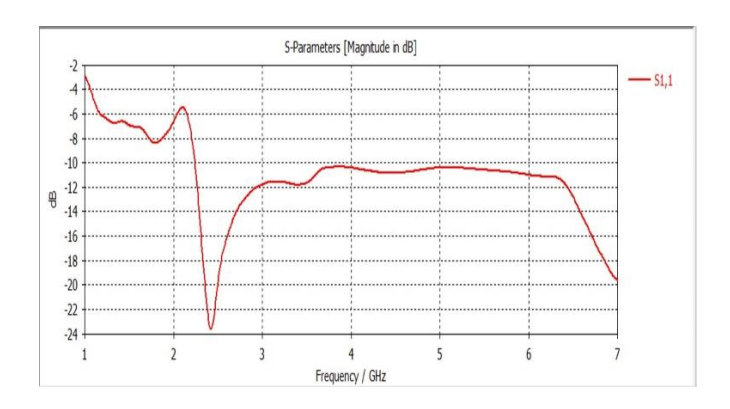
Ch.V.Sai Revanth ,M.Hadi Abbas

Introduction:

The advent of wearable devices in healthcare applications has given rise to a pressing needfor compact and efficient multiple-input multiple-output (MIMO) antennas capable of operating over a wide frequency range. The proximity of antennas in on-body or wearable systems introduces a critical concern: mutual coupling, which, if not addressed, can significantly degrade the overall performance of the communication system.

Researchers and engineers have dedicated considerable efforts to address this challenge, proposing innovative antenna designs and techniques to suppress mutual coupling and ensure reliable communication in diverse environments. Wen et al.'s work stands out in this endeavor, introducing a compact, low-profile MIMO antenna that utilizes a miniature circular high- impedance surface specifically tailored for wearable applications. This design emphasizes the importance of maintaining a small form factor while achieving effective mutual coupling suppression. Similarly, Biswas and Chakraborty have contributed to this field by proposing a compact wearable MIMO antenna with improved port isolation for ultra-wideband applications, focusing on achieving enhanced isolation between antenna elements.

Antenna design strategies have expanded to include the incorporation of textile materials, which cater to the specific requirements of body-centric wireless communications. Sun et al. presented a textile ultra-wideband antenna designed for stable performance in on-body applications. Such designs not only consider electromagnetic performance but also account for the comfort and flexibility required for integration into wearable devices. The economically available CST software is used to simulate the performance of the design antenna and to illustrate the S11 and S12 characteristics of the designed antenna is shown.



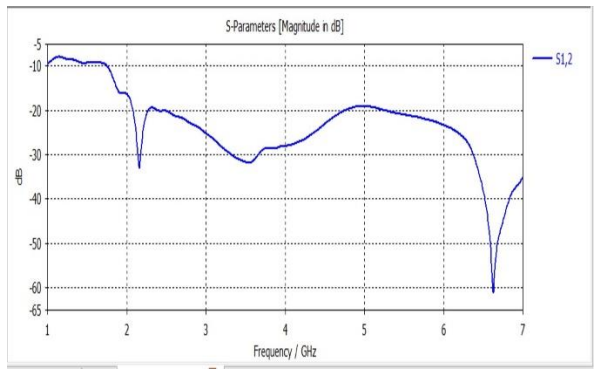


Fig 1: S11 plot of the Base antenna

Fig 2: S12 plot of the Base antenna

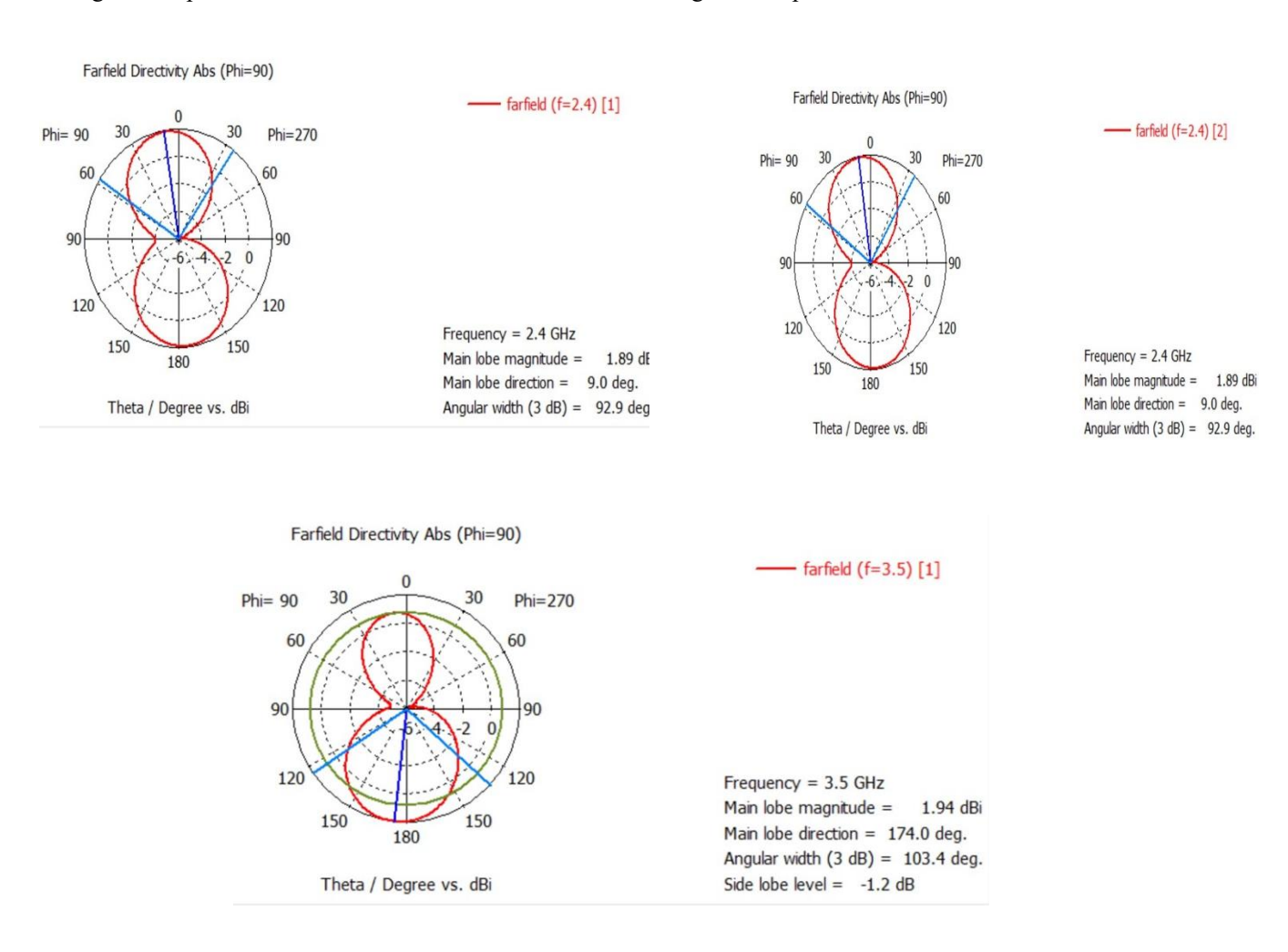


Fig 3: Directivity

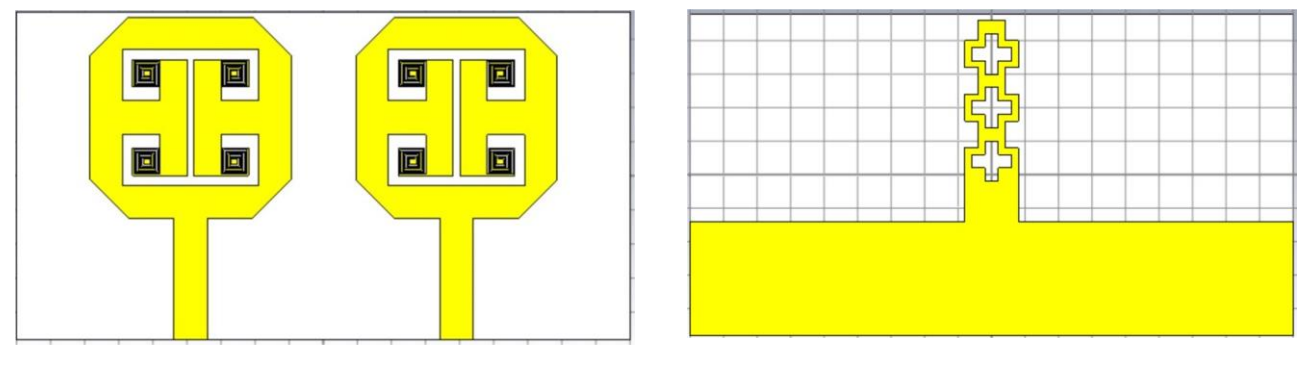


Fig4 :FRONT VIEW

Fig 5: BACK VIEW

In the above proposed antenna intended for operation within the frequency range of (2.13-2.36 GHz) and (4.7-20) GHz. The antenna is engineered to resonate at specific frequencies, namely 2.23, 5.44, 8.23, and 9.41 GHz. To enhance its performance, we introduced a decoupling element within the MIMO antenna design. By reducing inter-element coupling, we aim to minimize interference and achieve improved signal quality. This antenna design will make it suitable for biomedical applications, providing better reliability and accuracy.

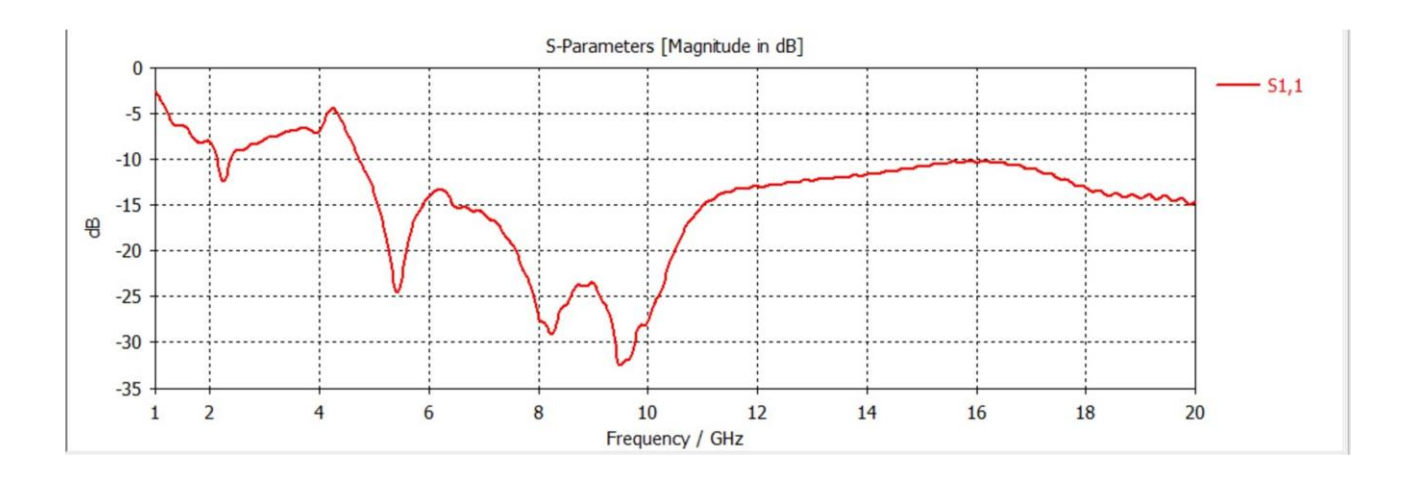


Fig6: S11 plot of the proposed antenna

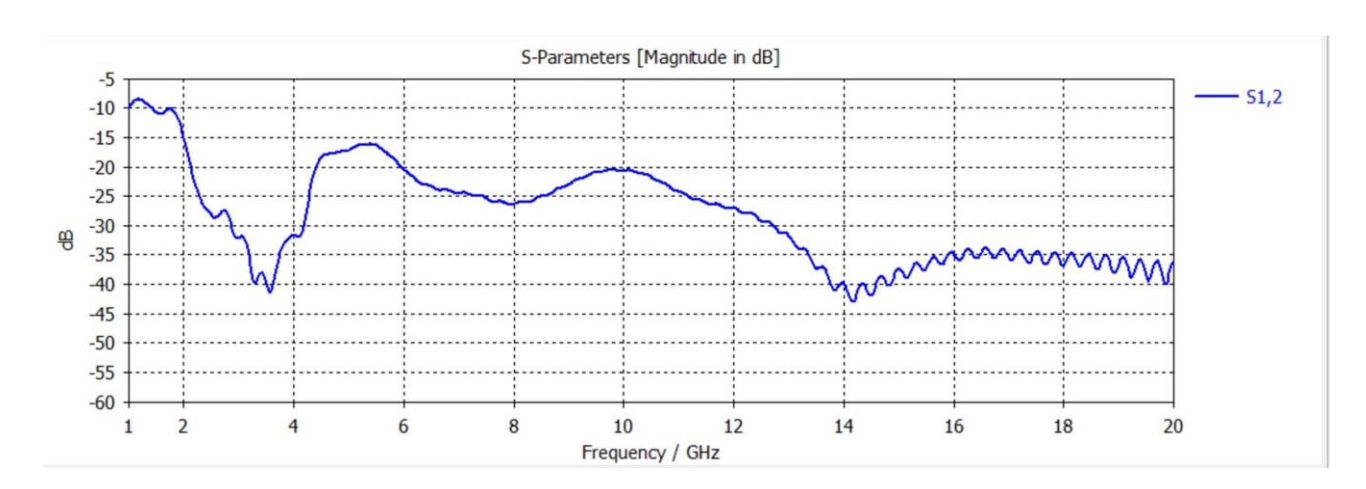


Fig7: S12 plot of the proposed antenna

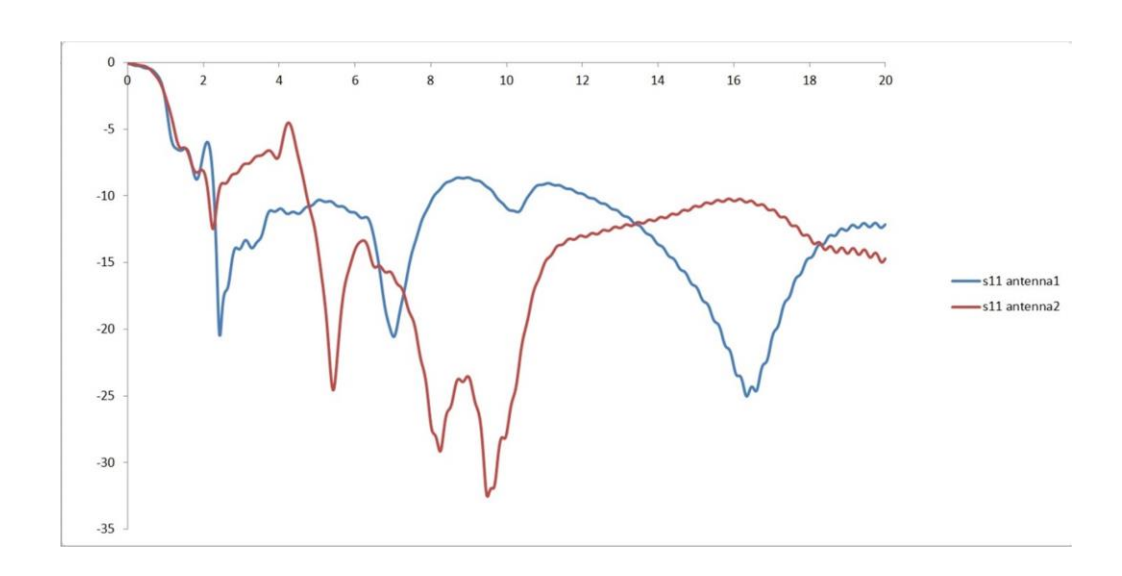


Fig 8: S-Parameter Antenna1(Base) VS Antenna2(Proposed)

ANALYSIS OF SMART PARKING SYSTEM USING MACHINE LEARNING

Ch.Kowshik ,N.Kaushik ,Y.Yaswanth

Introduction:

Modern society is witnessing a rapid population growth each day, and people are purchasing vehicles for their convenience so that they can travel between places. Since vehicle density is increasing rapidly, particularly during peak hours, finding a parking space to leave a vehicle can be difficult for users. Machine learning applications will be used to create a smart parkingsystem based on this framework. There is a mobile application being developed for users to beable to check the accessibility of parking spots from their mobile devices. By introducing a smart parking system in metropolitan cities, one can reduce the amount of fuel utilized and environmentally harmful pollution which are potential difficulties. In this project, The user canalso check the real time parking space availability in mobile application. Hence we propose a framework for a Smart Parking System that will provide an optimal solution for parking in themetropolitan city.

Smart parking systems have gained significant attention as urban areas grapple with increasing traffic congestion and limited parking spaces. Machine learning has emerged as a powerful toolto optimize parking management and enhance the overall parking experience for users. This research presents an in-depth analysis of a smart parking system that leverages machine learning techniques to improve parking efficiency, reduce environmental impact, and enhanceuser satisfaction.

These systems use a variety of sensors and technologies to collect data about parking availability, traffic conditions, and other factors. This data can then be used to provide real-time information to drivers and parking operators, and to optimize the use of parking resources. Machine learning (ML) is a powerful tool that can be used to improve the performance of smartparking systems.

Smart parking systems are a promising technology that has the potential to significantly improve the efficiency and convenience of parking. Machine learning is a key enabling technology for smart parking systems, and it is being used to develop new and innovative solutions to the challenges of parking management. In order to create a model that predicts the available parking slots using different machine learning techniques and to analyze the obtained results in each case, implementing a smart parking system using machine learning involves several steps, from data collection and preprocessing to model development and system deployment. Below, I outline the key steps tocreate a basic smart parking system using machine learning:

1. Data Collection:

• Collect data on parking space occupancy. You can use various sensors such as cameras,ultrasonic sensors, or magnetic sensors to monitor parking spaces. Ensure that the dataincludes information on occupancy status and timestamps.

2. Data Preprocessing:

• Clean and preprocess the collected data. This may involve handling missing data, filtering noise, and converting timestamps into a usable format. You should also label the data as "occupied" or "available."

3. Data Labeling:

• Label the data based on the occupancy status of parking spaces. You can manually labela portion of the data and use it as the ground truth for training your machine learning model.

4. Feature Engineering:

• Extract relevant features from the data that can help the machine learning model make predictions. Features may include time of day, day of the week, and historical occupancy patterns.

5. Model Selection:

- Choose a suitable machine learning model for occupancy prediction. Common choicesinclude:
- Logistic Regression
- Decision Trees
- Random Forest
- Support Vector Machines
- Neural Networks (deep learning)

6. Model Evaluation:

• Assess the model's performance using evaluation metrics such as accuracy, precision, recall, and F1-score. Fine-tune the model as necessary.

7. Communication Network:

• Ensure that there is a reliable communication network in place to transmit data betweensensors, the central server, and the user interface.

8. Deployment:

• Deploy the smart parking system in your target location, such as a parking facility or acity. Ensure that all components are working together seamlessly.

9. Data Privacy and Security:

• Implement data privacy and security measures to protect user data and ensure that the system complies with relevant regulations.

Creating a smart parking system using machine learning can be a complex undertaking, but it has the potential to greatly enhance the parking experience for users and improve the efficientuse of parking resources. Make sure to consider the specific requirements and constraints of your project during each step of the implementation process.

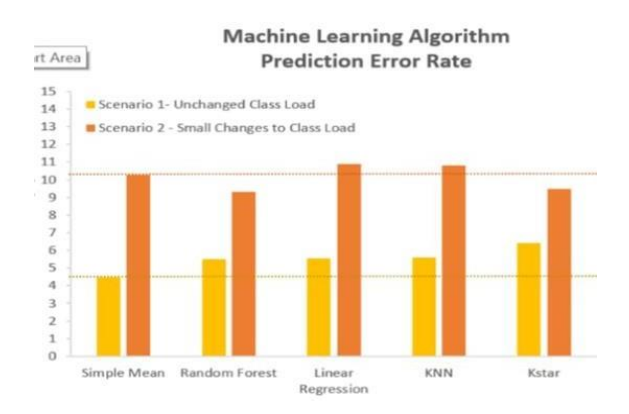




Fig 1 Analysis of ML Algorithms

Fig 2 Predicted Parking Slots Occupancy

Smart parking systems using different machine learning algorithms and their accuracy are determined. Smart parking systems using machine learning algorithms have the potential to significantly improve the parking experience for both drivers and parking lot operators. By using machine learning to collect and analyze data about parkinglot occupancy, traffic flow, and other factors, smart parking systems can help drivers to find parking spaces more quickly and easily, while also helping parking lot operators to improve efficiency and reduce costs. Another key benefit of smart parking systems using machine learning algorithms is that they can improve customer satisfaction. By making it easier and more convenient for people to find parking spaces, smart parking systems can lead to increased business activity in areas with smart parking systems. Overall, the analysis of smart parking systems using machine learning algorithms has shown that these systems have the potential tomake parking more efficient, convenient, and cost-effective for everyone involved.

SMART BOT FOR FACE RECOGNITION AND VOICE CONTROLS

E. AdityaVardhan, B. Pooja, B.KumarSai

Introduction:

The combination of learning algorithms and computer vision has given rise to novel applications that are redefining the way people interact with machines in an era of constantly evolving technology. The "Smart Bot for Face Recognition and Voice Controls" is an interesting and innovative project that combines these technologies to produce a smart, interactive, and user-friendly system. The basic elements of the project are face recognition and voice control technologies, that when combined provide a smooth and clear user experience. These technologies can recognize people based on their facial traits and comprehend spoken instructions, making machine contact more natural and user-friendly

The goal of this project is to create a smart bot that combines face recognition and voice commands to give a smooth and common user experience. This creative bot may be used in a number of situations, including home automation, security systems, and customer service applications. It provides an extensive range of convenience and security benefits by combining the capabilities of facial recognition with voice commands.

The two primary components of this project are:

- Facial Recognition: The project uses computer vision and learning algorithms to identify and verify people based on facial attributes. This technology can be utilized for more than only user recognition; it can also be used for emotion analysis and gender identification. Furthermore, face recognition plays an important role in improving security and access management, making it an essential tool for smart homes, businesses, and public areas.
- Voice Controls: The voice control component makes use of speech recognition algorithms to allow users to interact with the system by speaking commands. This improves accessibility while also providing a hands-free and simple way to manage multiple gadgets and applications. Voice commands may be used to do things like adjust lights, manage smart appliances, create reminders, and more.







Fig-1. Prototype of the proposed smart bot

FLOW CHART AND ALGORITHM:

The below flow chart describes how the process isgoing to run.

Step-1:start

Step-2: the raspberry pi cam starts capturing the images

Step-3: it compares the captured faces with the faces stored in the databases

Step-4: if the faces matches? Yes- greets the person with the name stored in database

Step-5: no- just it says welcome without any name

Step-6: provides additional information regarding date and time

Step-7: also accepts our commands to provide certain information

Step-8: stop

Fig-7 shows the flow chart for the smart bot

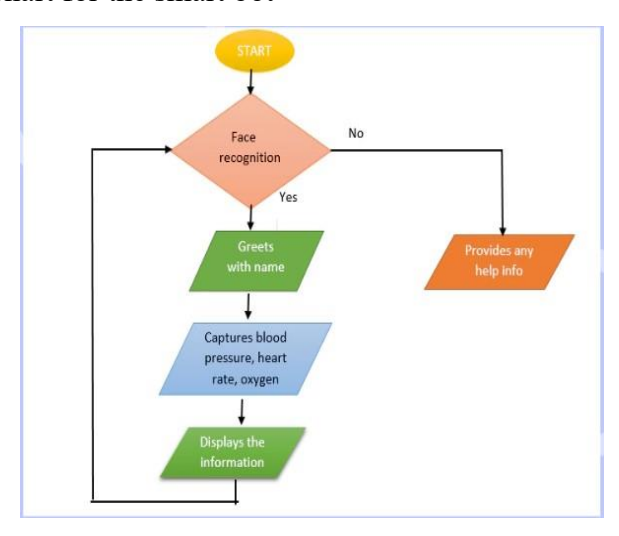


Fig-2: Flow chart

Install the latest version of OS in the raspberry pi module. After that we need to make sure that we have installed the latest version of python software because we have developed a python code for face recognition. For this purpose we require some modules as mentioned above we need to install all those modules. Fig -8 shows the raspberry pi setup. Once the raspberry pi is ready we need to connect a raspberry pi cam or web cam to the raspberry pi and a speaker to greet the person.





Fig-3: Raspberry pi module setup

The webcam connected to the raspberry pi starts recording the video. CV2 module ensures that an image should be taken from the video in order to detect the person. Fig-9 shows the webcam used for face recognition and the code. In the developed code we included how to train the raspberry pi module to detect the face of the person. In the code itself we have imported the modules required which are downloaded before which makes user interface a little bit easier. We just need to run the program all the activities are inbuilt. It runs and detects the face if the persons image is already present in the database.



Fig-4: Code for face recognition and webcam

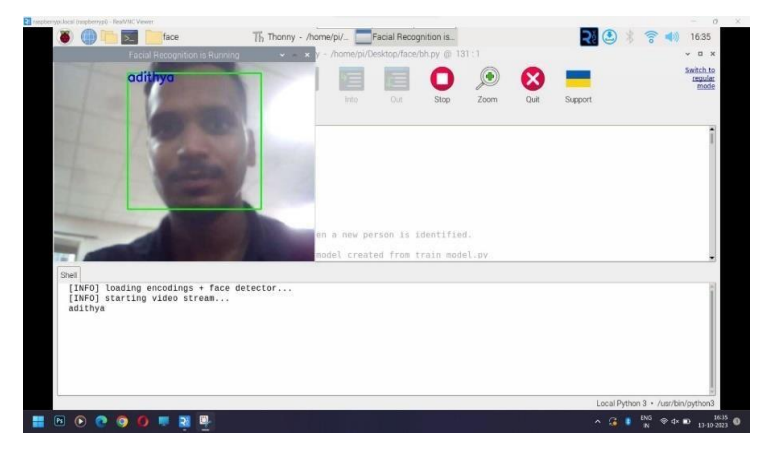




Fig-5: Output of trained face-1

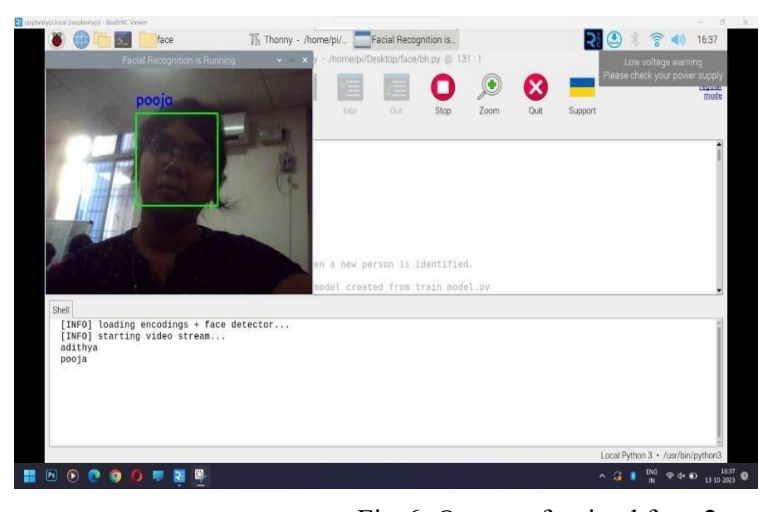




Fig-6: Output of trained face-2

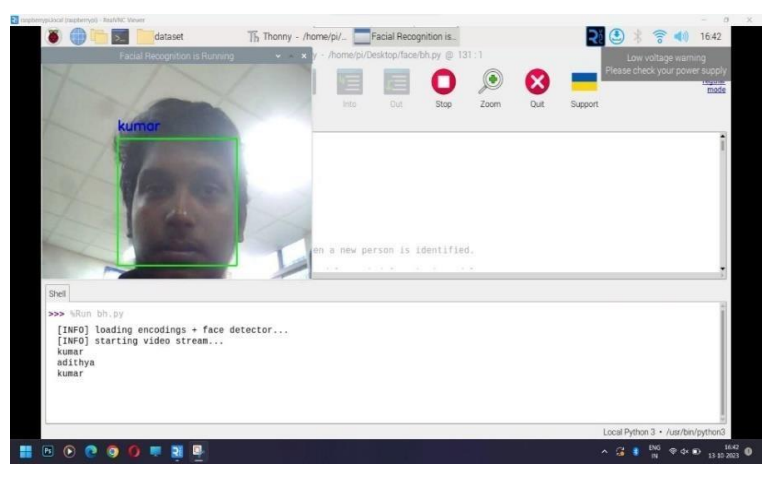




Fig-7: Output of trained face-3

As mentioned above after detecting the face of the person it should greet the person with the name which is stored in the data base for example hello welcome Adithya. For this purpose also we need to install certain modules lie espeak, pyttsx6, speech recognition etc.. and these modules are also included in the code to make if easy because total process is in one code. Fig-13 shows the speakers used for our smart bot and the code. After running the code we see that the command given in the code in addition to the name of the person stored in the database willbe outputted through the speaker .we can hear the voice and we feel like the bot is greeting us. And after that it also accepts our commands as input and provide the required information for us. We just trained our raspberry pi in such a way.



```
ngine.runAndWait()
  h sr.Microphone() as source:
                                  print("Say")
audio_data = r.record(source, duration=5)
text = r.recognize_google(audio_data)
                                  print(text)
if(text=="yes"):
                                                with sr.Microphone() as source:
                                                print("Say")
audio_data = r.record(source, duration=5)
if(text=="hello"):
    current_date = datetime.now()
                                                       formatted_date = current_date.strftime("%dth %B %Y")
print(formatted_date)
current_time = datetime.now().time()
                                                       Outlean_time - datetame.now().time()
formatted_time = current_time.strftime("%1 %M %p").lstrip('0')
print( formatted_time)
engine.say("Melcome to VRSidhhartha Engineering College")
engine.say("Today is")
                                                       engine.say(formatted_date)
engine.say("Time is")
                                                       engine.say(formatted time)
                                                 engine.runAndWait()
elif(text=="who are you"):
   engine.say("I am APK Smart Bot working with raspberry pi")
                                                       engine.runAndWait()
                                                 elif(text="seminar hall"):
   engine.say("take right and then left you will find seminar hall ")
   engine.runAndWait()
                                                 elif(text=="rest rooms"
                                                                                         or text=="restroom" or text=="toilet"or text="toilets"):
                                                       engine.say("you can find at the corners ")
engine.runAndWait()
                                                elif(text=="HOD room"):
                                                       engine.say("right side of the block beside steps ")
engine.runAndWait()
                                             engine.say("Have a good day ")
engine.runAndWait()
```

Fig-8: speakers and the code

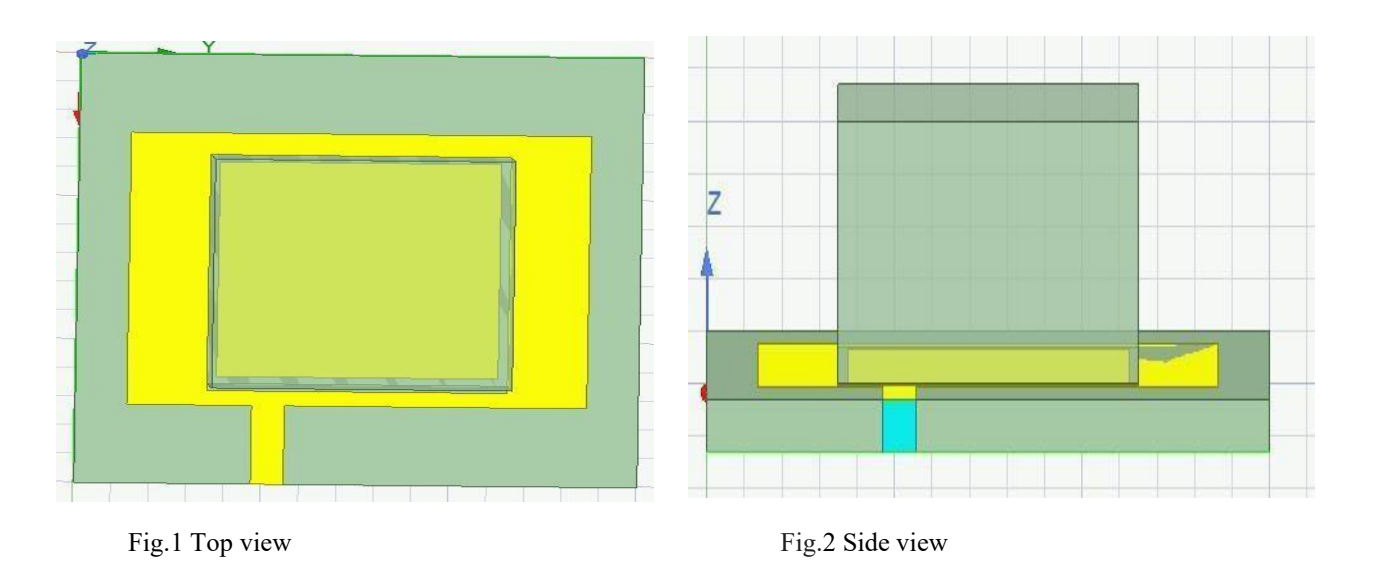
DESIGN AND IMPLEMENTATION OF C BAND DIELECTRIC RESONATOR

A.R. V. Manoj Kumar, sk. Ashraf, B. Yaswanth

INTRODUCTION:

As we progress towards a future that is more connected than ever, the demand for high-speed data transmission is more critical than ever. The introduction of 5G technology has altered the way we interact with the internet. Designing an antenna that can operate over a broad frequency range while maintaining a compact form factor is one of the fundamental obstacles to reaching this goal. Dielectric resonator antennas (DRAs), which have special characteristics and may function in a variety of frequency bands, have recently come to be recognized as a possible solution to this issue. We outline the design and analysis of a dual-band DRA that is tailored for 5G applications in this work. We demonstrate that our antenna can perform well interms of bandwidth, gain, and radiation efficiency, making it a possible candidate for next-generation wireless communication systems.

In the context of 5G technology, there is an increasing need for high-speed data transmission, which has led researchers to look at new antenna designs that can support the high data rates and frequencies necessary for 5G networks. A form of electromagnetic resonator that relies on the resonant characteristics of a dielectric material to operate is the dielectric resonator antenna (DRA), which is one such solution.



The completed dielectric resonator antenna is seen in Figure 1a. For clarification, the aerial's top and perspective views have been included. At first, only the micro strip line's rectangular patch resonator is constructed. The absence of metal is a crucial element of the dielectric resonator when conducting loss is severe at high frequencies. Metallic losses have a substantial effect on the traditional conductor-based antenna. These antennas have a high aerial gain because of their great radiation efficiency.

The antenna was designed using an alumina material with a dielectric constant of 9.9 and a loss tangent of 0.0001 due to its inexpensive cost and widespread availability. The ground's length and breadth are 30mm and 30mm, respectively. The dimensions of the FR-4 substrate are 30mmx30mmx2mm in length, breadth, and height fig1b. The patch's length and breadth are then 19mm by 24.5 mm. Then we added a slit that was 15 mm long and 15 mm wide. In order to activate the dielectric material, the aperture coupling technique involves electromagnetically coupling a fieldproduced by a conducting patch.

Conducting patches are stimulated via micro strip feed excitation. As compared to the patchantenna, the micro strip feed approach requires the least amount of design complexity. The excited patch further induces the field, which is coupled to the DR. An aperture coupler is used to activate the DR. The widely used FR-4 substrate is utilized in the construction of the dielectric reflector (DR)aerial. Standard copper sheets that are 70 micrometers thick were taken into consideration for modeling on top of the FR4 dielectric resonator. The dielectric resonator has dimensions of 16mm in height, breadth, and length. Rectangular micro strip feeding is one type of feeding technique used in the development of micro strip antennas. This technique uses a rectangular micro strip line to feed the antenna. The rectangular micro strip line, a thin strip of conducting material, is put on top of the dielectric substrate, which is then placed on top of the ground plane.

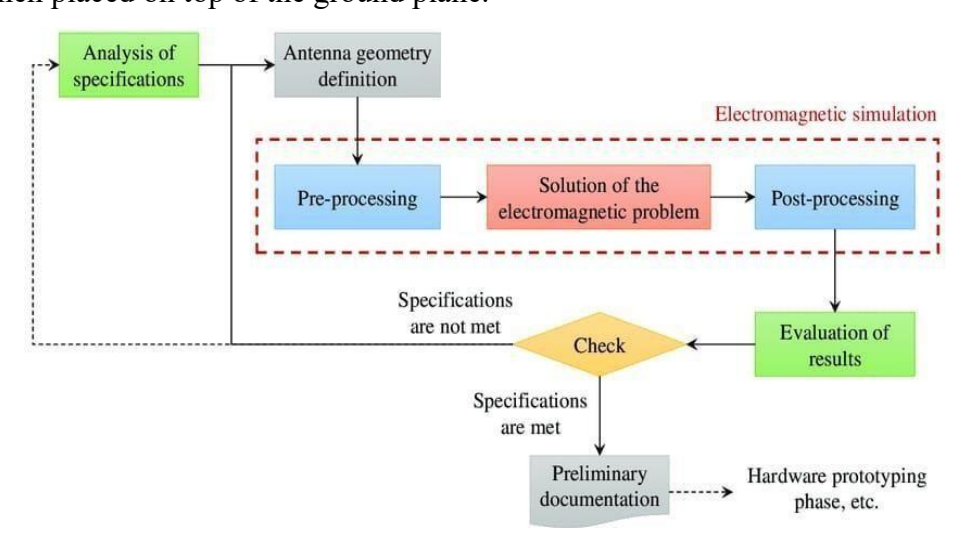


Fig 1: Flow chart

The characteristic impedance of the antenna is designed to match the rectangular microstrip line. This ensures the most effective power transfer from the feedline to the aerial. The width and length of the rectangular microstrip line are critical design elements that must be carefully specified in order to guarantee accurate impedance matching. Rectangular microstrip feeding has the benefit of facilitating simple integration with other parts, including as filters, amplifiers, and phase shifters. By utilizing numerous feeding locations, the feeding approach can also be employed to offer multi-frequency operation. Rectangular microstrip feeding has certain drawbacks, though, including the potential for radiation leakage from the feedline and the challenge of obtaining broadband impedance matching.

Techniques like radiation pattern optimization and impedance matching networks can be used toget around these restrictions. S-parameters (or scattering parameters) are used to describe how energy can propagate through an electric network. S-Parameters are used to describe the relationship between different ports, when it becomes especially important to describe a network in terms of amplitude and phase versus frequencies, rather than voltages and currents. From the S-parameter matrix, you can calculate characteristics of linear networks such as gain, loss, impedance, phase group delay, and voltage standing wave ratio (VSWR).

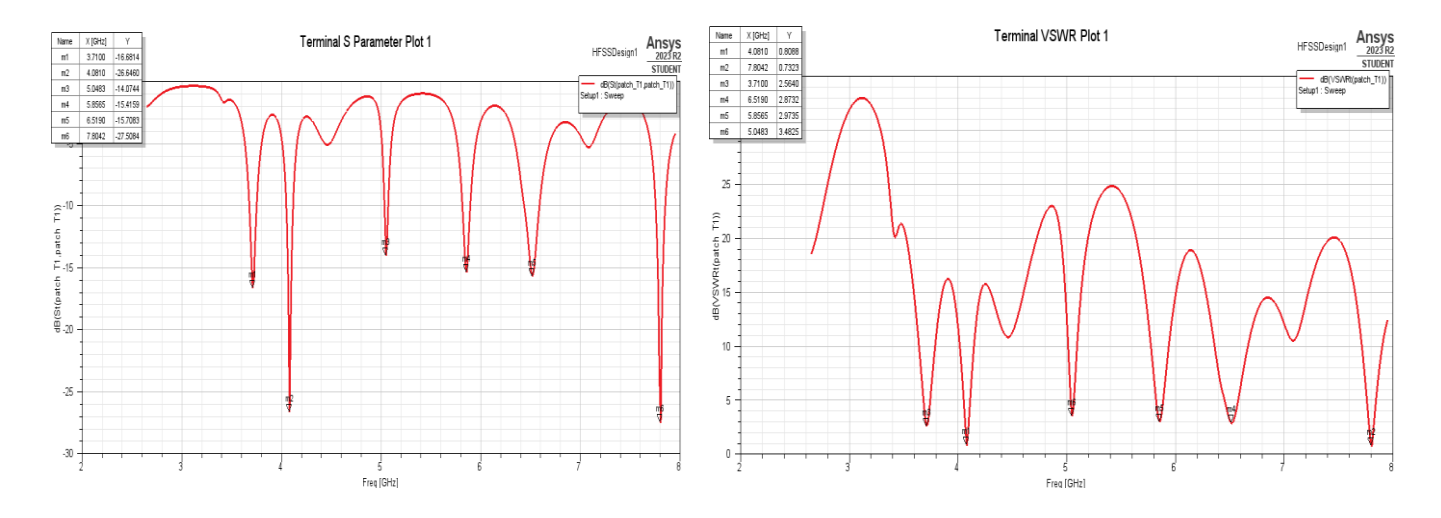


Fig 2: S parameter plot

Fig 3: VSWR Plot

VSWR (Voltage Standing Wave Ratio) is a measure of how efficiently radio-frequency power is transmitted from a power source, through a transmission line, into a load .In an ideal system, 100% of the energy is transmitted. VSWR value under 2 is considered suitable for most antenna applications. The antenna can be described as having a "Good Match". So when someone says that the antenna is poorly matched, very often it means that the VSWR value exceeds 2 for a frequency of interest. VSWR is a very important parameter in RF transmission systems where a high VSWR canreduce the power delivered to an antenna or system significantly. The efficiency with which radio-frequency power is transported from a power source, through a transmission line, and into a load is gauged by the VSWR.

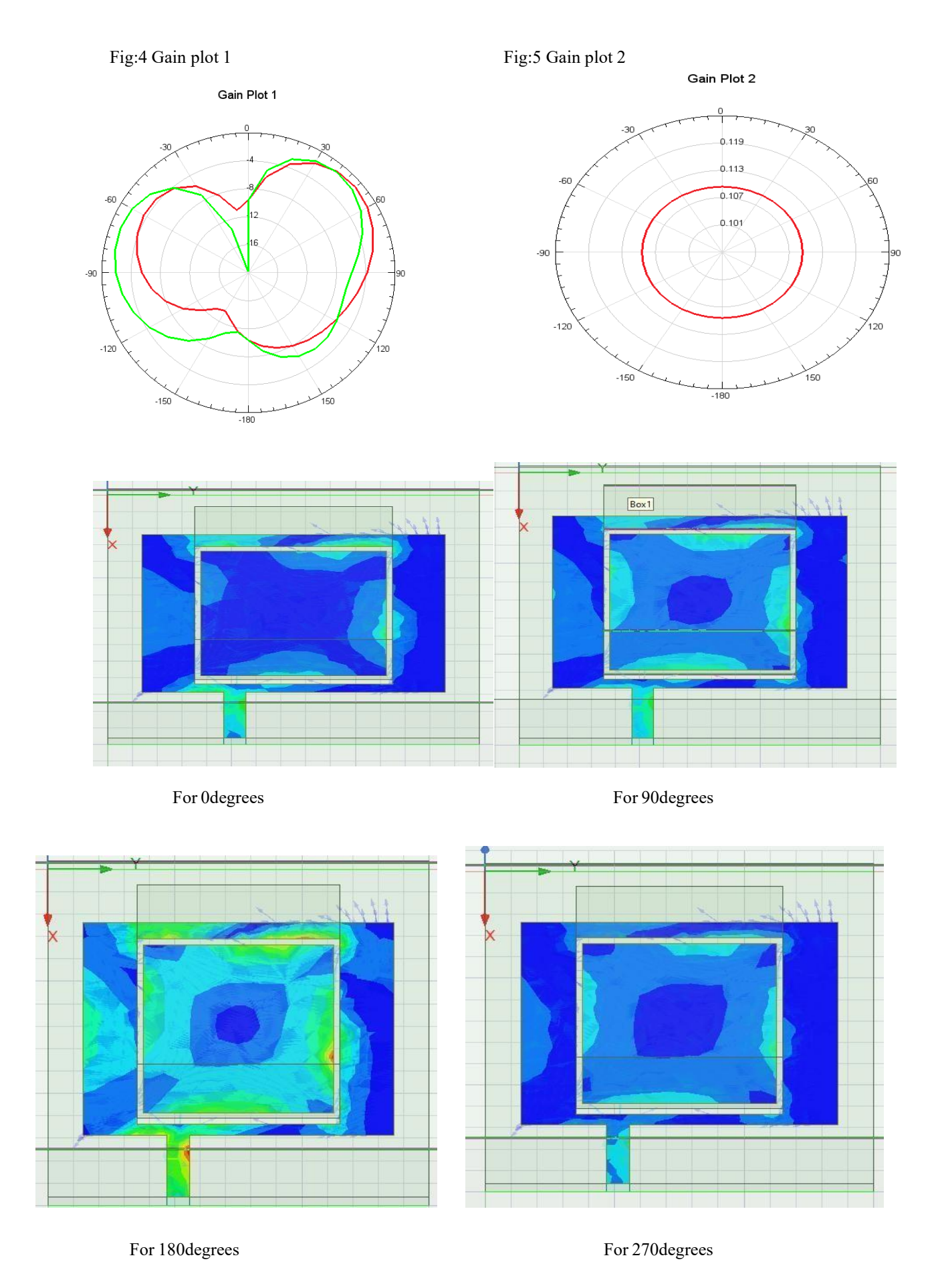


Fig 6 Surface Current Distribution

Gain Plot 3

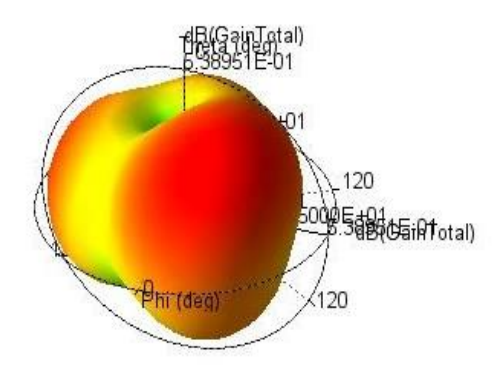


Fig 7 Gain Plot

The gain of an antenna in a given direction is defined as the ratio of the intensity, in agiven direction, and the radiation intensity that would be obtained if the power accepted by the antenna were radiated isotropic.

PHYSICAL LAYER SECURITY ANALYSIS OF NOMANETWORK WITH COOPERATIVE RELAYING AND RIS UNDER DIFFERENT JAMMING CONSTRAINTS

D.B.S.Rohan, P.Naga Sridhar, D.Kumar Reddy

INTRODUCTION

Among 5G wireless networks, non-orthogonal multiple access (NOMA) has gained agreat deal of attention, enabling multiple user connections and smarter spectrum use for enhanced data rate. NOMA utilizes power domain multiplexing, allowing diverseusers to efficiently share channel resources with suitable power levels within the sametime or frequency. To ensure data retrieval from combined signals of NOMA users, NOMA deploys successive-interference-cancellation (SIC) at the receiver. Moreover, for improved coverage and reliability, integrating NOMA with cooperative relaying has garnered substantial interest in recent times. Cooperative NOMA employs conventional relaying techniques to boost performance for distant users dealing with weak channel conditions.

A NOMA DF relay-based system is examined for its secrecy performance. Extensive MATLAB simulations using the Monte Carlo approach are used for validation. The main emphasis is on contrasting the CJ scheme with other jamming and non-jamming approaches, revealing insight on their relative usefulness in various contexts.

The investigation explores into the proposed system's Secrecy Outage Probability (SOP) at both NOMA users under various jamming conditions. Figure 2 depicts the SOP analysis for the remote user (U1) vs various Signal-to-Noise Ratios (SNR). Notably, when compared to other jamming circumstances, the CJ technique performsbetter, with less secrecy outage.

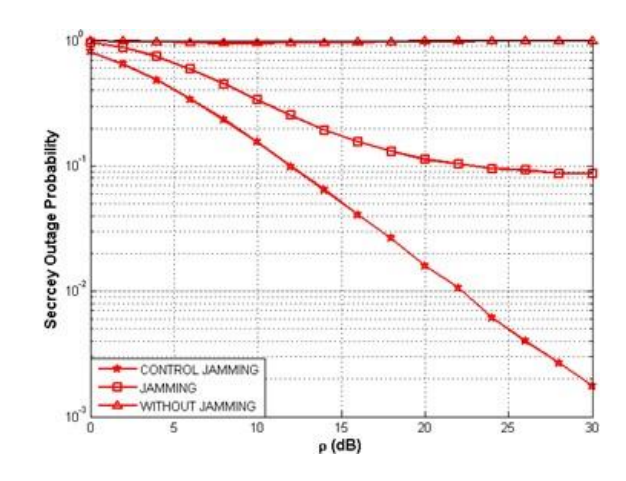


Fig 1: SOP vs SNR at U1

An example of how the jammer-to-eavesdropper distance (d_{je}) impacts the SOP performance at user U_1 can be seen in Figure 3. Notably, the CJ strategy outperforms other strategies in terms of outage performance. Surprisingly, SOP performance diminishes as the distance between jammer and eavesdropper grows. This decrease can be ascribed to the jamming signal's diminished efficacy in

confounding the eavesdropper's reception across longer distances. These findings emphasize the complex interplay between distance, jamming, and secrecy when evaluating system performance.

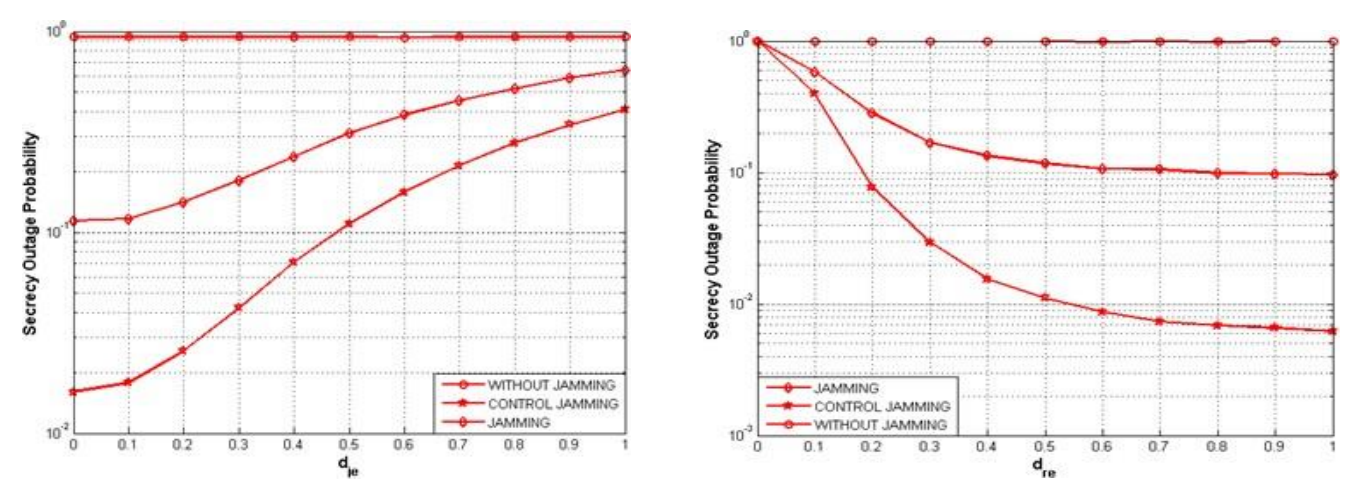


Fig 2 Impact of die on SOP at U1

 $Fig3: Influence\ of\ d_{re}\ on\ SOP\ at\ U_{1}$

A notable trend emerges: SOP performance experiences enhancement with increasing d_{re}. This pattern can be attributed to the diminished likelihood of eavesdropping on relay-to-destination transmission as the relay and eavesdropper are spatially separated. When the relays are positioned in close proximity to the eavesdropper, however, SOP performance deteriorates due to heightened vulnerability. The Constant Jamming (CJ) scheme consistently exhibits superior SOP performance compared to alternative jamming strategies. There is a distinct trend: U2 has lower SOP values, which can be attributed to advantageous channel circumstances along the jammer-to-U2 and relay-to-U2 links. The dominance of the Constant Jamming (CJ) strategy is notable, as indicated by its constantly superior SOP performance when compared to the 'J' and WJ (Wiretap Jamming) conditions. This gap stems from NOMA user U2's intelligent interference signal processing in the CJ scenario, which contributes to its improved secrecy outage performance.

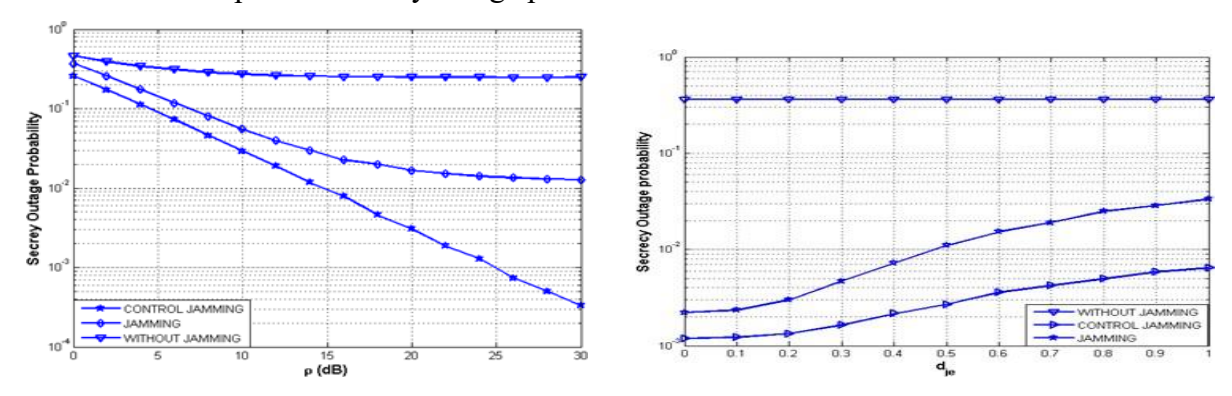
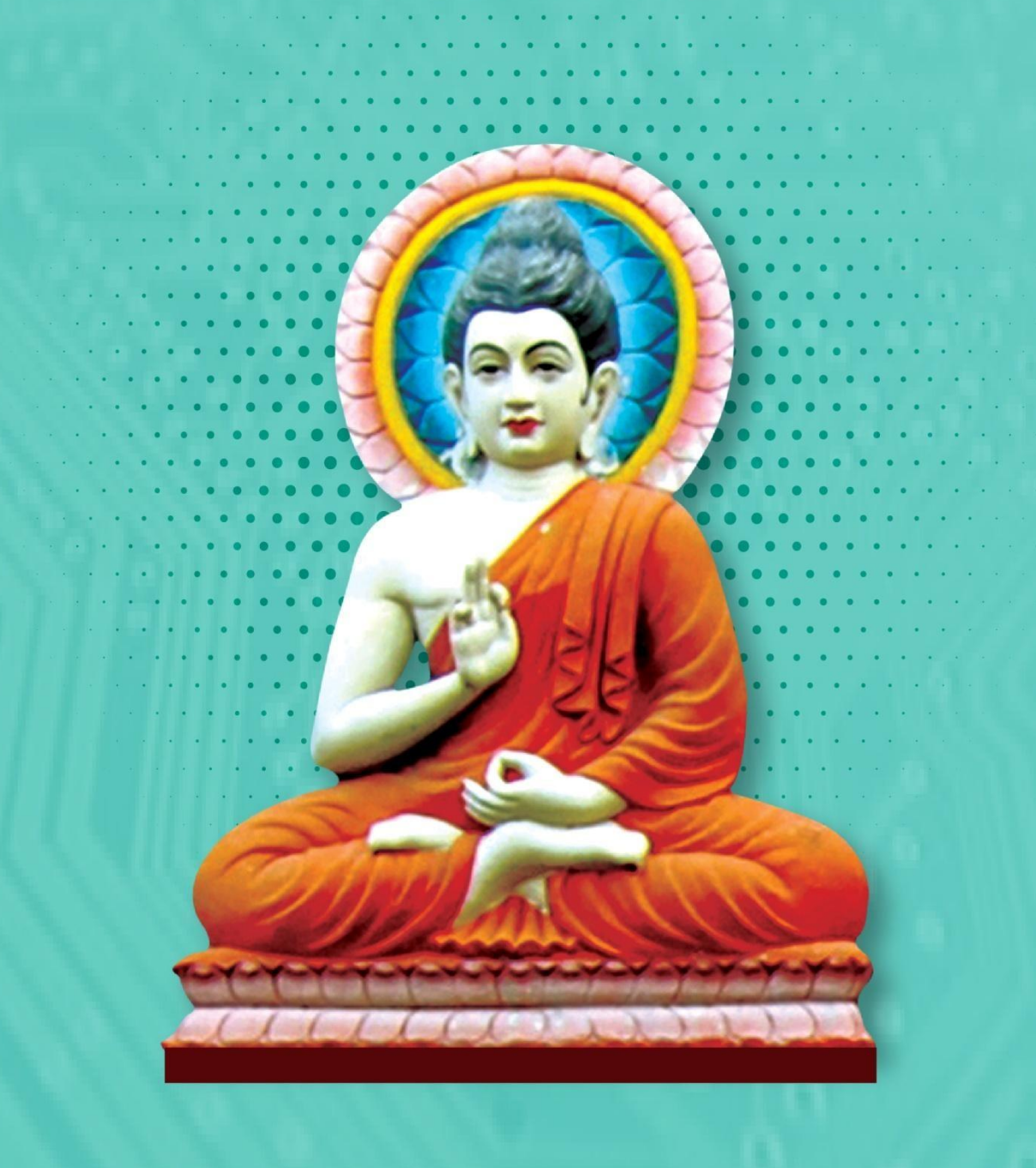


Fig 4: SOP vs SNR with different jamming conditions at U2

According to Figure, various jamming settings affect SOP at user U2 under various jammer-to-eavesdropper distances (dje). Notably, a unique trend emerges: SOP performance improves as the

jammer-to-eavesdropper distance decreases. The counteractive effects of jamming signals on eavesdropper capabilities can be explained by the jamming signal's counteractive effect, especially if the eavesdropper is near the jammer. This performance highlights the effectiveness of the CJ method, which constantly minimize SOP compared to both jamming and non-jamming options in terms of SOP, demonstrating its enhanced secret preservation capabilities. The CJ scheme effectively safeguards the confidential-information of both users from intruder attacks. The study focuses on minimizing the SOP of NOMA users while adhering to total power constraints. Through a comprehensive analysis and comparison with other jamming conditions, it is demonstrated that the CJ scheme significantly improves secrecy performance. The evaluation of the network's physical layer security, considering the SOP under CJ conditions, further strengthens the findings. These findings demonstrate the value and potential of the CJ scheme in boosting NOMA network security, providing valuable insights for future research in the field of secure wireless communications.





VELAGAPUDI RAMAKRISHNA SIDDHARTHA ENGINEERING COLLEGE

(AUTONOMOUS)
(Sponsored by Siddhartha Academy of General & Technical Education)